Part IV
Ecological Aspects and Adaptation

Chapter 11
Chemical Ecology of Poisonous Butterflies: Model or Mimic? A Paradox of Sexual Dimorphisms in Müllerian Mimicry

Ritsuo Nishida

Abstract A number of butterfly species are toxic or unpalatable against predators by developing mechanisms either to biosynthesize such noxious elements de novo or to acquire directly from the poisonous host plants for their own defense. Most of these "poisonous butterflies" exhibit aposematically colored wing patterns that are often associated either with Batesian or Müllerian mimicry species to form a "mimicry ring." This review focuses on unpalatable chemical elements potentially operating in three typical mimicry rings: (1) the tiger *Danaus* mimicry ring, (2) the *Idea* mimicry ring, and (3) the red-bodied swallowtail mimicry ring, in association with their mimetic wing patterns. Female-limited polymorphisms are a common feature of the Batesian mimicry but not in Müllerian mimicry, because such diversification is unfavorable for the models. I present here some unique cases of sexual dimorphisms within the putative Müllerian mimicry complexes. A *Danaus chrysippus*-mimicking nymphalid, *Argyreus hyperbius*, is a typical example of the female-limited dimorphic mimics. However, *A. hyperbius* were found to be poisonous with toxic cyanogenic glycosides (linamarin and lotaustralin). Likewise, a pipevine swallowtail, *Atrophaneura alcinous*, which sequesters toxic aristolochic acids, exhibits sexually dimorphic color patterns (male, black; female, smoky brown). A sympatric diurnal zygaenid moth, *Histia flabellicornis*, is mimetic to *A. alcinous* males rather than the females and stores cyanogenic glycosides. The moth is regarded as a Müllerian ally that may have stabilized the wing coloration mutually with those of *A. alcinous* males. On the contrary, a diurnal "swallowtail moth," *Epicopeia hainesii*, mimics the brighter wing color of *A. alcinous* females. Possible adaptation mechanisms on these paradoxical mimicry patterns are discussed.

Keywords Batesian mimicry • Müllerian mimicry • Aposematism • Unpalatability • Sequestration • Defense substance • Pharmacophagy • Sexual dimorphism • Sexual selection • Mimicry ring

---

The original version of this chapter was revised. An erratum to this chapter can be found at https://doi.org/10.1007/978-981-10-4956-9_18

R. Nishida (✉)
Discipline of Chemical Ecology, Kyoto University, Sakyo-ku, Kyoto 606-8502, Japan
e-mail: ritz@kais.kyoto-u.ac.jp

T. Sekimura, H.F. Nijhout (eds.), *Diversity and Evolution of Butterfly Wing Patterns*, DOI 10.1007/978-981-10-4956-9_11

11.1 Introduction

The monarch butterfly, *Danaus plexippus* (Danainae: Nymphalidae), is an exemplar of the model/mimic relationships in butterflies. The larvae feed on milkweed plants (Asclepiadoideae of the family Apocynaceae) and selectively accumulate toxic cardenolides (cardiac glycosides, CGs) from the host plants and pass over to the adults (Reichstein et al. 1968). CGs are powerful heart poison and induce emesis to predatory birds (Brower 1984). If a "hungry blue jay" ingested a monarch butterfly, the sequestered CGs in the butterfly body tissues strongly induced emesis (Brower 1969). After such a noxious experience, the bird would never eat the butterflies with the same wing pattern again. Predatory birds avoid the butterflies primarily because they experience an obnoxious "bitter" taste and/or emesis after ingestion. This results in a visually conditioned aversion toward prey with similar appearance, allowing for the evolution of Batesian mimicry (Brower 1969). Therefore, the monarch is considered to be a typical poisonous model butterfly. The viceroy, *Limenitis archippus* (Nymphalinae, Nymphalidae), was initially thought to be a typical example of Batesian mimicry. However, the viceroy was shown to be fairly unpalatable to some predators (Ritland and Brower 1991; Prudic et al. 2007). Moreover, monarch can sometimes be palatable (or nontoxic) particularly if the larvae grew up on the nontoxic or low-CG milkweed plants (Brower 1969). Thus, the situation between the models and mimics may be interchangeable as in this case, and if both are unpalatable mimicking to each other, it forms an association of the Müllerian mimicry type, rather than Batesian (Rothschild 1979; Huheey 1984).

Unpalatability or distastefulness is strongly linked to the toxicity of the sequestered defense substances, as in human taste (Brower 1984), and thus, the predator effectively avoids toxic prey before ingestion. Visually oriented, avian predators are the most effective selective pressure to contribute to the formation of mimicry butterflies in conjunction with the distastefulness of the model species. The evolution of mimicry is highly dependent on both the visual and chemosensory (gustatory/olfactory) physiology of the predatory animals in addition to the intrinsic toxicity of the model butterfly (Brower 1984; Nishida 2002). However, knowledge on the chemistry of defensive agents stored in each species within the mimicry rings is often scarce (Trigo 2000; Nishida 2002). I highlight chemical backgrounds of acquired defensive elements among some aposematic Asian butterfly species in the following three typical/putative mimicry rings:

(1) The tiger *Danaus* mimicry ring
(2) The *Idea* mimicry ring
(3) The red-bodied swallowtail mimicry ring

The female-limited mimetic dimorphisms are a common feature of the Batesian mimics as in the *Papilio polytes* of the red-bodied swallowtail mimicry ring (Turner 1978). By contrast, Müllerian mimics lack strong sexual dimorphism, presumably due to density-dependent selection, where the divergence of a morph is disadvantageous in the toxic model (Mallet and Joron 1999). However, some exceptional

cases of sexual dimorphisms can be seen within the putative Müllerian mimicry complexes in the above mimicry rings (1) and (3). My particular attention is focused on those sexually dimorphic species where both sexes were confirmed to harbor noxious chemicals – to evaluate their adaptive characteristics within the mimicry rings.

11.1.1 Tiger Danaus Mimicry Ring

Although the monarch butterfly, *Danaus plexippus*, and other milkweed butterflies sequester CGs from the *Asclepias* hosts in the body tissues and become unpalatable to bird predators, some of the butterfly populations often lack CGs as mentioned above. Similar to the American *Danaus* spp., the Old World milkweed butterfly, *Danaus chrysippus* (so-called plain tiger, widely distributed from Africa to tropical Asia) is assumed to be "poisonous" with its conspicuous appearance with a black apex and white subapical spots on the forewing in blight tawny-orange background coloration, likely as a typical model for various mimicry species (Smith 1973) (Figs. 11.1 and 11.2). *D. chrysippus* feeds exclusively on the Asclepiadoideae and presumed to sequester toxic cardenolides from its host milkweed plants during the

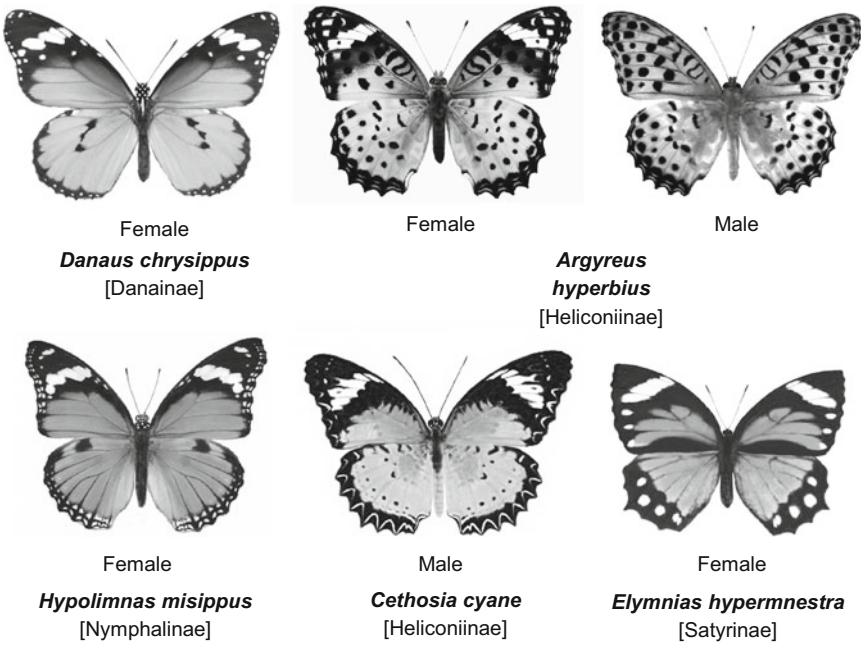

Fig. 11.1 The tiger Danaus mimicry ring. Note that some species in this figure may not occur in the same habitat

Fig. 11.2 (**a**) *Danaus chrysippus* female, (**b**) *Argyreus hyperbius* female, (**c**) *A. hyperbius* male

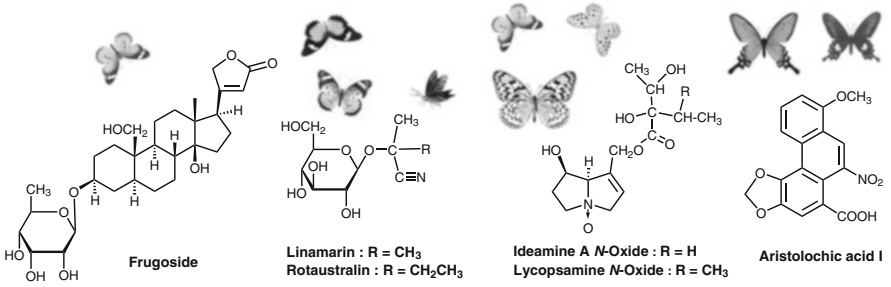

Fig. 11.3 Typical defensive substances in aposematic butterflies

larval stage. However, they are known to be poor and inconsistent sequesterers of CGs (Schneider et al. 1975; Rothschild et al. 1975; Mebs et al. 2005).

In order to confirm the toxicity of a local population of *D. chrysippus* in Okinawa, we examined CG contents in their body tissue. A relatively polar CG, frugoside (Fig. 11.3), was characterized as the major sequestrate in *D. chrysippus* adults raised on *Asclepias curassavica* (Wada et al. unpublished). While calotropin and calactin are CGs known as typical sequestrates in *D. plexippus* raised on *A. curassavica* (A), these less polar CGs were not found as prominent components in *D. chrysippus*, suggesting a selective or differential accumulation of CG species as in the case between *D. plexippus* and *D. gilippus* (Cohen 1985; Mebs et al. 2012). In addition, males of *D. chrysippus* frequently visit plants containing poisonous pyrrolizidine alkaloids (PAs) and pharmacophagously sequester the alkaloids in the body tissues both as a defense substance and pheromone precursors (Edgar et al., 1979; Boppré, 1986) (see also Sect. 11.2). Since *D. chrysippus* males in Okinawa frequently visit PA-containing plants such as *Eupatorium* (Asteraceae) and *Heliotropium* (Boraginaceae), they are assumed to be protected dually both by CGs and PAs. Nevertheless, a more detailed spatiotemporal dimensional survey of sequestered defensive elements is needed further to clarify the "palatability spectrum," because the distribution of *D. chrysippus* is widespread throughout the African-Asian tropical and subtropical regions up to Okinawa in association with their local mimics as discussed below.

There are a variety of butterfly species that closely resemble wing color patterns of *D. chrysippus*, particularly within Nymphalidae to form a "tiger Danaus mimicry ring" in Asian regions (Fig. 11.1):

Danaus genutia (striped tiger) (Danainae: Nymphalidae): This butterfly resembles *D. chrysippus* but with conspicuous black stripes on both fore- and hindwings. These two coinhabiting *Danaus* species, widely distributed throughout India, South Asia, and Japan, are regarded as Müllerian mimics, as both species feed on the milkweed subfamily Asclepiadoideae, although the ability of sequestration of CGs from their host *Cynanchum liukiuense* in Okinawa is unknown. Males of these two species show strong affinity to PA-containing plants and are considered to obtain alkaloids both as defensive measure as well as sex pheromone precursors.

Hypolimnas misippus (danaid eggfly) (Nymphalinae: Nymphalidae): Females are known polymorphic and the plain tiger mimic occurs sympatrically with *D. chrysippus* in Asia (Gordon and Smith, 1998). Since the larvae feed on the "presumably innocuous plant" *Portulaca oleracea* (Portulacaceae), this butterfly is thought to be a palatable mimic.

Elymnias hypermnestra (common palmfly) (Satyrinae: Nymphalidae): Some populations are sexually dimorphic. While the males mimic *Euploea* species, the females mimic *Danaus* spp. (Yata and Morishita 1985). The larvae feed on the palm family Arecaceae (Ackery and Vane-Wright 1984).

Cethosia cyane (leopard lacewing) (Heliconiinae: Nymphalidae): There are several lacewing species mimicking the wing patterns of *D. chrysippus*. Their larvae feed on Passifloraceae, the subfamily of which is known to biosynthesize toxic cyanogenic glycosides (CNs) (Nahrstedt and Davis 1985).

Argyreus hyperbius (Indian fritillary) (Heliconiinae: Nymphalidae): This species is sexually dimorphic and the females have similar patterns to *D. chrysippus* but with additional black spots scattered on the dorsal wings (Fig. 11.2). The female has been considered to be a Batesian mimic (Su et al. 2015). The larvae feed on Violaceae plants similar to many other related species in the tribe Argynnini in Japan. Since the toxicity of this butterfly is unknown, we examined the possible defensive substance in the body as described below.

Among the species listed above, only females are mimetic to *D. chrysippus* in *H. misippus*, *A. hyperbius*, and *E. hypermnestra*, whereas males are considered to be pre-existing morphs at least in the case of the former two, as typical examples of sexual dimorphism. Female-limited wing pattern dimorphism in the butterfly mimicry rings seems restricted to Batesian mimicry, whereas Müllerian mimics lack strong sexual dimorphism (Mallet and Joron 1999). An increase of palatable mimetic pattern relative to a model would weaken the mimetic advantage in Batesian mimicry by negative frequency-dependent selection, whereas an increase of unpalatable mimetic pattern becomes more favorable in Müllerian mimicry by positive density-dependent selection (Turner 1978; Mallet and Joron 1999). If this theory is applicable, both *H. misippus* and *A. hyperbius* would be palatable Batesian mimics of the model *Danaus*. This would also be supported by chemical

constituents in their host plants; both *Portulaca* and *Viola* are presumably "nontoxic" (the former often listed as a local edible wild vegetable). However, the chemical analysis of *A. hyperbius* butterfly bodies revealed the presence of highly toxic cyanogenic glycosides (CNs), linamarin and lotaustralin, both in males and females (raised on wild *Viola yedoensis* as well as cultivated varieties of pansy, *V. tricolor* during the larval stage) in substantial quantities (contents of total CNs: females, 300–400 μg; males 100–250 μg/body) (Nakade et al. unpublished) (Fig. 11.3). Since these CNs were not detected in the host *Viola* plants, *A. hyperbius* seems to biosynthesize these toxic compounds from amino acids, as in *Heliconius* butterflies (Nahrstedt and Davis 1985). It is also known that some of monomorphic *Cethosia* spices store linamarin and lotaustralin (Nahrstedt and Davis 1985).

Here *A. hyperbius* butterfly is determined to be poisonous despite its sexual dimorphism in wing pattern, to form the *Danaus* (male + female) – *Cethosia* (male + female) – *Argyreus* (female) Müllerian mimicry ring. It is noted that a number of *Cethosia* lacewings exhibit a black-spotted wing pattern similar to that of *A. hyperbius* rather than that of *D. chrysippus* which entirely lacks such "leopard"--spotted patterns, suggesting a closer reciprocal interaction between these two taxa within the Heliconiinae in the South Asian regions. We still do not know whether the other sexually dimorphic nymphalids, *H. misippus* and *E. hypermnestra*, store any unpalatable allelochemicals or not.

11.1.2 Idea *Butterfly Mimicry Ring*

A giant butterfly, *Idea leuconoe* (mangrove tree nymph) (Danainae: Nymphalidae), is a primitive danaine species, having a wingspan of 120–140 mm with black markings and veins on the white wing background (Fig. 11.4). Although the butterfly is not aposematic in coloration, compared to other toxic butterflies, it is highly conspicuous in the subtropical forests flying slowly and gracefully under the high predatory avian pressure such as the blue rock thrush, *Monticola solitarius*. The butterfly (originated in Okinawa) accumulates large quantities of PAs (ideamines A, B, and C, lycopsamine, parsonsine) as *N*-oxides from the host *Parsonsia laevigata* (Apocynaceae) during the larval stage (Nishida et al. 1991; Kim et al. 1994) (Fig. 11.3). The total alkaloids often exceed 3 mg/insect, suggesting a high unpalatability to potential predators.

Although males of most danaine butterflies show strong affinity to PAs during adult stage and accumulate PAs by foraging pharmacophagously from various plant sources to obtain defensive agents, as well as pheromone precursors, by visiting PA-containing plants (Ackery and Vane-Wright 1984), *I. leuconoe* and some other related *Idea* species in Southeast Asia likely obtain PAs not pharmacophagously but directly from the apocynad hosts during the larval stage. *I. leuconoe* is highly adapted to PAs not only by sequestering PAs for defense (allomone) but also for specific oviposition cues (kairomone) in females (Honda et al. 1997) and precursors

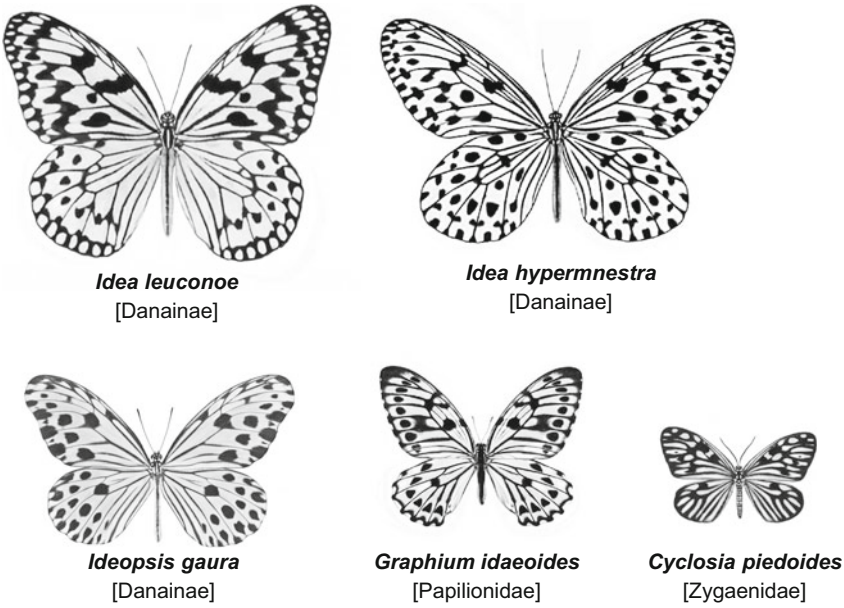

Fig. 11.4 The *Idea* mimicry ring. Note that some species in this figure may not occur in the same habitat

of volatile sex pheromone in males (Nishida et al. 1996). Such a tight linkage with PAs seems to represent an ancestral feature of the Danainae, from which the secondary colonization of the Danainae on PA-free plants (such as Asclepiadaceae) might have taken place with retention of the PA-mediated allomonal and pheromonal systems via pharmacophagous acquisition of the precursors from nonhost PA plants (Edgar 1984; Nishida 2002). *I. hypermnestra* (Fig. 11.4) and *I. lynceus*, both sympatric in Peninsular Malaysia, sequester a series of PA *N*-oxides, tentatively assigned from the hemolymph of the wild adults in the spectrometric analysis (Nishida unpublished). These two species are regarded as the Müllerian mimics in the rainforest habitat.

Beside these two giant *Idea* species, a smaller danaine species, *Ideopsis gaura*, often share the same habitat in Southeast Asia (Fig. 11.4). Its larvae feed on the Apocynaceae, but sequestration of toxic elements from the host is unknown. *I. gaura* males frequently visit PA-containing *Eupatorium* flowers (Asteraceae). A PA *N*-oxide of lycopsamine (or its stereoisomers) was detected by mass spectrometry from the body extracts of *I. gaura* males (captured in Penang, Malaysia) (Nishida unpublished). Thus, these three coinhabiting danaines seem to form a Müllerian mimicry association within the subfamily Danainae.

A Southeast Asian satyrine species, *Elymnias kuenstleri* (Nymphalidae), is also known to mimic *Idea* spp., which is analogous to the relationship between *Elymnias hypermnestra* and *D. chrysippus* in the tiger Danaus mimicry ring (Fig. 11.1). There are several swallowtail butterfly species mimetic to *Idea* spp. or *Ideopsis gaura*, such as *Graphium idaeoides* (Fig. 11.4), *G. delessertii*, and a whitish morph of

Papilio memnon (Papilionidae), which are assumed to be Batesian mimics of *Idea* spp.

The wing pattern of a day-flying *Cyclosia pieriodes* (false *Idea* moth, Zygaenidae) (Fig. 11.4) resembles that of *Idea* spp. or *Ideopsis gaura*. Although the defense substance has not been examined, it is likely that the moth stores some CNs, as many other unpalatable zygaenids are known to biosynthesize/store linamarin and lotaustralin (Holzkamp and Nahrstedt 1994; Nishida 1994). The wingspans between the putative model giant *Idea* spp. (or medium-size *I. gaura*) and minute *C. pieriodes* may be beyond comparison for the insectivorous birds. However, the exquisite wing color pattern may be a more significant factor to develop mimicry beyond their size in the avian vision, probably involving a psychological effect (Wickler 1968; Halpin et al. 2013).

11.1.3 Red-Bodied Swallowtail Mimicry Ring

As quoted by Wallace, the common rose, *Pachliopta aristolochiae*, and many other "red-bodied swallowtails" in the tribes Troidini (Papilionidae) are known as unpalatable models for various Batesian mimicry complexes particularly in the genus *Papilio* (Uésugi 1996) (Fig. 11.5). These troidines feed selectively on the pipevine family, Aristolochiaceae, and sequester toxic aristolochic acids (AAs) (Fig. 11.3) in the body tissues (Euw et al. 1968; Nishida and Fukami 1989; Wu et al. 2000). One of the pipevine swallowtails, *Atrophaneura alcinous*, from mainland Japan exhibits sexual dimorphism to some degree, in that the dorsal wings of males are typically jet black, while the females' are gray or smoky brown with some variations in the degree of darkness; the underside hindwings have long tails and a row of pink or orange spots at the edge in both sexes; the lateral sides of the abdomen are red with a black spot on each segment in both sexes (Fig. 11.5b, e, f).

A day-flying swallowtail moth, *Epicopeia hainesii* (Epicopeiidae) (Fig. 11.5c, d), has a red abdomen and a similar color pattern on the wings with long swallowtail projections as those in *A. alcinous*, although the body size is much smaller than that of *A. alcinous* (Fig. 11.5d–f and 11.6). The brighter gray or smoky brown-color tone and the black veins on the dorsal wings of *E. hainesii* are strikingly similar to those of *A. alcinous* females but not much of males. It suggests a unique case of mimicry in that the moth adopts one of the sexes of the toxic model. Both *A. alcinous* and *E. hainesii* are considered to be more or less sympatric in forests and grasslands in the middle to southern part of Japan. However, *E. hainesii* is distributed further to northern Japan, including Hokkaido, where its putative model *A. alcinous* is absent (Inoue, 1978). In the absence of a model species, there may be no protection from predation (Prudic and Oliver, 2008), unless other defensive measures are present. Since *E. hainesii* is warningly colored with red body even without the presence of the model swallowtail, it strongly implies that this moth is also unpalatable,

Fig. 11.5 The red-bodied butterflies and moths. (**a**) *Pachliopta aristolochiae* female, (**b**) *Atrophaneura alcinous* female, (**c**) *Epicopeia hainesii* female, (**d**) *Histia flabellicornis* female secreting defensive foams containing linamarin (*orange arrow*). (**e**) *A. alcinous* female, (**f**) *A. alcinous* male, (**g**) *E. hainesii* male, (**h**) *H. flabellicornis* male

although their palatability is unknown. The larval host, *Cornus controversa* (Cornaceae), is not known to contain typical noxious elements such as CGs, PAs, and CNs. The moth does not seem to secrete glandular defense substance. Preliminary chemical analysis of the whole-body extracts of *E. hainesii* revealed some unidentified polar compounds on the thin-layer chromatography, which did not match with CNs such as linamarin and lotaustralin (Nishida unpublished). Further studies are needed to substantiate possible unpalatability of *E. hainesii*. There is a

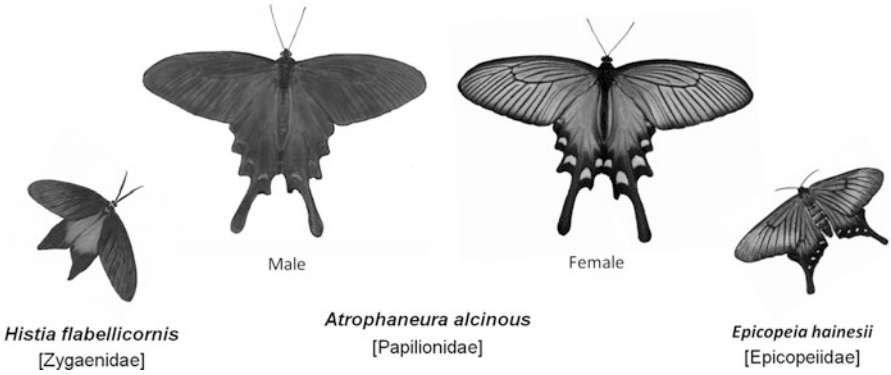

Fig. 11.6 The red-bodied swallowtail mimicry ring. Note that some species in this figure may not occur in the same habitat

spectacular array of red-bodied *Atrophaneura/Pachliopta–Epicopeia* mimicry rings distributed in East Asia further to examine in view of Batesian/Müllerian mimicry associations.

Histia flabellicornis moth (Zygaenidae) is a red-bodied diurnal moth resembling *A. alcinous* with black forewing and metallic blue hindwing coloration (larval host: *Bischofia javanica*, Euphorbiaceae) (Fig. 11.5d, h). *H. flabellicornis* is subdivided into many subspecies, and their distribution from Southeast Asia to Taiwan and Okinawa (but not inhabited in Japan's mainland) overlaps that of the red-bodied swallowtails (*Atrophaneura* and *Pachliopta*). The adults secrete toxic linamarin and hydrogen cyanide (HCN) as a foam when disturbed, suggesting the moth to be a Müllerian mimicry ally with *A. alcinous* in Okinawa (Nishida 1994). Although the degree of mimesis is imperfect in size, shape, and coloration, the wing color of *H. flabellicornis* relatively resembles males of *A. alcinous* but less resembles the females. This situation is contrary to the *A. alcinous–E. hainesii* mimicry association pattern, where the mimesis is biased to the females. The metallic blue burnish characteristic to *H. flabellicornis* hindwings may appear less similar to the *A. alcinous* male wing coloration. However, under the strong subtropical sunlight, dorsal wings of *A. alcinous* males (Fig. 11.5f) in Iriomote Island (Okinawa) shine in a metallic blue as in *H. flabellicornis* wings (Fig. 11.5h). *A. alcinous* males may have developed an implementation of structural coloration interacting with *H. flabellicornis* through visual selection by avian predators. Thus, even though the Müllerian association between these two species may be loose, the mimicking pattern may represent a rare case of sexual dimorphism in the toxic model, which might have stabilized the wing morph only in male. As illustrated in Fig. 11.6, the above two cases exemplify a symmetrical relationship of sexual dimorphism in *A. alcinous*, interacting adaptively with either one of the (putative) Müllerian mimic moths (*H. flabellicornis* and *E. hainesii*).

11.2 Discussion

As presented in those three mimicry rings, the chemistry of the unpalatable elements stored in the butterflies is the critical factor to understand the nature of aposematic wing coloration and mimicry – otherwise a conclusion of adaptive coloration must be tentative (Nishida 2002). Besides, "unpalatability" itself is hard to determine (Mallet and Joron 1999) due to the variable ecological and physiological milieus of both the preys and predators. The quality and quantities of defensive substances in presumptive model butterflies often depend on allelochemicals from the host plants, which may result in a variation in palatability, individually or among local communities, which complicates the mimicry association (Nishida 2002). Thus, Batesian and Müllerian mimicries may be interchangeable depending on the "palatability spectrum" of the prey butterflies as well as the "predatory spectrum" of the potential selective pressure (Huheey 1984; Turner 1984). The predatory spectra may involve variations in chemosensory and toxicological sensitivity/susceptibility of the predators. The sensory sensitivity in insectivorous animals may be different greatly among the species, and such variation in response to chemicals or preferences may often be seasonal particularly during highly predacious period and abundance of preys such as breeding seasons (Fink and Brower 1981; Glendinning and Brower 1990). We certainly need to know both prey/predatory spectra in time and space to understand the overall scheme of the existing mimicry rings (Joron and Mallet 1998).

Two instances of sex-limited dimorphisms were presented here in the Müllerian mimicry complexes – the tiger Danaine mimicry ring (*Argyreus hyperbius*) and the red-bodied swallowtail mimicry ring (*Atrophaneura alcinous*). In a toxic model, the diversification of its wing morphology would decrease their fitness due to a "number-dependent selection" as originally stated by Müller (Turner 1978; Mallet and Joron 1999). This widely accepted rule is not supported by the cases noted above. Such paradoxical examples are also known in *D. chrysippus* in Africa (Owen et al. 1994) and *Heliconius numata* in South America (Brown and Benson 1974).

In the *A. alcinous* (male)–*H. flabellicornis* (both sexes) co-mimicking association of the red-bodied mimicry ring, the defensive allelochemicals (AAs and CNs) fulfill the requirement of potential unpalatability that would reciprocally enhance their fitness through Müllerian mimicry. In the case of the *A. alcinous* (female)–*E. hainesii* (both sexes) co-mimicking association, the chemistry of the latter is still unclear, although the moth is suspected to be a Müllerian mimic as mentioned above. The root cause triggering female-limited wing pattern dimorphism in *A. alcinous* may be attributed to an escape from an overload of potential Batesian mimics, similar to the case of polymorphism in *D. chrysippus* in Africa under the high population density of palatable *Hypolimnas* (Smith et al. 1993). Several Rutaceae-feeding black swallowtails such as *Papilio macilentus* and *P. protenor* (females of the former are highly mimetic to *A. alcinous* males) often share the same microhabitat spatiotemporally in the middle part of Japan. Potential higher

predation on females due to behavioral vulnerability may underlie behind this mechanism (Ohsaki 1995 2005). Thus, in addition to the chemistry, further studies are warranted especially on the geographical variations of wing color in both the butterflies and moths but also on the potential interspecific impacts from co-occurring Batesian mimics.

In the *A. hyperbius* (female)–*D. chrysippus* (both sexes) co-mimicking association, both are protected by unpalatable elements (CNs, CGs, and PAs). The black-spotted wing pattern in *A. hyperbius* males resembles that of the co-occurring woodland fritillaries such as *Argynnis paphia* (silver-washed fritillary) and *Argyronome ruslana*. We have recently shown that adults (both sexes) of these fritillary species sequester CNs in their body in substantial quantities (Nakade, Naka et al. unpublished), likely to form a "leopard fritillary mimicry ring," apparently excluding *A. hyperbius* females from the ring. These chemical evidences support that sexual dimorphism is feasible not only in Batesian mimicry but also in Müllerian mimicry, if the other sexual morph is consolidated by a member of other mimetic toxic species, probably to receive better protection than staying in the same color patterns. This would invoke arguments on the sexual selection vs. natural selection. Certainly, additional work is needed to support this hypothesis.

Another type of sexually restrictive feature in the mimicry syndromes can be seen in the specific exocrine organs developed on the wings and/or body, which disseminate odoriferous substances, often accompanied by morphological differences between the sexes. Troidine males such as *A. alcinous* emit characteristic odors from androconial scales on the inner margins of the hindwings (Honda 1980), which represents a structural–chemical dimorphism. Although sex-pheromonal roles of these male-specific scents are mostly unknown, the conspicuous smell of *A. alcinous* males may be attributed to an "odor aposematism," alerting the presence of systemic toxins (AAs) to enhance its visual aposematism (Nishida and Fukami 1989).

In many *Danaus* butterfly species, males pharmacophagously accumulate specific alkaloids from PA-containing plants during adult stage and use these chemicals for their own defense as well as precursors of sex pheromone disseminated from male-specific hairpencil organs (Boppré 1984). In this case, only males become a model with defensive PAs, possibly dually protected also by CGs originating from the larval host plant, representing a sexual "chemical dimorphism" by the sequestered defense substances. In this process, females may also be indirectly protected by visual automimicry, even if they do not have any defensive chemicals (Brower 1969). In the queen butterfly, *Danaus gilippus*, a portion of male's PAs may be transferred to females during copulation as a nuptial gift potentially to protect the female and eventually to eggs and thus to ensure protection of the male's progeny (Eisner and Meinwald 1995).

In contrast, a primitive danaine, *Idea leuconoe*, acquires PAs from the apocynad host during the larval stage (both sexes), and males convert a portion of sequestered PAs to volatile pheromone components to entice females (Nishida et al. 1996). In this hairpencil pheromone system, females assess the quality of protectiveness of a male during the precopulatory behavior (Nishida 2002). PA-derived pheromone

Fig. 11.7 *Idea leuconoe* female in a typical acceptance posture, visually and chemically stimulated by a paper model of male wings with a paper disk treated with the hairpencil extract (male pheromone). The female is arrested, curling her abdomen downward

system thus plays a decisive role in sexual selection of danaine butterflies (Eisner and Meinwald 1987; Nishida 2002). In indoor behavioral tests of *I. leuconoe*, both virgin males and females visually responded to a "fluttering" paper model of *I. leuconoe* (wing image printed on the copy paper) as shown in Fig. 11.7 (Nishida et al. 1996). When the model was scented with crude extracts of hair pencils from mature males (0.1 male equivalent/paper disk), receptive females usually landed on the nearby herbage with abdomen-curling posture (Fig. 11.7). Interestingly, if a fluttering "solid white model + pheromone" was presented instead of the "patterned model + pheromone," many virgin females approached and touched the model, some occasionally exhibiting the typical mate-acceptance posture, whereas none even approached a fluttering "solid black model + pheromone" (Nishida, unpublished). This clearly indicates that the females can select males by both visual and chemical cues and in lesser degrees by vision. If this is the case in nature, non-mimetic males would also be selected by a female by chance, in that the androconial chemical stimulus is sufficient to induce her acceptance, although *Idea* butterflies are basically monomorphic. This suggests an importance of chemical factors together with visual components, which then might facilitate the evolution of a new wing pattern through sexual selection (cf. Turner 1984; Krebs and West 1988).

In addition, males of *Idea* spp. also manipulate the conspicuous white/yellow eversible tufts of hair pencils on the dorsum of the abdomen for defense, by extruding them reflexively to emit a strong odor of phenol and/or *p*-cresol together with other volatiles whenever frightened by predators (Schulz and Nishida 1996). This exemplifies a male-specific aposematic scent operating concurrently with aposematic coloration of defensive organs (Nishida et al. 1996). Interestingly, one of the Idea-mimicking swallowtails, Graphium delessertii, exhibits a conspicuous yellow mark on the inner edge of the hindwings, as though an Idea male in captivity were displaying hair pencils. This could possibly evoke an additional psychological impression upon avian predators. In this case, only males become a template for the mimic.

Batesian or Müllerian mimicry – whichever the case – the evolutionary convergence of morphological characters between the models and mimics seems to have been greatly assisted by chemical elements including wing pigments and subject, concomitantly, to both natural and sexual selections.

Acknowledgments Special thanks are due to the late Miriam Rothschild for the discussion on this subject. I thank Hiroki Takamatsu, Aya Nakade, Atsushi Wada, and Hajime Ono of Kyoto University and Hideshi Naka of Tottori University for the project on *Argyreus hyperbius*. I am grateful to H. Frederik Nijhout and Atsushi Honma for reviewing the manuscript.

References

Ackery PR, Vane-Wright RI (1984) Milkweed butterflies. British Museum (Natural History), London

Boppré M (1984) Chemically mediated interactions between butterflies. In: Vane-Wright RI, Ackery PR (eds) The biology of butterflies. Academic, London, pp 259–275

Boppré M (1986) Insects pharmacophagously utilizing defensive plant chemicals (pyrrolizidine alkaloids). Naturwissenschaften 73:17–26

Brower LP (1969) Ecological chemistry. Sci Am 220:22–29

Brower LP (1984) Chemical defence in butterflies. In: Vane-Wright RI, Ackery PR (eds) The biology of butterflies. Academic, London, pp 109–134

Brown KS, Benson WW (1974) Adaptive polymorphism associated with multiple Müllerian mimicry in *Heliconius numata* (Lepid.: Nymph.) Biotropica 6:205–228

Cohen JA (1985) Differences and similarities in cardenolide contents of queen and monarch butterflies in Florida and their ecological and evolutionary implications. J Chem Ecol 11:85–103

Edgar JA (1984) Parsonsieae: ancestral larval foodplants of the Danainae and Ithomiinae. In: Vane-Wright RI, Ackery PR (eds) The biology of butterflies. Academic, London, pp 91–93

Edgar JA, Boppré M, Schneider D (1979) Pyrrolizidine alkaloid storage in African and Australian danaid butterflies. Experientia 35:1447–1448

Eisner T, Meinwald J (1987) Alkaloid-derived pheromones and sexual selection in Lepidoptera. In: Prestwich GD, Blomquist GJ (eds) Pheromone biochemistry. Academic, Orlando, pp 251–269

Eisner T, Meinwald J (1995) The chemistry of sexual selection. Proc Natl Acad Sci U S A 92:50–55

Euw JV, Reichstein T, Rothschild M (1968) Aristolochic acid-I in the swallowtail butterfly *Pachliopta aristolochiae* (Fabr.) (Papilionidae). Isr J Chem 6:659–607

Fink LS, Brower LP (1981) Birds can overcome the cardenolide defense of monarch butterflies in Mexico. Nature 291:67–70

Glendinning JI, Brower LP (1990) Feeding and breeding responses of five mice species to overwintering aggregations of the monarch butterfly. J Anim Ecol 59:1091–1112

Gordon IJ, Smith DAS (1998) Genetics of the mimetic African butterfly *Hypolimnas misippus*: hindwing polymorphism. Heredity 80:62–69

Halpin C, Skelhorn J, Rowe C (2013) Predators' decisions to eat defended prey depend on the size of undefended prey. Anim Behav 85:1315–1321

Holzkamp G, Nahrstedt A (1994) Biosynthesis of cyanogenic glucosides in the Lepidoptera: Incorporation of [U-^{14}C]-2-methylpropanealdoxime, 2S-[U-^{14}C]-methylbutanealdoxime and D,L-[U-^{14}C]-*N*-hydroxyisoleucine into linamarin and lotaustralin by the larvae of *Zygaena trifolii*. Insect Biochem Molec Biol 24:161–165

Honda K (1980) Odor of a papilionid butterfly: odoriferous substances emitted by *Atrophaneura alcinous alcinous* (Lepidoptera: Papilionidae). J Chem Ecol 6:867–873
Honda K, Hayashi N, Abe F et al (1997) Pyrrolizidine alkaloids mediate host-plant recognition by ovipositing females of an Old World danaid butterfly, *Idea leuconoe*. J Chem Ecol 23:1703–1713
Huheey JE (1984) Warning coloration and mimicry. In: Bell WJ, Cardé RT (eds) Chemical ecology of insects. Chapman and Hall, London, pp 257–297
Inoue H (1978) Genus *Epicopeia* Westwood from Japan, Korea and Taiwan, Lepidoptera: Epicopeiidae. Tyo to Ga (Trans Le Soc Jpn) 29:69–75
Joron M, Mallet J (1998) Diversity in mimicry: paradox or paradigm. Trends Ecol Evol 13:461–466
Kim CS, Nishida R, Fukami H, Abe F, Yamauchi T (1994) 14-Deoxyparsonsianidine *N*-oxide: A pyrrolizidine alkaloid sequestered by the giant danaine butterfly, *Idea leuconoe*. Biosci Biotech Biochem 58:980–981
Krebs RA, West DA (1988) Female mate preference and the evolution of female-limited Batesian mimicry. Evolution 42:1101–1104
Mallet J, Joron M (1999) Evolution of diversity in warning color and mimicry: polymorphisms, shifting balance, and speciation. Annu Rev Ecol Syst 30:201–233
Mebs D, Reuss E, Schneider M (2005) Studies on the cardenolide sequestration in African milkweed butterflies (Danaidae). Toxicon 45:581–584
Mebs D, Wagner MG, Toennes SW et al (2012) Selective sequestration of cardenolide isomers by two species of *Danaus* butterflies (Lepidoptera: Nymphalidae: Danainae). Chemoecology 22:269–272
Nahrstedt A, Davis RH (1985) Biosynthesis and quantitative relationships of the cyanogenic glucosides, linamarin and lotaustralin, in genera of the Heliconiini (Insecta: Lepidoptera). Comp Biochem Physiol 82B:745–749
Nishida R (1994/1995) Sequestration of plant secondary compounds by butterflies and moths. Chemoecology 5(6):127–138
Nishida R (2002) Sequestration of defensive substances from plants by Lepidoptera. Annu Rev Entomol 47:57–92
Nishida R, Fukami H (1989) Ecological adaptation of an Aristolochiaceae-feeding swallowtail butterfly, *Atrophaneura alcinous*, to aristolochic acids. J Chem Ecol 15:2549–2563
Nishida R, Kim CS, Fukami H, Irie R (1991) Ideamine *N*-oxides: Pyrrolizidine alkaloids sequestered by a danaine butterfly, *Idea leuconoe*. Agric Biol Chem 55:1787–1797
Nishida R, Schulz S, Kim CS et al (1996) Male sex pheromone of the giant danaine butterfly, *Idea leuconoe*. J Chem Ecol 22:949–972
Ohsaki N (1995) Preferential predation of female butterflies and the evolution of Batesian mimicry. Nature 378:173–175
Ohsaki N (2005) A common mechanism explaining the evolution of female-limited and both-sex Batesian mimicry in butterflies. J Anim Ecol 74:728–734
Owen DF, Smith DAS et al (1994) Polymorphic Müllerian mimicry in a group of African butterflies: a reassessment of the relationship between *Danaus chrysippus, Acraea encedon* and *Acraea encedana* (Lepidoptera: Nymphalidae). J Zool 232:93–108
Prudic KL, Oliver JC (2008) Once a Batesian mimic, not always a Batesian mimic: mimic reverts back to ancestral phenotype when the model is absent. Proc R Soc B 275:1125–1132
Prudic KL, Khera S et al (2007) Isolation, identification, and quantification of potential defensive compounds in the viceroy butterfly and its larval host-plant, Carolina willow. J Chem Ecol 33:1149–1159
Reichstein T, Jv E, Parsons JA, Rothschild M (1968) Heart poison in the monarch butterfly. Science 161:861–866
Ritland DB, Brower LP (1991) The viceroy is not a Batesian mimic. Science 350:497–498
Rothschild M (1979) Mimicry, butterflies and plants. Symb Bot Upsal 22:82–99

Rothschild M, Jv E, Reichstein T et al (1975) Cardenolide storage in *Danaus chrysippus* (L.) with additional notes of *D. plexippus* (L.) Proc Roy Soc London (B) 190:1–31
Schneider D, Boppré M, Schneider H et al (1975) A pheromone precursor and its uptake in male *Danaus* butterflies. J Comp Physiol 97:245–256
Schulz S, Nishida R (1996) The pheromone system of the male danaine butterfly, *Idea leuconoe*. Bioorg Med Chem 4:341–349
Smith DAS (1973) Batesian mimicry between *Danaus chrysippus* and *Hypolimnas misippus* (Lepidoptera) in Tanzania. Nature 242:129–131
Smith DAS, Owen DF, Gordon IJ et al (1993) Polymorphism and evolution in the butterfly *Danaus chrysippus* L. (Lepidoptera: Danainae). Heredity 71:242–251
Su S, Lim M, Kunte L (2015) Prey from the eyes of predators: Color discriminability of aposematic and mimetic butterflies from an avian visual perspective. Evolution 69:2985–2994
Trigo JR (2000) The chemistry of antipredator defense by secondary compounds in neotropical Lepidoptera: facts, perspectives and caveats. J Braz Chem Soc 11:551–561
Turner JRG (1978) Why male butterflies are non-mimetic: natural selection, sexual selection, group selection, modification and sieving. Biol J Linn Soc 10:385–432
Turner JRG (1984) Mimicry: the palatability spectrum and its consequences. In: Vane-Wright RI, Ackery PR (eds) The biology of butterflies. Academic, London, pp 141–161
Uésugi K (1996) The adaptive significance of Batesian mimicry in the swallowtail butterfly, *Papilio polytes* (Insecta, Papilionidae): Associative learning in a predator. Ethology 102:762–775
Wickler W (1968) Mimicry in plants and animals. Wiedenfeld and Nicholson, London
Wu TS, Leu YL, Chan YY (2000) Aristolochic acids as a defensive substance for the aristolochiaceous plant-feeding swallowtail butterfly, *Pachliopta aristolochiae interpositus*. J Chin Chem Soc 47:221–226
Yata O, Morishita K (1985) Butterflies of the South East Asian Islands, vol II. Pieridae and Danaidae. Plapac Co Ltd, Tokyo

Chapter 12
A Model for Population Dynamics of the Mimetic Butterfly *Papilio polytes* in Sakishima Islands, Japan (II)

Toshio Sekimura, Noriyuki Suzuki, and Yasuhiro Takeuchi

Abstract Based on recent progresses of both experiment and mathematical analysis, we present an extension of the model for population dynamics of the mimetic swallowtail butterfly *Papilio polytes* in Sakishima Islands, Japan (Sekimura et al. J Theor Biol 361:133–140, 2014). The model includes four major variables, that is, population densities of three kinds of butterflies (two female forms f. *cyrus* and f. *polytes* and the unpalatable butterfly *Pachliopta aristolochiae*) and their predator. In this extension, we introduce difference in the predation rate between two forms f. *cyrus* and f. *polytes*. We still assume that both the benefit of mimicry for the mimic f. *polytes* and the cost for the model are dependent on their relative frequencies, i.e., the mortality of the mimic by predation decreases with increase in frequency of the model, while the mortality of the model increases as the frequency of the mimic increases. Taking the density-dependent effect by carrying capacity into account, we set up an extended model system consisting of three ordinary differential equations (ODEs), analyze it mathematically, and provide computer simulations that confirm the analytical results.

Keywords *Papilio polytes* • Batesian mimicry • Population dynamics • Mathematical model • Computer simulations • Relative abundance of the mimic • Sakishima Islands

T. Sekimura (✉)
Department of Biological Chemistry, Graduate School of Bioscience and Biotechnology, Chubu University, Kasugai, Aichi 487-8501, Japan
e-mail: sekimura@isc.chubu.ac.jp

N. Suzuki • Y. Takeuchi
Department of Physics and Mathematics, College of Science and Engineering, Aoyama Gakuin University, Sagamihara, Kanagawa 252-5258, Japan

T. Sekimura, H.F. Nijhout (eds.), *Diversity and Evolution of Butterfly Wing Patterns*, DOI 10.1007/978-981-10-4956-9_12

12.1 Introduction

P. polytes is a mimetic swallowtail butterfly species widely distributed across India and Southeast Asia, including Southeast of China, the Philippines, Taiwan, and the Ryukyu Islands of Japan (Clarke and Sheppard 1972). *P. polytes* exhibits the female limited polymorphism, that is, the female is polymorphic, whereas the male is monomorphic and exhibits a white bar on the black hindwing. In the Ryukyu Islands located in the southwest of Japan, the female of *P. polytes* has two different forms, the mimetic form f. *polytes* and the nonmimetic form f. *cyrus* resembling the monomorphic male in appearance. The form f. *polytes* mimics the unpalatable butterfly *Pachliopta aristolochiae* as a mimetic model, which has a large white area in the center and a row of submarginal red spots on the black hindwing (Fig. 12.1). Mimicry in the female of *P. polytes* is known to be Batesian mimicry.

Yamauchi (1994) built a population dynamic model of Batesian mimicry, in which two populations of both model and mimic species were considered. The dynamic model has two components, growth at intrinsic growth rate and carrying capacity and reduction by predation. The probability of a predator catching prey on an encounter was assumed to depend on the frequency of the mimic. He applied the dynamic model to field records of butterflies in Ryukyu Islands, and his model has successfully explained some features, e.g., multiple dynamic equilibria between the model and the mimic in the field. However, his model did not account for realistic

Fig. 12.1 The female limited polymorphism of the mimetic butterfly *Papilio polytes* and the model butterfly *Pachliopta aristolochiae*. *Top left*: *P. polytes* f. *cyrus* (nonmimetic form). *Top right*: *P. polytes* f. *polytes* (mimetic form). *Bottom left*: *P. polytes* male. *Bottom right*: the model *Pachliopta aristolochiae*

model-mimic systems such as polymorphism in *P*. *polytes* and intraspecific competition between the mimic f. *polytes* and the non-mimic f. *cyrus*.

Sekimura et al. (2014) presented a mathematical model for population dynamics of *P*. *polytes* observed in the Sakishima Islands (i.e., the Miyako Islands and the Yaeyama Islands), which are the southernmost island group of the Ryukyu Islands, Japan (Fig. 12.2). The model system consists of three ordinary differential equations (ODEs), in which variables are population densities of three butterflies, the unpalatable butterfly *P*. *aristolochiae* and two female forms of *P*. *polytes*. The model was constructed on the basis of field data in the islands and also experimental data in the laboratory. Using mathematical analysis and computer simulations of the system equations, they clarified the logical relationship hidden behind field data on the population dynamics of the mimetic butterfly *P*. *polytes* in Sakishima Islands. In particular, they discussed both temporal change in the relative abundance (RA) since 1975 in Miyako-jima Island and variation in the RA in Sakishima Islands.

Before going into details of our extended model and results, we summarize field data briefly in Sect. 12.2 and describe main features of mimicry of *P*. *polytes* in Sect. 12.3.

12.2 Field Records of *Papilio polytes* Observed in Sakishima Islands

12.2.1 Observation of Temporal Change in the Population of the Mimetic Female of P. polytes *in Miyako-jima Island*

Uesugi (1992) observed temporal change of the relative abundance of the mimic f. *polytes* in all the females of *P*. *polytes* for 14 years from 1975 to 1989 after the establishment of the model *P*. *aristolochiae* in the land. Here, the relative abundance (RA) of the mimic denotes the population ratio of f. *polytes* to all the two forms (f. *cyrus* and f. *polytes*) and is defined as follows:

$$\mathrm{RA} = \frac{\text{population of the mimic f. } \textit{polytes}}{\text{population of the non-mimic f. } \textit{cyrus} + \text{population of the mimic f. } \textit{polytes}} \times 100 \ (\%)$$

The observational result revealed that the RA increases with the date like the sigmoidal curve, and in 1985 about 10 years after starting observation, the RA reached at a saturated value (or the value of equilibrium) of about 50% (Fig. 12.5a).

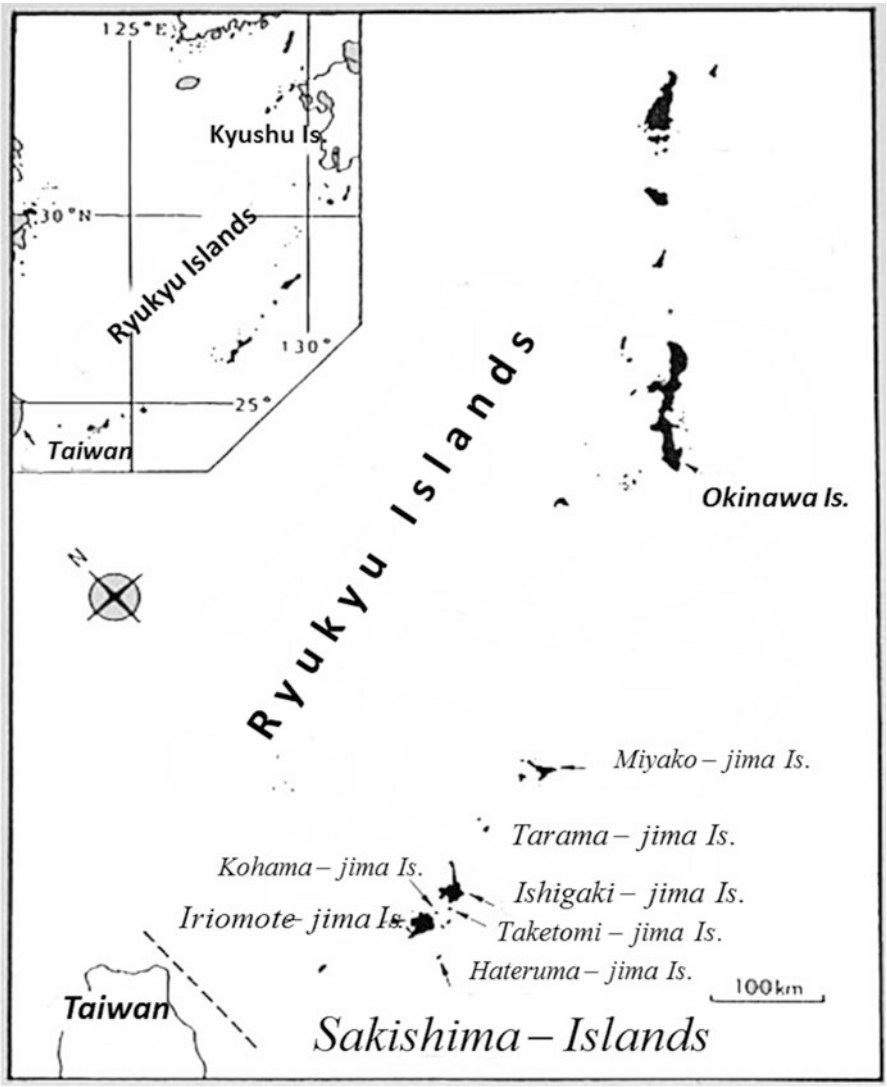

Fig. 12.2 Map of the Sakishima Islands, Japan. The Sakishima Islands are located at the southeast end of Japan and part of the Ryukyu Islands, which include both the Miyako Islands and the Yaeyama Islands. The Miyako Islands include Miyako-jima Is., Tarama-jima Is., etc., and the Yaeyama Islands include Ishigaki-jima Is., Hateruma-jima Is., Iriomote-jima Is., Taketomi-jima Is., Kohama-jima Is., etc.

12.2.2 Variation in the Relative Abundance (RA) in Sakishima Islands

Uesugi (1992) also observed variation in the RA in Sakishima Islands. In order to investigate the relationship between two populations of the model *P. aristolochiae* and the mimic f. *polytes*, he recorded three populations of the model and two female forms of *P. polytes* in seven islands from island to island in the Sakishima Islands in 1982, 14 years after the establishment of the model in the Yaeyama Islands. The horizontal axis in Fig. 12.5b shows the advantage index (AI) of Batesian mimicry, which is defined to be the population ratio of the model to all the related butterflies as follows:

$$\mathrm{AI} = \frac{\text{population of the model}}{\text{population of the model} + \text{populations of f. } cyrus \text{ and f. } polytes} \times 100 \ (\%)$$

The vertical axis in Figs. 12.5a and 12.5b is the relative abundance (RA), which denotes the population rate of the form f. *polytes* to all two forms (f. *cyrus* and f. *polytes*).

Field data, which is shown by solid circles in Fig. 12.5b, clearly shows the positive correlation between the AI and the RA, which means that the higher the population ratio of the model butterfly in an island, the higher the ratio of the mimetic female to all females in the island.

12.3 Extended Mathematical Model for Population Dynamics of *P. polytes*

We first summarize fundamental facts on the mimicry, which will allow us to design the content of the mathematical model of three variables, that is, three kinds of populations of the model *P. aristolochiae*, the mimic f. *polytes*, and the non-mimic f. *cyrus*.

12.3.1 Fundamental Facts on the Mimicry of P. polytes

12.3.1.1 Difference in Predation Risk Between Two Forms f. *polytes* and f. *cyrus*

The butterfly *P. polytes* has two female forms: one is the non-mimic f. *cyrus* that resembles the monomorphic male with a white bar on the black hindwing, while the other is the mimic f. *polytes* that resembles the unpalatable butterfly species *P. aristolochiae* (Fig.12.1). The mimetic form f. *polytes* is considered to have an

advantage over f. *cyrus* with respect to protection from predation, when it lives in sympatry with the model *P. aristolochiae*. In reality, Uesugi (1996) examined the idea positively by learning experiments. Unexperienced birds, brown-eared bulbuls, *Hypsipetes amaurotis oryeri* as predators, were first trained to take food from two feeders in a cavity and then offered *P. aristolochiae* in one of the feeders. After experiencing an uncomfortable encounter with this butterfly, the birds reduced the frequency of taking regular food from the feeder where the butterfly had been placed. On the other hand, Ohsaki (1995) paid attention to the rates of beak marks by predators on wings of both palatable and unpalatable butterflies. By analyzing the number of beak marks on butterfly wings caught in Borneo, he found that by comparing the species *P. polytes* and the model species *P. aristolochiae*, nonmimetic females were selectively attacked, while males, mimetic females, and models were attacked less. Thus, the mimic f. *polytes* is considered to gain benefit of reduced predation risk by living in sympatry with the model *P. aristolochiae*.

However, we should note an experimental result on survival rates of the mimetic form f. *polytes*, the nonmimetic form f. *cyrus*, and male in Taketomi-jima Is., where the model *P. aristolochiae* and the mimetic female f. *polytes* are both absent (Uesugi 1997). Uesugi (1997) used a releasing and re-catching method, that is, he released at first 300 butterflies into the field and then caught again released butterflies day after day for a week in the field. The result was remarkable, that is, the survival rate of the mimetic f. *polytes* was statistically significantly lower than those of the nonmimetic f. *cyrus* and male. This means that the mimetic f. *polytes* has received an apparent disadvantage for survival in Taketomi-jima Is. in comparison with the nonmimetic f. *cyrus* and male.

12.3.1.2 Males Prefer the Non-mimic f. *cyrus* to the Mimic f. *polytes*?

The mimetic female f. *polytes* might be less distinguishable than the nonmimetic female f. *cyrus* by the male, because the form f. *polytes* resembles a different species *P. aristolochiae*, while the form f. *cyrus* resembles the male of the same species. This means that f. *cyrus* could get more chances to mate with the male than f. *polytes*. In reality, Uesugi (1997) counted mating times of young butterflies of both f. *cyrus* and f. *polytes* just after emergence. The result was striking to show that f. *polytes* had no approach from the male and no count, while f. *cyrus* could mate with the male. From the viewpoint of making offspring, the non-mimic f. *cyrus* has an advantage over the mimic f. *polytes*. Thus, viewing from the preference of the male to females in the species, the mimicry is not always beneficial.

12.3.1.3 Physiological Life Span of Two Forms f. *cyrus* and f. *polytes*

Ohsaki (2005) measured physiological life spans of flying three types (the male, the non-mimic f. *cyrus*, and the mimic f. *polytes*) in Itami City Museum of Insects, Japan, and found that the order of the life span length is as follows: f. *cyrus* > the male > f. *polytes*. The problem is why the life span of the mimic f. *polytes* is the shortest. To explain the reason, Ohsaki proposed a hypothesis that the mimic f. *polytes* pays an additional cost for producing red colored pigments (carotenoid) by activating biochemical reaction networks in cells. The hypothesis coincides with the result that the bigger the red colored area on the wing that the butterfly has, the shorter the physiological life span that the butterfly has.

On the other hand, by using *P*. *polytes* caught in Okinawa Island, Kinjyo (2000) showed that the physiological life span of f. *cyrus* and f. *polytes* is dependent on the feeding condition. For example, there is no statistically significant difference in the life span when both f. *cyrus* and f. *polytes* are fed in a good condition, under which honey is given every day (i.e., the mean life span, 23.5 days for f. *cyrus* and 22 days for f. *polytes*, respectively). When butterflies are fed in other conditions, under which plain water or no honey is given, mean life spans of the non-mimic f. *cyrus* become 8.8 days (with plain water) and 5.3 days (with no food), and those of the mimic f. *polytes* become 7.8 days (with plain water) and 4.6 days (with no food), respectively. This result shows that in nature, when environmental condition or food conditions (e.g., long rainy weather, dry weather) become worse, the life span of both f. *cyrus* and f. *polytes* becomes shorter rapidly. In any case, the result shows that the life span of f. *cyrus* is somewhat longer than that of f. *polytes*.

For the last several years, Sekimura measured the life span of both f. *cyrus* and f. *polytes* in the laboratory and found that in a regular condition at 25 °C room temperature, there was no statistically significant difference in the life span of both f. *cyrus* and f. *polytes* under different feeding conditions (Fig. 12.3).

12.3.2 *Mathematical Model of Three ODEs for Population Dynamics of* P. polytes *with Intraspecific Competition*

In order to analyze field data summarized in Sect. 12.2, we present here a mathematical model for population dynamics of *P*. *polytes*. The model system consists of three ordinary differential equations (ODEs), in which variables are population densities of three butterflies, the unpalatable butterfly *P*. *aristolochiae* and two female forms of *P*. *polytes*. The male of *P*. *polytes* is not included directly in the system but included indirectly through parameter values such as intraspecific competition coefficients.

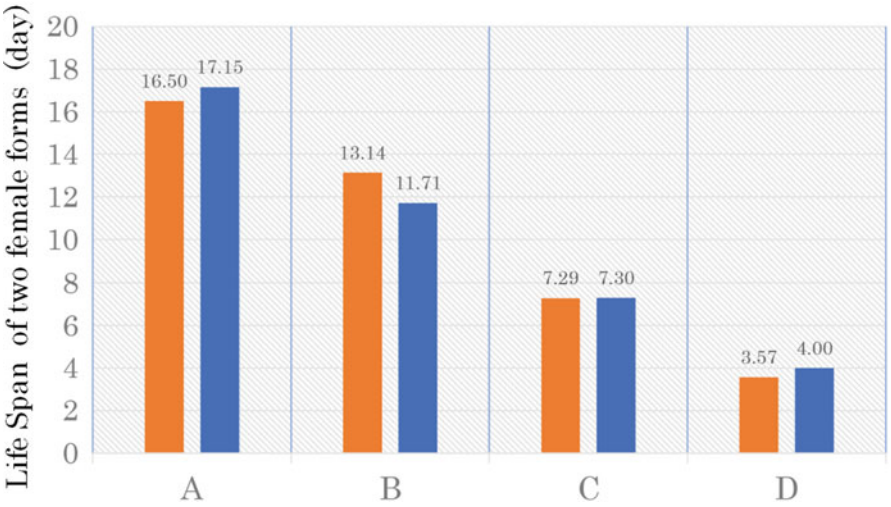

Fig. 12.3 Phylogenetic life span of two female forms f. *cyrus* and f. *polytes* under the feeding condition. The horizontal axis indicates the feeding condition. "A" is the condition under which Calpis (or Calpico) water (i.e., Japanese milk-based soft drink) is given twice a day; "B" is the condition under which the Calpis water with doubling dilution is given twice a day; "C" is the condition under which only water is given twice a day; "D" is the condition under which nothing is given after hatching. The left side (*orange-colored*) column of each condition corresponds to the average life span of f. *cyrus*, and the right side (*blue colored column*) is that of f. *polytes*. The number upon each column indicates the average life span. For example, the number 16.50 upon the left column of the condition "A" is the average life span (days) of 10 (f. *cyrus*) individuals. Numbers of individuals used in the experiment are as follows: numbers of (f. *cyrus*) individuals, 10 for the feeding condition "A," 7 for "B," 14 for "C," and 14 for "D," respectively, and numbers of (f. *polytes*) individuals: 13 for the feeding condition "A," 7 for "B," 10 for "C," and 10 for "D," respectively. According to our statistical analysis of the data, there is no statistically significant difference in the physiological life span between two forms f. *cyrus* and f. *polytes* for all feeding conditions A–D. In contrast, the data analysis has made it clear that there exists statistically significant effect of the feeding condition (*A–D*) on difference in the life span

We denote four population densities of the model *P. aristolochiae*, the mimic f. *polytes*, the non-mimic f. *cyrus*, and predator as n_1, n_2, n_3, and p, respectively. Changes of the densities in time become the following three ODEs:

$$\frac{dn_1}{dt} = n_1\left\{r_1\left(1-\frac{n_1}{K_1}\right) - \alpha\left(\frac{n_2}{n_1+n_2}\right)p\right\} \tag{12.1}$$

$$\frac{dn_2}{dt} = n_2\left\{r_2\left(1-\frac{n_2+a_{23}n_3}{K_2}\right) - \beta_2\left(\frac{n_2}{n_1+n_2}\right)p\right\} \tag{12.2}$$

$$\frac{dn_3}{dt} = n_3\left\{r_3\left(1-\frac{n_3+a_{32}n_2}{K_3}\right) - \beta_3 p\right\} \tag{12.3}$$

where the population density of predator p is given as a fixed parameter value. In the system Eqs. (12.1), (12.2), and (12.3), we evaluated the density effect or saturation effect by using carrying capacities K_1, K_2, K_3 $(=K_2)$ for *P. aristolochiae*, f. *polytes*, and f. *cyrus,* respectively. We assume that K_2, K_3 have the same value since both f. *polytes* and f. *cyrus* are females in the same species. Growth rates of three butterflies are denoted by r_1, r_2, r_3, respectively. In Eqs. (12.2) and (12.3), we introduced an intraspecific competition between f. *polytes* and f. *cyrus* through competition coefficients (a_{23}, a_{32}). The intraspecific competition effect includes competitions for resources such as nectar and indirectly the male as noted in Sect. 12.3.1.2. The term $(n_2/(n_1+n_2))$ multiplied by p in Eqs. (12.1) and (12.2) represents the effect of mimicry, that is, the negative density effect implying that the increase in the density of f. *polytes* n_2 causes the decrease in both densities of *P. aristolochiae* and f. *polytes*, n_1 and n_2. Parameters α, β_2, β_3 represent difference in the predation rate among *P. aristolochiae*, *P. polytes* f. *polytes*, and f. *cyrus,* respectively, and it would be reasonable to assume the inequality $\alpha < \beta_2, \beta_3$, because *P. aristolochiae* is an unpalatable butterfly species. In Sect. 12.3.1.1, we noted the result on beak marks by predators showing that nonmimetic females were selectively attacked, while males, mimetic females, and model butterflies were attacked less. This fact is evaluated mathematically in the second term of Eqs. (12.2) and (12.3) by multiplying p by $(n_2/(n_1+n_2))$ (<1) for the mimic f. *polytes*, while by 1 for the non-mimic f. *cyrus*.

12.4 Mathematical Analysis of the System Equations and Computer Simulations

12.4.1 Mathematical Analysis

Based on discussions in Sect. 12.3.1, we consider and analyze mathematically the following three cases of the system Eqs. (12.1), (12.2), and (12.3) classified by growth rate and predation rate of two forms f. *polytes* and f. *cyrus*: (a) case 1, $r_2 < r_3$ and $\beta_2 = \beta_3 (=\beta)$; (b) case 2, $r_2 = r_3$ and $\beta_2 > \beta_3$; and (c) case 3, $r_2 = r_3$ and $\beta_2 = \beta_3 (=\beta)$.

12.4.1.1 Case 1: $r_2 < r_3$ and $\beta_2 = \beta_3 (=\beta)$

This is just the case that was analyzed in our previous paper (Sekimura et al. 2014), where following inequalities were assumed, $r_2 < r_3$, i.e., (growth rate of f. *polytes*) < (growth rate of f. *cyrus*), and $\alpha < \beta$, i.e., (predation rate of *P. aristolochinae*) < (predation rate of f. *polytes*).

We put one more assumption on the survival of f. *cyrus*, $r_3 > \beta p$, i.e., the growth rate of f. *cyrus* is larger than the predation rate. Note that the population n_3 tends to zero when $r_3 \leq \beta p$, since $\mathrm{d}n_3/\mathrm{d}t \leq 0$.

We summarize here main analytical results and computer simulations by solving the system Eqs. (12.1), (12.2), and (12.3).

[Result C1-1] The change of relative abundance (RA) of the mimic in the female of *P. polytes* with respect to the carrying capacity K_1 of the model is positive, that is,

$$\frac{d}{\mathrm{d}K_1}\left(\frac{n_2}{n_2+n_3}\right) = \frac{\mathrm{d}(RA)}{\mathrm{d}K_1} > 0 \tag{12.4}$$

[Result C1-2] The change of the advantage index (AI) with respect to the carrying capacity K_1 of the model is positive:

$$\frac{d}{\mathrm{d}K_1}\left(\frac{n_1}{n_1+n_2+n_3}\right) = \frac{\mathrm{d}(AI)}{\mathrm{d}K_1} > 0 \tag{12.5}$$

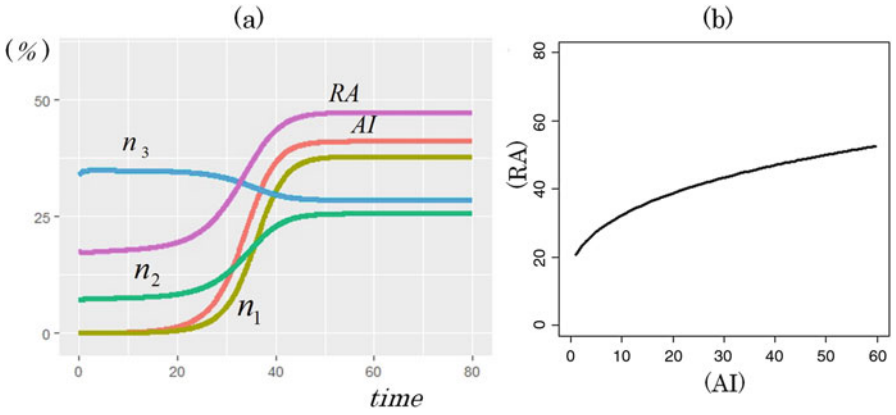

Fig. 12.4 Simulation results on temporal changes of all related quantities
(**a**) The *blue line* denotes the population density n_3 of the non-mimic f. *cyrus*, the *green line* is the density n_2 of the mimic f. *polytes*, the *purple line* is the RA, the *orange line* is the AI, and the *ocher line* denotes the density n_1 of the model *P. aristolochiae*, respectively. Parameter values used in numerical simulations are as follows, and the stability condition for the positive equilibrium is satisfied with these parameter values:
$r_1 = 0.5, r_2 = 1.0, r_3 = 2.0; K_1 = 50, K_2 = 50; a_{23} = {}^{23}0.5, a_{32} = 0.35; p = 0.5; \alpha = 0.6, \beta_2 = \beta_3 = 1.0; n_{10} = 0.01, n_{20} = 7.2, n_{30} = 34$ (initial values)
(**b**) Numerical simulation results of the positive dependence of the RA on the AI. Parameter values used in the numerical simulation are all the same as in Fig. 12.4a

From inequalities (12.4) and (12.5), we see that the ratio of change of the relative abundance (RA) to change of the advantage index (AI) with respect to the carrying capacity K_1 of the model is also positive:

$$\frac{d(RA)}{dK_1} / \frac{d(AI)}{dK_1} > 0 \tag{12.6}$$

The inequality (12.6) provides the analytical evidence for the field record on the positive dependence of the RA on the AI in Sakishima Islands in Fig.12.5b (Uesugi 1992) noted in Sect. 12.2.2.

Parameter values used in numerical simulations of Figs. 12.4, 12.5a and 12.5b are chosen as follows, so as to satisfy the existence and stability condition for the equilibrium of all the three population densities $E_{123} = (n_1, n_2, n_3)$, $r_1 = 0.5$, $r_2 = 1.0$, $r_3 = 2.0$, $K_1 = 50$, $K_2 = 50$, $a_{23} = 0.5$, $a_{32} = 0.35$, $p = 0.5$, $\alpha = 0.6$, $\beta = 1.0$, $n_{10} = 00.1$, $n_{20} = 7.2$, and $n_{30} = 34$, where n_{i0} denotes the initial value of n_i.

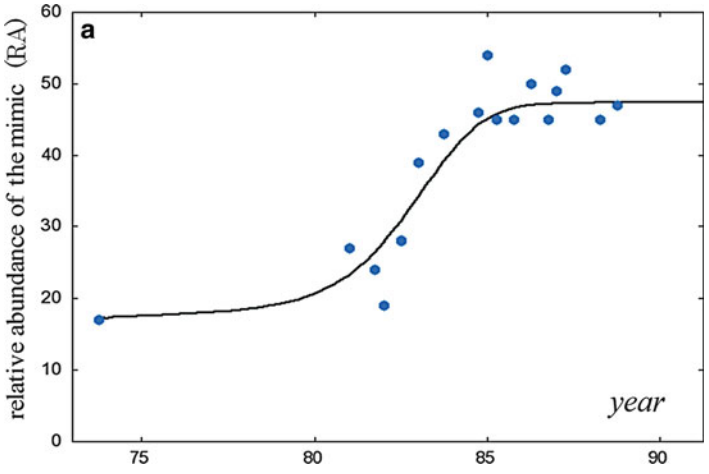

Fig. 12.5a Temporal change in the population of the mimetic female of *P. polytes* on Miyako-jima Island and its numerical simulation results

Solid circles (●) show temporal change in the relative abundance (RA) of the mimetic form f. *polytes* to all the females of *P. polytes* for 14 years after the establishment of the model *P. aristolochiae* on Miyako-jima Is. in 1975. The *solid line* shows numerical simulation results of temporal change in the RA by use of the Eqs. (12.1), (12.2), and (12.3). Parameter values used in numerical simulations are all the same as in Fig. 12.4a, and the stability condition for the positive equilibrium is satisfied with these parameter values:

$r_1 = 0.5, r_2 = 1.0, r_3 = 2.0; K_1 = 50, K_2 = 50; a_{23} = {}^{23}0.5, a_{32} = 0.35; p = 0.5; \alpha = 0.6, \beta_2 = \beta_3 = 1.0; n_{10} = 0.01, n_{20} = 7.2, n_{30} = 34$ (initial values)

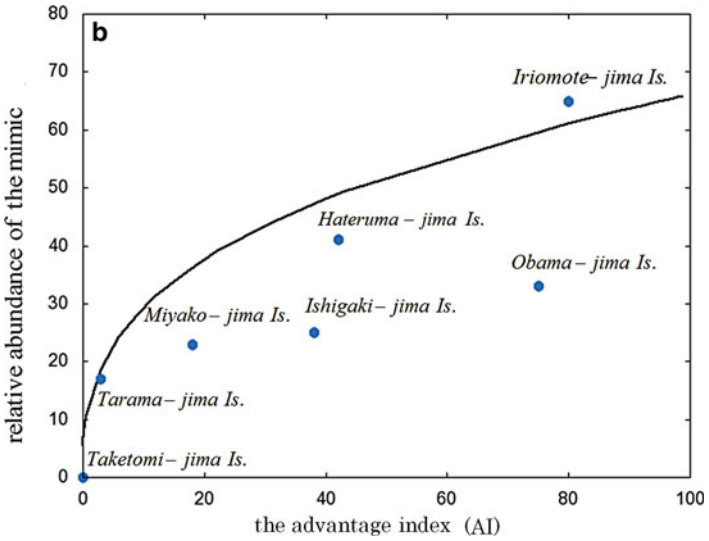

Fig. 12.5b Variation in the relative abundance (RA) in Sakishima Islands and its numerical simulation results

The horizontal axis shows the advantage index (AI), which is defined as the number ratio of the model to all the related butterflies (the model and two female forms of *P. polytes*). The vertical axis is the relative abundance (RA). *Solid circle* (●) represents the RA corresponding to the AI on each Island of 7 Islands (i.e., Taketomi-jima Is., Tarama-jima Is., Miyako-jima Is., Ishigaki-jima Is., Hateruma-jima Is., Obama-jima Is., and Iriomote-jima Is.) in Sakishima Islands (From Uesugi 1992). The *solid line* (i.e., Fig. 12.4b) represents numerical simulation results by use of the Eqs. (12.1), (12.2), and (12.3), which clearly show the positive dependence of the RA on the AI with a convexity. The inequality (6), which is an analytical result of the system equations, provides the theoretical basis on the positive dependence. Parameter values used in the numerical simulation are all the same as in Fig. 12.5a.

12.4.1.2 Case 2: $r_2 = r_3$ and $\beta_2 > \beta_3$

This is the case corresponding to experimental results noted in the last paragraphs of Sects. 12.3.1.3 and 12.3.1.1, that is, (a) there is no statistically significant difference in the life span of both f. *cyrus* and f. *polytes* (i.e., $r_2 = r_3$), and (b) the survival rate of mimetic f. *polytes* is statistically significantly lower than that of nonmimetic f. *cyrus* (i.e., $\beta_2 > \beta_3$) (this result was obtained by an experiment in Taketomi-jima Is. (Uesugi 1997), where the model *P. aristolochiae* and the mimetic female f. *polytes* are both absent) (Uesugi 1991, 1992).

[Result C2-1] First consider the system Eqs. (12.1), (12.2), and (12.3) under the condition $n_{10} = 0, n_{20} > 0$ and $n_{30} > 0$. The setting of initial parameter values corresponds to the situation of Taketomi-jima Is. The uniqueness of the solution of the system implies that $n_1(t) = 0, n_2(t) > 0$ and $n_3(t) > 0$ for any $t > 0$. Then the solution $n_2(t)$ and $n_3(t)$ satisfies

$$\frac{dn_2}{dt} = n_2\left\{r_2 - \beta_2 p - r_2\left(\frac{n_2 + a_{23}n_3}{K_2}\right)\right\} \tag{12.7}$$

$$\frac{dn_3}{dt} = n_3\left\{r_3 - \beta_3 p - r_3\left(\frac{n_3 + a_{32}n_2}{K_3}\right)\right\}, \tag{12.8}$$

which is a traditional Lotka-Volterra competition model. Suppose that $r_i > \beta_i p$ for i = 2, 3 (otherwise species i always tends to zero). It is easy to show that:

1. $n_2(t) \to 0$ for any $n_{20} > 0$ and $n_{30} > 0$, when

$$a_{23} > \frac{1 - \beta_2 p/r_2}{1 - \beta_3 p/r_3} \quad \text{and} \quad a_{32} < \frac{1 - \beta_3 p/r_3}{1 - \beta_2 p/r_2} \tag{12.9}$$

2. $n_2(t) \to 0$ for some $n_{20} > 0$ and $n_{30} > 0$, when

$$a_{23} > \frac{1 - \beta_2 p/r_2}{1 - \beta_3 p/r_3} \quad \text{and} \quad a_{32} > \frac{1 - \beta_3 p/r_3}{1 - \beta_2 p/r_2}. \tag{12.10}$$

Mathematically we can prove that the equilibrium point $E_3 = \left(0, \frac{K_3}{r_3}(r_3 - \beta_3 p)\right)$ is globally stable for system (12.7) and (12.8) under the condition (12.9). Also E_3 and $E_2 = \left(\frac{K_2}{r_2}(r_2 - \beta_3 p), 0\right)$ are locally stable under (12.10). Note that under the parameter values for case 1,

$$a_{23} < \frac{1 - \beta_2 p/r_2}{1 - \beta_3 p/r_3} \quad \text{and} \quad a_{32} > \frac{1 - \beta_3 p/r_3}{1 - \beta_2 p/r_2} \tag{12.11}$$

are satisfied, and f. *polytes* and f. *cyrus* can coexist at the positive equilibrium point when *P. aristolochiae* is absent.

[Result C2-2] Now let us choose the parameter values for case 2 as $r_1 = 0.5$, $r_2 = 1.0$, $r_3 = 1.0$, $K_1 = 50$, $K_2 = 50$, $a_{23} = 1$, $a_{32} = 0.3$, $p = 0.5$, $\alpha = 0.6$, $\beta_2 = 0.8$, $\beta_3 = 0.7$, $n_{10} = 0.01$, $n_{20} = 1$, *and* $n_{30} = 34$. This case corresponds to an expectation of the population dynamics of butterflies after introducing the model *P. aristolochiae* into Taketomi-jima Is. The different choices between this case 1 are $r_2 = r_3 = 1.0$, $\beta_2 > \beta_3$, and the smaller initial value for f. *polytes*, since the above parameters satisfy condition (12.9) and only f. *cyrus* remains when *P. aristolochiae* is absent. Figure 12.6a shows that the introduction of the model yields the stable coexistence of *P. aristolochiae*, f. *polytes*, and f. *cyrus*. Further Fig. 12.6b shows the positive dependence of the RA and the AI.

[Result C2-3] The above results imply that the qualitative properties obtained for case 1 still hold true for case 2.

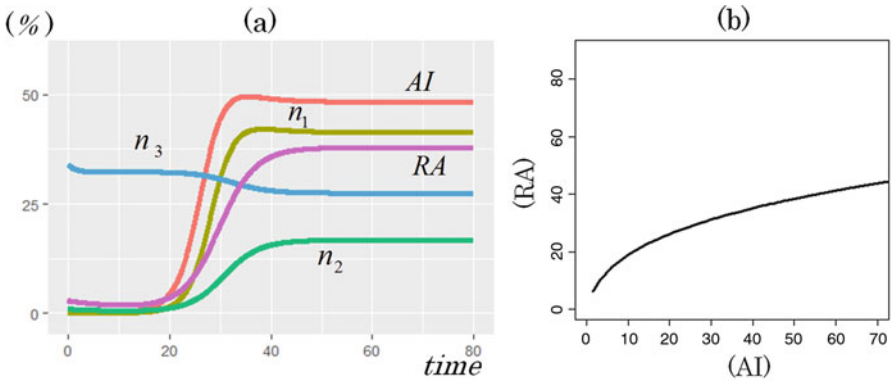

Fig. 12.6 Simulation results on temporal changes of all related quantities
(**a**) The *blue line* denotes the population density n_3 of the non-mimic f. *cyrus*, the *green line* is the density n_2 of the mimic f. *polytes*, the *purple line* is the RA, the *orange line* is the AI, and the *ocher line* denotes the density n_1 of the model *P. aristolochiae*, respectively. Parameter values used in numerical simulations are as follows, and the stability condition for the positive equilibrium is satisfied with these parameter values:
$r_1 = 0.5, r_2 = 1.0, r_3 = 1.0; K_1 = 50, K_2 = 50; a_{23} = {}^{23}1, a_{32} = 0.3; p = 0.5; \alpha = 0.6, \beta_2 = 0.8, \beta_3 = 0.7; n_{10} = 0.01, n_{20} = 1, n_{30} = 34$ (initial values)
(**b**) Numerical simulation results of the positive dependence of the RA on the AI. Parameter values used in the numerical simulation are all the same as in Fig. 12.6a

12.4.1.3 Case 3: $r_2 = r_3$ and $\beta_2 = \beta_3$ ($=\beta$)

Now consider case 3. We adopt the parameter values $a_{23} = 1.1$, $a_{32} = 0.1$, $\beta = 1$ and the same values for the remaining as case 2. Similar case 2, the parameters satisfy condition (12.9). Figure 12.7 shows the similar property as Fig. 12.6.

Finally, we note mathematical results in a compact way in Sect. 12.4 as follows,

Let us define the right-hand sides of the inequality in (12.9), (12.10), and (12.11) as

$$a_{23}^c = \frac{1 - \beta_2 p/r_2}{1 - \beta_3 p/r_3} \quad \text{and} \quad a_{32}^c = \frac{1 - \beta_3 p/r_3}{1 - \beta_2 p/r_2}. \tag{12.12}$$

It is easy to check that $a_{23}^c = a_{32}^c = 1$ for case 3 and $a_{23}^c < 1, a_{32}^c > 1$ for case 1 and 2.Since the condition $a_{23} > a_{23}^c$ implies that f. *polytes* goes extinct under the competition with f. *cyrus* ($n_2(t) \to 0$) when *P. aristolochiae* is absent, both cases 1 and 2 enlarge the possibility for the extinction of f. *polytes* when *P. aristolochiae* is absent. The results obtained in Sect. 12.4 show that f. *polytes* can coexist with f. *cyrus* under the invasion of *P. aristolochiae* even f. *polytes* has disadvantageous property as case 1 (relatively small intrinsic growth rate) or case 2 (relatively small survival rate under that predation). Note that the same result can be obtained the case where $\frac{\beta_2}{r_2} > \frac{\beta_3}{r_3}$.

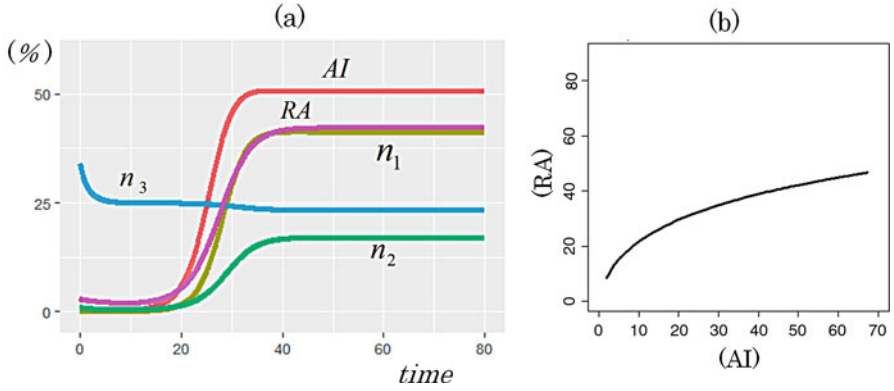

Fig. 12.7 Simulation results on temporal changes of all related quantities
(**a**) The *blue line* denotes the population density n_3 of the non-mimic f. *cyrus*, the *green line* is the density n_2 of the mimic f. *polytes*, the *purple line* is the RA, the *orange line* is the AI, and the *ocher line* denotes the density n_1 of the model *P. aristolochiae*, respectively. Parameter values used in numerical simulations are as follows, and the stability condition for the positive equilibrium is satisfied with these parameter values:

$r_1 = 0.5, r_2 = 1.0, r_3 = 1.0; K_1 = 50, K_2 = 50; a_{23} = {}^{23}1.1, a_{32} = 0.1; p = 0.5; \alpha = 0.6, \beta_2 = \beta_3 = 1.0; n_{10} = 0.01, n_{20} = 1, n_{30} = 34$ (initial values)
(**b**) Numerical simulation results of the positive dependence of the RA on the AI. Parameter values used in the numerical simulation are all the same as in Fig. 12.7a

12.5 Summary and Discussions

Based on new experimental results, we presented an extension of the model for population dynamics of the mimetic butterfly *P. polytes* in Sakishima Islands, Japan (Sekimura et al. 2014). We introduced here difference in the predation rate between two female forms f. *polytes* and f. *cyrus* by parameters β_2, β_3, respectively. The new model system (12.1), (12.2), and (12.3) still includes three major effects: (a) self-density effect by carrying capacity; (b) mimetic effect, that is, the probability that a predator attacks prey on an encounter is proportional to the relative frequency of the mimic among the model and the mimic; and (c) intraspecific competition between two forms f. *polytes* and f. *cyrus* for resources such as nectar and, indirectly, the male. As to growth rate and predation rate, we took account two cases ($r_2 < r_3$) and ($r_2 = r_3$) into consideration and assumed the inequality $\alpha < \beta_2, \beta_3$ among predation rates of the model *P. aristolochiae*, f. *polytes*, and f. *cyrus*, respectively.

Using mathematical analysis and computer simulations of the system equations, we extended the possibility of the logical relationship on the population dynamics

of the mimetic butterfly *P. polytes* in Sakishima Islands. In particular, we discussed both temporal change in the relative abundance (RA) and variation in the RA in Sakishima Islands. We estimated conditions for existence of equilibrium solutions of butterfly populations by making a comparison between experimental results and mathematical analyses of the model equations. Our results show that one of key factors to understand field data is the carrying capacity K_1 of the model in each island. The positive dependence of the RA on the AI originates from the result that changes of both the relative abundance (RA) and the advantage index (AI) with respect to the carrying capacity K_1 are positive.

The results in Sect. 12.4 have shown that both cases with respect to production rate: ($r_2 < r_3$) and ($r_2 = r_3$) could be possible to reproduce experimental data on the population dynamics of the mimetic butterfly *P. polytes* in Sakishima Islands. The first case: ($r_2 < r_3$) means that the mimicry of *P. polytes* requires a kind of genetic change in production rate of the mimetic form f. *polytes* to reproduce the data. On the other hand, the second case ($r_2 = r_3$) means that in order to reproduce the data, changes in ecological factors such as intraspecific competition coefficients (a_{23}, a_{32}) and predation rate β_2, β_3 are required for the mimicry of *P. polytes* without any genetic change. We think that it is not enough to determine at the moment which case is the real case that occurred in Sakishima Islands, because experiments on butterflies in both the field and the laboratory are somewhat subtle. We hope that much reliable experiments will be done to understand the reality in the future.

Finally, we hope that the mathematical analysis and computer simulations in the paper provide the theoretical basis on the female limited polymorphism of *P. polytes* in Sakishima Islands.

References

Clarke CA, Sheppard PM (1972) The genetics of the mimetic butterfly *Papilio Polytes* L. Proc R Soc Lond B 263:431–458

Kinjyou A (2000) Mimetic relationship in swallowtail butterflies in the Ryukyus. Nat Insects 36 (12):24–27 (In Japanese)

Ohsaki N (1995) Preferential predation of female butterflies and the evolution of batesian mimicry. Nature 378:173–175

Ohsaki N (2005) A common mechanism explaining the evolution of female-limited and both-sex Batesian mimicry in butterflies. J Anim Ecol 74:728–734

Sekimura T, Fujihashi Y, Takeuchi Y (2014) A model for population dynamics of the mimetic butterfly *Papilio polytes* in the Sakishima Islands, Japan. J Theor Biol 361:133–140

Uesugi K (1991) Temporal changes in records of the mimetic butterfly *Papilio polytes* with establishment of its model *Pachiliopta aristolochiae* in the Ryukyu Islands. Jpn J Ent 59 (1):183–198

Uesugi K (1992) Polymorphism of the mimetic butterfly *Papilio Polytes*, L. Insectalium 22:4–10. (In Japanese)

Uesugi K (1996) The adaptive significance of Batesian mimicry in the butterfly, *Papilio Polytes* (Insecta, Papilionidae): Associative learning in a predator. Ethology 102:762–775
Uesugi K (1997) Iden 51(2):68–71 (In Japanese)
Yamauchi A (1994) A population dynamic model of the Batesian mimicry. Res Popul Ecol 53:295–315

Chapter 13
Evolutionary Trends in Phenotypic Elements of Seasonal Forms of the Tribe Junoniini (Lepidoptera: Nymphalidae)

Jameson W. Clarke

Abstract Seasonal polyphenism in insects is the phenomenon whereby multiple phenotypes can arise from a single genotype depending on environmental conditions during development. Many butterflies have multiple generations per year, and environmentally induced variation in wing color pattern phenotype allows them to develop adaptations to the specific season in which the adults live. Elements of butterfly color patterns are developmentally semiautonomous allowing for detailed developmental and evolutionary changes in the overall color pattern. This developmental flexibility of the color pattern can result in extremely diverse seasonal phenotypes in a single species. In this study, we asked the following questions: (a) How do wing phenotype elements such as shape and pattern vary between seasonal forms? (b) Can this variation be explained phylogenetically? (c) If so, what are the various pattern development strategies used to achieve crypsis in the dry season form? To answer these questions, we used high-resolution images to analyze pattern element variation of 34 seasonally polyphenic butterfly species belonging to the tribe Junoniini (Lepidoptera: Nymphalidae). We show that forewing shape and eyespot size both vary seasonally and that the methods by which phenotype elements change in the dry season forms are different in different clades and may therefore have independent and diverse evolutionary origins.

Keywords Polyphenism • Seasonal polyphenism • Shape polyphenism • Color pattern • Pattern evolution • Pattern element • Junoniini • *Junonia* • *Precis*

13.1 Introduction

Seasonal polyphenism in insects is the phenomenon whereby multiple phenotypes can arise from a single genotype depending on environmental conditions during development. Brakefield and Shapiro more formally define seasonal polyphenism

J.W. Clarke (✉)
Department of Biology, Duke University, Durham, NC 27705, USA
e-mail: jameson.clarke@duke.edu

T. Sekimura, H.F. Nijhout (eds.), *Diversity and Evolution of Butterfly Wing Patterns*, DOI 10.1007/978-981-10-4956-9_13

as the expression of a repeating pattern of changing phenotypes under the control of some environmental factor (Brakefield et al. 1996). Many butterflies have multiple generations per year, and environmentally induced variation in wing color pattern allows them to develop adaptations to the specific season in which the adults live. For example, when predators and prey are both plentiful during the spring or wet season, large striking eyespots may serve to deter or deflect predators (Prudic et al. 2015). In contrast, during the autumn or dry season when prey are scarce, having large striking eyespots might increase the chances of being detected by a predator, and benefit may be obtained by a more cryptic coloration (Brakefield and Larsen 1984).

Because it is potentially adaptive to have specialized forms for predictable environmental heterogeneity, seasonal polyphenism is not uncommon and is most often seen in families Hesperiidae, Lycaenidae, Pieridae, and of course Nymphalidae (Brakefield and Larsen 1984). The elements of butterfly color patterns are developmentally semiautonomous allowing for detailed developmental and evolutionary changes in the overall color pattern (Nijhout 1991). This developmental flexibility of the color pattern can result in extremely diverse seasonal phenotypes within and among species. Seasonal forms of some species, such as *Precis octavia*, can be so different that they were thought to be a distinct species prior to laboratory experiments that demonstrated that alternative color patterns could be induced by rearing the larvae under varying conditions of temperature and photoperiod (McLeod 1968).

Although the genetic, developmental, and hormonal control of seasonal polyphenism are becoming increasingly understood, there are relatively few studies that examine the evolution of the pattern elements of seasonal forms (Rountree and Nijhout 1995; Monteiro et al. 2015; Oostra et al. 2011). Therefore we asked the following questions: (a) How do wing phenotype elements such as shape and pattern differ between seasonal forms? (b) Can this variation be explained phylogenetically? (c) If so, what are the various pattern strategies used to achieve crypsis in the dry season form? To answer these questions, we analyzed pattern element variation of 34 seasonally polyphenic butterfly species belonging to tribe Junoniini.

The tribe Junoniini (Lepidoptera: Nymphalidae: Nymphalinae) is one of six major tribes in the subfamily Nymphalinae and is comprised of 85 species in 6 genera: *Hypolimnas* (26 spp.), *Precis* (17 spp.), *Salamis* (3 spp.), *Yoma* (2 spp.), *Protogoniomorpha* (2 spp.), and *Junonia* (35 spp.) (Kodandaramaiah 2009). The tribe is estimated to have evolved approximately 30–40 million years ago originating in Africa and spreading throughout Asia and Oceania primarily (Wahlberg et al. 2005; Kodandaramaiah and Wahlberg 2007). Most of the genera diverged approximately 25 million years ago with the exception of *Yoma* and *Protogoniomorpha* which split approximately 5 million years later (2006). Species belonging to this tribe are noted for being swift fliers, having medium to large body sizes, and exhibiting striking polyphenic forms such as the model organism *Junonia coenia* making the tribe an ideal target taxon for this study (Win et al. 2016).

We show that forewing shape and eyespot size both vary seasonally in the Junoniini and that the methods by which phenotype elements change in the dry

season forms are different in different clades and may therefore have independent and diverse evolutionary origins.

13.2 Methods

Phenotypic variation in the seasonal forms of the Junoniini was measured and assessed using high-resolution digital images and image processing software. Specimens were acquired from the Museum of Natural History in London and the Smithsonian National Museum of Natural History. Images received from the London Museum were on 35 mm photographic film and were digitized using an EPSON Perfection V600 flatbed digital scanner. Images of the Smithsonian specimens were captured at a fixed distance from the specimen using a Nikon CoolPix P600 16.1 megapixel digital camera. All images were taken with a millimeter ruler for scale.

Specimens were selected for analysis to maximize phylogenetic coverage of tribe Junoniini by including representatives from each of the major genera (*Hypolimnas*, *Junonia*, *Precis*, *Protogoniomorpha*, *Salamis*, and *Yoma*) as well as two out-groups (*Anartia* and *Kallimoides*). Selected Junoniini specimens were labeled and organized into the following functional groups corresponding to major clades within the tribe's phylogeny: upper *Junonia*, Asian *Junonia*, lower *Junonia*, *Yoma*, *Precis*, and *Hypolimnas* (Fig. 13.1a). The lower *Junonia* was treated as a clade for comparative purposes despite its status as an unresolved polytomy. Species were selected that had at least four replicates of comparable quality. To eliminate confounding effects of regional variation and sexual dimorphism, specimens were sexed and selected from the same geographic region. If the species had distinct seasonal phenotypes, these were confirmed by the date of collection and comparison to previous descriptions in the literature. The resulting sample was comprised of 34 species from Africa, Asia, Oceania, and North America.

Size and position of pattern elements of the ventral hind wing were measured by generating landmark points in the image processing software ImageJ v1.51g (Schneider et al. 2012). The ventral surface was chosen because butterflies most often have their wings folded showing the ventral pattern when not in flight. The hind wing was chosen to maximize the amount of visible wing surface since it overlaps in front of the forewing when viewed from the ventral side of the animal. For each image, landmark distances were converted from pixels to millimeters using a 20 mm scale. To normalize the size and relative distances between pattern elements according to the size of the wing on which they appear, a proxy for wing size was generated using the perimeter of a triangle formed using the distances between the root node of the venation system, the Cu2 vein terminus, and the Rs vein terminus, abbreviated RCR triangle (Fig. 13.1b – e).

For the Sc+R1, Rs, M1, M2, M3, and Cu1 cells of the ventral hind wing, the following measurements were taken:

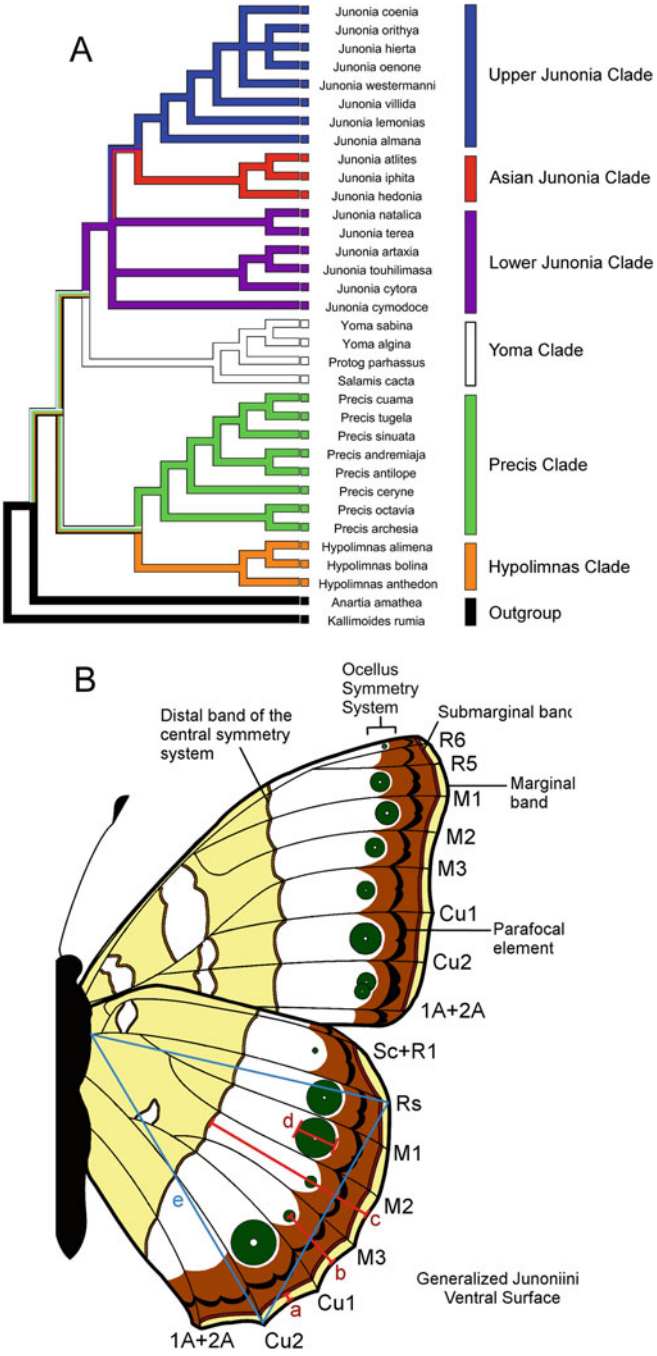

Fig. 13.1 (**a**) Phylogeny of the Junoniini (Lepidoptera: Nymphalidae: Nymphalinae) species used in this study grouped by reference clade. Tree topology based on Kodandaramaiah and Wahlberg (2007). (**b**) Diagram of measurements on a generalized Junoniini ventral wing surface including (*a*) submarginal band proximity [NSP], (*b*) eyespot proximity [NEP], (*c*) central symmetry system

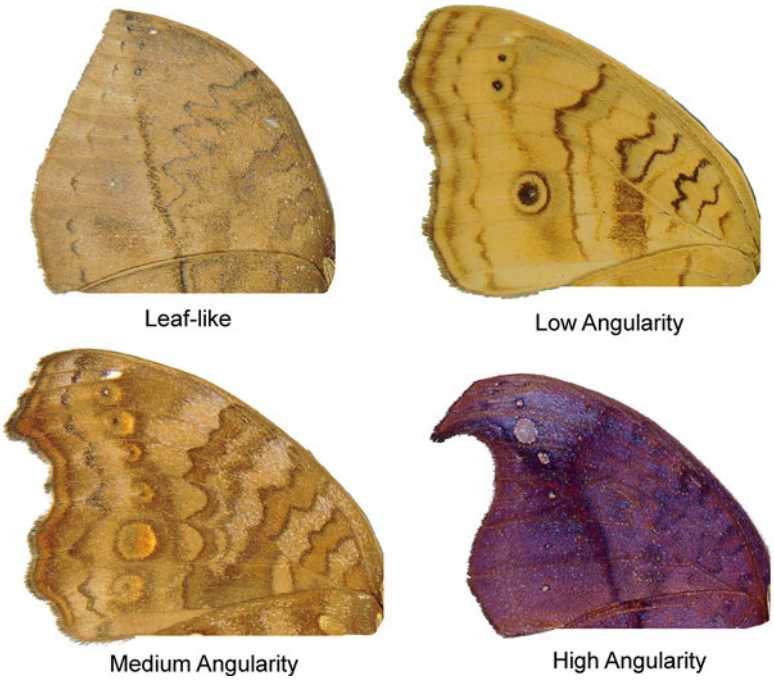

Fig. 13.2 Qualitative categorization of four forewing apex shape classifications observed in the dry season form. Note the increasing acuteness of the angle formed by the margins immediately flanking the M1 terminus as the apex increases in angularity from low to high. Note also that the M1 terminus angle is not present in the leaflike morphotype

(a) [NSP] normalized submarginal band proximity – the distance between the wing margin and the submarginal band divided by the RCR triangle (Fig. 13.1b – a)
(b) [NEP] normalized eyespot proximity – the distance between the wing margin and the focus of the eyespot divided by the RCR triangle (Fig. 13.1b – b)
(c) [NCP] normalized central symmetry system proximity – the distance between the wing margin and the distal band of the central symmetry system divided by the RCR triangle (Fig. 13.1b – c)
(d) [NED] normalized eyespot diameter – the longest distance that intersects with the focus of an eyespot between the distal and the proximal borders of the eyespot divided by the RCR triangle (Fig. 13.1b – d)

The morphology of the forewing apex was categorized into four classifications: leaflike, low angularity, medium angularity, and high angularity (Fig. 13.2). To

Fig. 13.1 (continued) proximity [NCP], and (*d*) eyespot diameter [NED]. Measurements were size-normalized using (*e*) the perimeter of a triangle connecting the Rs and Cu2 termini to the root of the venation system [RCR triangle]. (Tree topology from Kodandaramaiah and Wahlberg 2007)

ensure the consistency of the shape classifications, specimens were independently classified by an outside researcher and by the authors. Each classification converged on the same subdivision of morphotypes.

All measurements, including absolute differences in measurements for each seasonal form, were entered into a character matrix using the software suite Mesquite version 3.04 (Maddison and Maddison 2015). To contrast pattern element data between seasonal forms, parsimony character state reconstructions were mapped to an existing tree topology based on a molecular phylogeny for tribe Junoniini (Kodandaramaiah and Wahlberg 2007) and mirrored to draw comparisons between seasonal forms.

13.3 Results

13.3.1 Variation by Pattern Element

Variation in pattern elements was dependent on the type of pattern element being measured. The normalized submarginal band proximity (NSP) to the margin of the wing did not vary significantly for any wing cell between seasonal forms or across clades. The normalized central symmetry system proximity (NCP) to the wing margin and the normalized eyespot proximity (NEP) to the wing margin did not vary significantly for any wing cell between seasonal forms, but did show clear differences between clades. Finally, the normalized eyespot diameter (NED) varied significantly between seasonal forms and also showed clear differences between clades. It should also be noted that it is likely that the parafocal element also varies between seasonal forms, but difficulty in consistently defining the boundaries of this pattern element led to its omission from this study.

13.3.2 Variation by Wing Cell

Variation in pattern elements was also dependent on the wing cell in which the pattern elements are located. There was little variation in NED, NSP, NCP, or NEP for wing cells Sc+R1, M2, and M3 between seasonal forms for all clades because these eyespots are typically reduced or absent in ventral hind wings in both the wet and dry season forms. In contrast, the Rs, M1, and Cu1 wing cells showed significant differences in NED and NCP across clades, but only NED varied significantly between seasonal forms. *Junonia almana* (Fig. 13.3) provides a clear example of the differences in seasonal eyespot size variation across wing cells. In this species, the Sc+R1 eyespot is absent in both seasonal forms. The M2 and M3 eyespots are absent in the wet season form, but are present and highly reduced in the

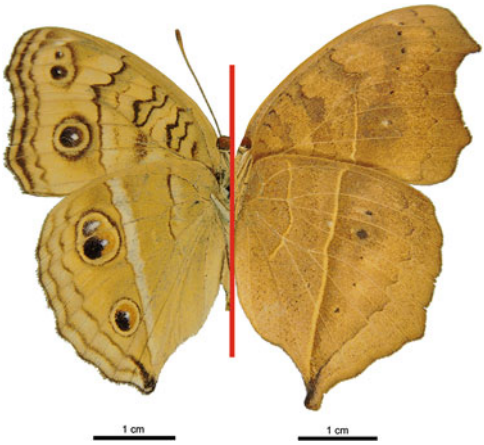

Fig. 13.3 *Junonia almana* seasonal forms. (*Left*) Wet season form exhibiting regions of high color contrast, large well-defined eyespots, and a low-angularity apex shape. (*Right*) Dry season form exhibiting low color contrast throughout the entire wing, drastically reduced eyespots, and a high-angularity forewing apex shape

dry season form. Finally, the Rs, M1, and Cu1 eyespots are large in the wet season form and highly reduced in the dry season form (Fig. 13.3).

13.3.3 Seasonal Eyespot Variation by Clade

Parsimony analysis of seasonal eyespot variation resulted in three similar parsimony character state reconstructions for the Rs, M1, and Cu1 eyespots when mapped to the molecular phylogeny. (Figs. 13.4, 13.5, and 13.6). However, the seasonal eyespot variation for each wing cell was not consistent across clades.

All species in the upper *Junonia* clade exhibited high seasonal eyespot size variation for the Rs, M1, and Cu1 eyespots with two exceptions: *J. westermanni* has no variation in the M1 eyespot (Fig. 13.5) and *J. hierta* in the Cu1 eyespot (Fig. 13.6).

The lower *Junonia* clade varied greatly both across species and by wing cell for seasonal eyespot size. For the Rs eyespot, most species showed no seasonal size variation except slightly in *J. cytora* and *J. touhilimasa* (Fig. 13.4). However, for the M1 and Cu1 eyespots, all of the species showed some seasonal size variation, though to different degrees, with the single exception of *J. cytora* in the Cu1 cell (Figs. 13.5 and 13.6).

The *Yoma* clade also exhibited a wide range of seasonal eyespot size variation. *Yoma algina* showed large seasonal eyespot size variation for the Rs, M1, and Cu1 eyespots, while its sister taxon *Y. sabina* showed only minimal variation in the Rs and M1 eyespots and no variation in the Cu1 eyespot. *Protogoniomorpha parhassus* exhibited seasonal eyespot size variation in the M1 and Cu1 eyespots but not the Rs eyespot. Finally, *Salamis cacta* showed no seasonal eyespot size variation whatsoever (Figs. 13.4, 13.5, and 13.8).

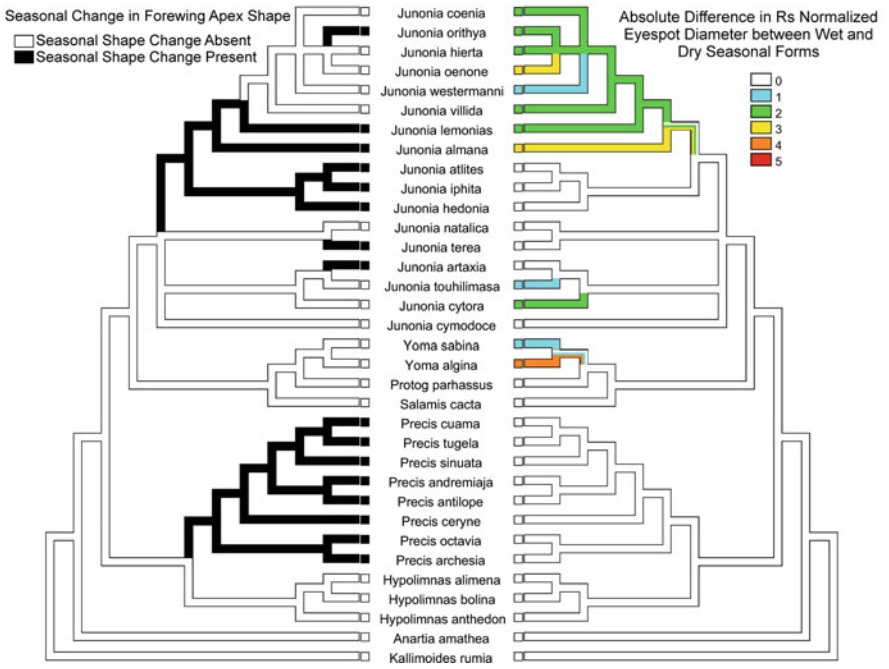

Fig. 13.4 Mirrored parsimony character state reconstructions for seasonal change in forewing apex shape class and the absolute difference in Rs normalized eyespot diameter between wet and dry season forms. Warmer colors represent a larger disparity between eyespot diameters of wet and dry forms (Tree topology from Kodandaramaiah and Wahlberg 2007)

Finally, the *Precis* clade, the *Hypolimnas* clade, and the Asian *Junonia* showed almost no seasonal eyespot size variation for any eyespot with one exception in *H. anthedon* which had the unusual characteristic of having no eyespots in (Figs. 13.4, 13.5, and 13.6).

13.3.4 Seasonal Forewing Apex Shape Change by Clade

The shape of the forewing apex varied both seasonally and by clade. The upper *Junonia* clade exhibited a mix of seasonal variation with shape change present only in *J. orithya*, *J. lemonias*, and *J. almana*. Similarly, in the lower *Junonia* clade, only two species, *J. terea* and *J. artaxia*, showed seasonal shape change of the forewing. The remaining clades, however, do not have this mix of shape change between seasonal forms. Neither the *Yoma* nor the *Hypolimnas* clades showed seasonal shape change. In contrast, both the Asian *Junonia* and *Precis* clades showed seasonal shape change in every species sampled (Fig. 13.7).

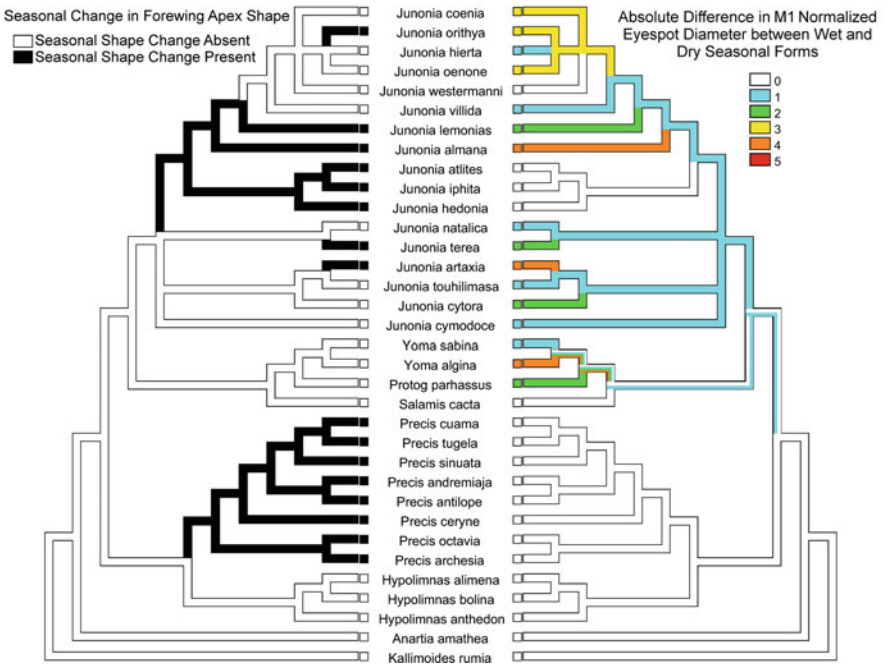

Fig. 13.5 Mirrored parsimony character state reconstructions for seasonal change in forewing apex shape class (*left*) and the absolute difference in M1 normalized eyespot diameter between wet and dry season forms (*right*). Warmer colors represent a larger disparity between eyespot diameters of wet and dry forms (Tree topology from Kodandaramaiah and Wahlberg 2007)

13.3.5 Shape Type and Shape Change

There exists an association between the shape of the forewing apex of the dry season form of a species and whether or not there was seasonal shape variation for that species. Species whose dry season form had a low angularity or leaflike forewing apex invariably did not exhibit seasonal forewing shape change (Fig. 13.7). Furthermore, species whose forewing apex varied seasonally did so according to a pattern of increasing angularity in the dry season form compared to the wet season form (Figs. 13.7 and 13.8 – bottom). Species with seasonal shape change whose wet season form had a low-angularity forewing apex had dry season forms with medium- or high-angularity forewing apex shapes. Similarly, species with seasonal shape change whose wet season form had a medium-angularity forewing apex had dry season forms with high-angularity forewing apex shapes. The result of this association is the general trend that species that exhibit seasonal change in forewing shape tend to have more high-angularity forewing morphologies, while species that do not exhibit seasonal change tend to have low-angularity forewing morphologies.

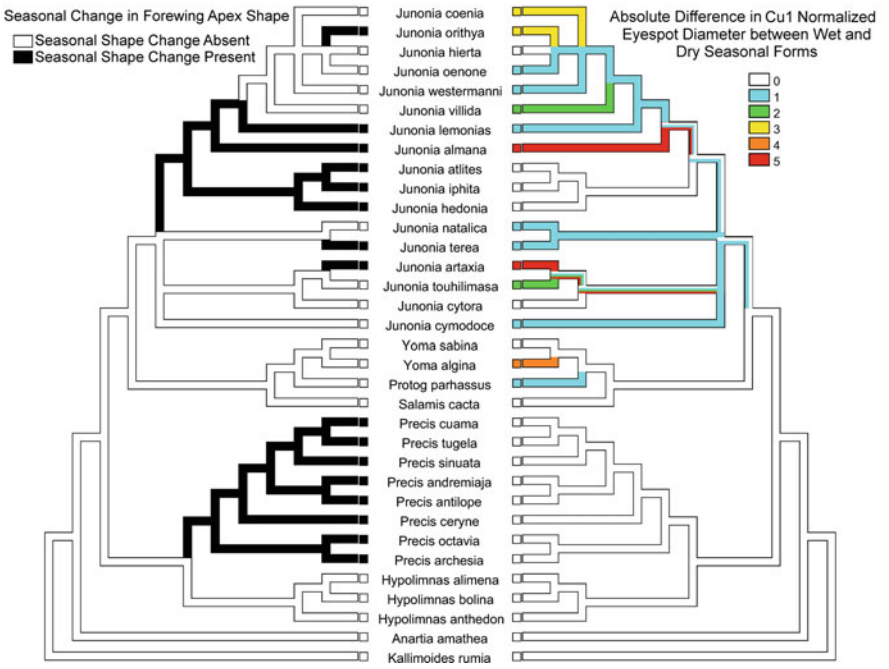

Fig. 13.6 Mirrored parsimony character state reconstructions for seasonal change in forewing apex shape class (*left*) and the absolute difference in Cu1 normalized eyespot diameter between wet and dry season forms (*right*). Warmer colors represent a larger disparity between eyespot diameters of wet and dry forms (Tree topology from Kodandaramaiah and Wahlberg 2007)

13.3.6 Discussion

The results of this investigation reveal a dynamic relationship between the components of a seasonally polyphenic phenotype and the pattern by which they evolve. They show that the phenotype elements of a seasonal form can be evolutionarily decoupled, that these plastic elements have responded to selective pressures in diverse ways, and that the diversity of these responses is reflected in the tribe's phylogenetic history. The different pattern elements of seasonally polyphenic forms do not evolve as a single cohesive unit.

The methods by which the seasonal forms have evolved in these butterflies also offer insight about how pattern elements are involved in responding to selection for crypsis in the dry season. The findings of this study suggest that the location of pattern elements on the wing does not change in the formation of alternative seasonal phenotypes. This suggests that either selection is not acting strongly on position or that element position is under some developmental constraint and therefore unable to respond to selective pressures. When considering the variation in the position of eyespots specifically, it seems more likely to be a lack of selection on position given that eyespot position is characteristically different among clades,

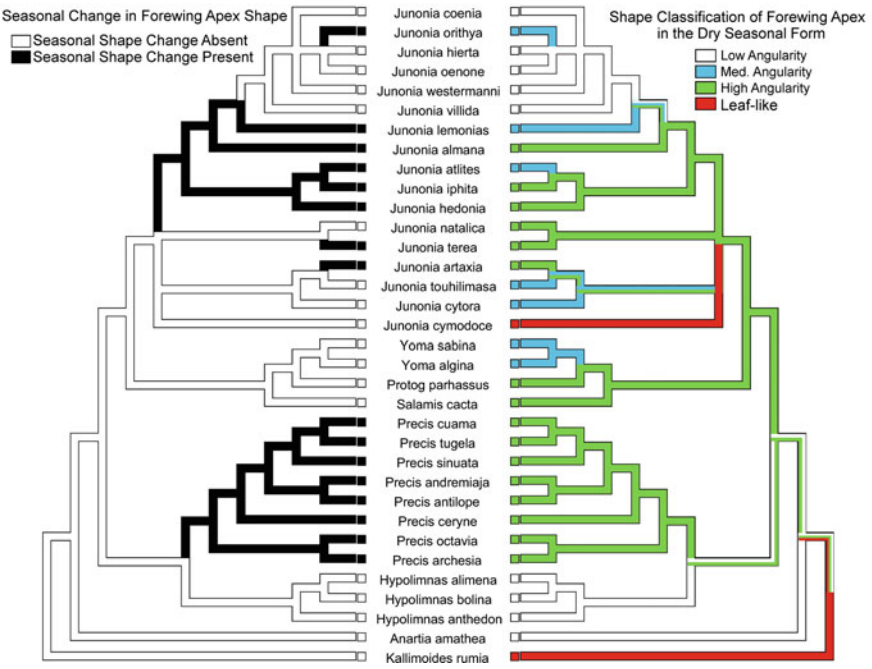

Fig. 13.7 Mirrored parsimony character state reconstructions for seasonal change in forewing apex shape class and the shape classification of the forewing apex in the dry season form. Note the association between exhibiting seasonal shape change and having higher forewing apex angularity in the dry season form (Tree topology from Kodandaramaiah and Wahlberg 2007)

implying at least some freedom from constraint during the early evolution of the major Junoniini clades.

However, the variation in eyespot size tells us a different story. In species where eyespot size is variable, the dry season form always has reduced eyespot size compared to the wet season form, suggesting a strong response to selection. At the same time, there is little variation in the wing cells in which large eyespots develop. For instance, the upper and lower *Junonia* clades all have stable large eyespots in the Rs, M1, and Cu1 wing cells and stable small eyespots in the M2 and M3 wing cells in the wet season form, whereas species in the *Precis* clade have stable small eyespots in all of the wing cells. There is no case where stable large eyespots have evolved in the M2 and M3 wing cells. Thus there appear to be constraints both on the capacity to have size-variable eyespots and on the wing cell in which the eyespot is found (Figs. 13.4 and 13.8 – bottom).

Similarly, in clades that have seasonal variation in wing shape, the dry season form always has a more angular or falcate forewing shape, again suggesting a strong response to selection (Figs. 13.7 and 13.8 – bottom). Other clades, by contrast, have evolved phenotypically stable low-angularity rounded (*Hypolimnas* clade) or high-angularity falcate (*Yoma* and Asian *Junonia* clades) wing shapes.

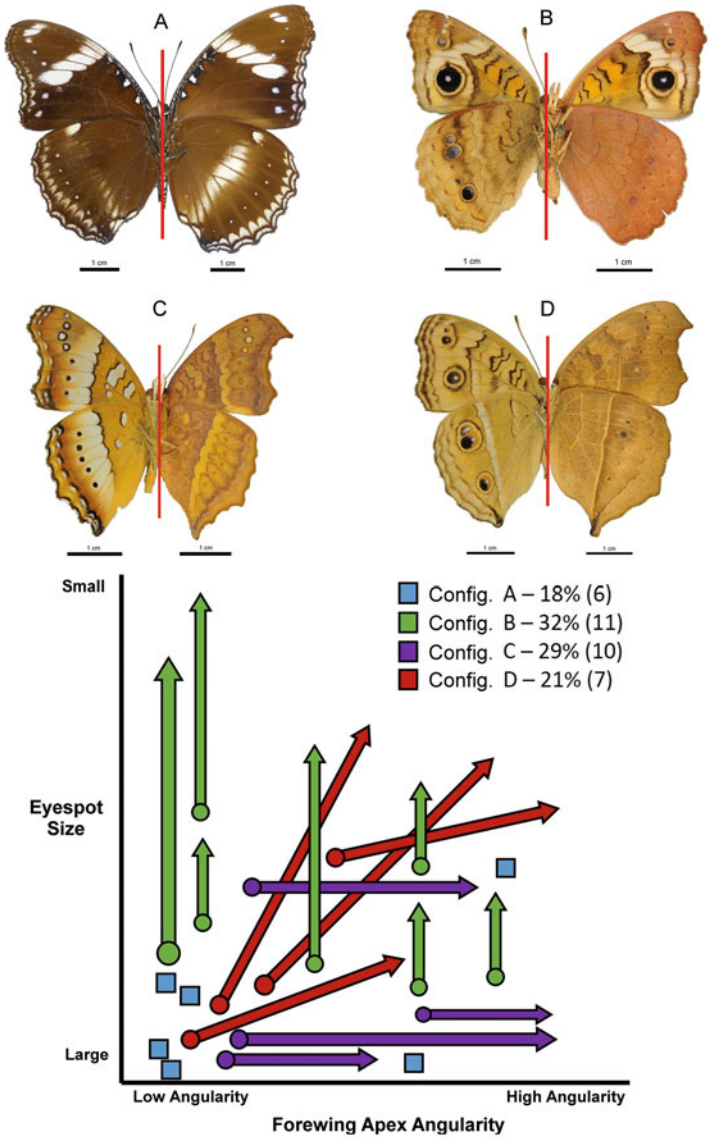

Fig. 13.8 *Top*: Plates representing four configurations found among Junoniini butterflies – (**a**) Neither forewing shape nor eyespot size vary seasonally; (**b**) Only eyespot size varies seasonally; (**c**) Only forewing shape varies seasonally; (**d**) Both forewing shape and eyespot size vary seasonally. Each plate is a composite of the wet season form (*left*) and the dry season form (*right*). *Bottom*: Schematic diagram of the relationship between seasonal changes in forewing shape and eyespot size. Wet season forms are shown as *circles*, dry season forms as *arrows*, and when the two forms overlap they are shown as *squares*. Note that the change for forewing shape is always from lower to higher angularity, and the change in eyespot size is always a reduction

Thus the Junoniini show both plastic alternative wing shape phenotypes and evolutionary fixation of the alternative shapes, and the fixation of either the low- or high-angularity wing shapes corresponds to major clade divergences in the phylogeny. This suggests that while the capacity to develop alternative wing shapes evolved early for the entire tribe, the fixation of alternative wing shapes occurred later in the establishment of the genera.

The decoupling of independent phenotype elements has allowed for the emergence of what we loosely refer to here as "phenotypic configurations" which can be thought of as arrangements of phenotype element variation. To illustrate this idea, we used only the combination of eyespot size variation and forewing apex shape variation which can be roughly categorized into the four configurations that represent butterflies whose seasonal forms exhibit no variation, size variation only, shape variation only, or both size and shape variation: Configurations A, B, C, and D, respectively (Fig. 13.8 – top).

The distribution of these configurations in the phylogeny shows some interesting patterns. First, each of the configurations corresponds to the clades described in Fig. 13.1 – top: the *Hypolimnas* clade shows almost no seasonal change in wing shape or eyespot size (Figs. 13.4 and 13.8 – top: Configuration A); the upper *Junonia* exhibit minimal seasonal change in wing shape, but exhibit great seasonal change in eyespot size (Figs. 13.4 and Fig. 13.8 – top: Configuration B); the inverse is true for the *Precis* and Asian *Junonia* clades whose members show almost no seasonal change in eyespot size, while they all exhibit seasonal change in forewing apex shape (Figs. 13.4 and Fig. 13.8 – top: Configuration C). Second, the relative frequency of these configurations and their position in the phylogeny show that species whose wing shape varies seasonally tend not to be the same species whose eyespot size varies seasonally, with a few exceptions. A highly angular wing shape in the dry season form seems to have evolved very early in the tribe but was lost independently in both *Hypolimnas* and upper *Junonia* (Fig. 13.4 right). Interestingly, the capacity to develop plastic seasonally distinct wing shapes may have evolved around the same time as the falcate wing shape but saw successive loss in H*ypolimnas*, *Yoma*, and some species in lower and upper *Junonia* (Fig. 13.4 left). An alternative interpretation might be that the capacity for wing shape change evolved multiple times – once in the *Precis* clade and once in genus *Junonia* with only the latter having some subsequent loss of the trait (Fig. 13.4 left).

Finally, the leaflike wing shape seems to have evolved independently with respect to the well-known leaf mimics of the genus *Kallimoides*. This raises some interesting questions regarding the importance of the phenotypic elements for crypsis. If a species can achieve crypsis by either reducing its eyespots or changing its wing shape from season to season, why do one or the other? Is the plasticity of one phenotype element enough to render the plasticity of another unnecessary? What, then, of species who have variation in both or neither of these elements?

Another interesting question regarding the interplay between phenotypic elements and their evolutionary trajectory is the role of color and contrast of the wing pattern. In the same way, the conspicuousness of an eyespot can be diminished by reducing its size; it can also be recolored or recontrasted to match the surrounding

region of the wing, which effectively achieves the same result. This is the case in *Precis atlites*, whose eyespots remain the same in size but become less bold and more similar in color to the background of the wing rendering them more difficult to detect. Although seasonal changes in color and contrast are widespread in the tribe, that is to say all of the dry season forms become duskier in color and less striking in the boldness of their patterns, it is unclear as to what extent changing color and contrast compensate for the inability to modify either wing shape or eyespot size. A detailed analysis of these elements will be presented in a separate paper.

The seasonally polyphenic forms of butterflies are often thought of as a single trait. In reality, because butterfly wing patterns are comprised of serially homologous phenotypic elements that are developmentally semiautonomous, they can be uncoupled, modified, and reconfigured to respond to selection and produce constraints in diverse ways. The seasonal forms of Junoniini butterflies have changed over time by invoking at least three distinct developmental mechanisms, including wing shape morphogenesis, pigment synthesis pathways, and pattern element positioning mechanisms. Rather than inheriting a seasonal form, these butterflies inherit the tools to create a seasonal form, and the methods by which they have convergently evolved to become cryptic are written in their evolutionary history.

Acknowledgments I am grateful to the Smithsonian Institution National Museum of Natural History and the National History Museum in London for access to their butterfly collections, Professor H.F. Nijhout for his direction and guidance, Richard Gawne and Kenneth McKenna for their helpful discussion and criticism, Leo Kerner for assistance in image databasing, the anonymous reviewers for their criticism and feedback, and the support of the following National Science Foundation grants awarded to H.F. Nijhout: IOS-0641144, IOS-1557341, and IOS-1121065.

References

Brakefield PM, Larsen TB (1984) The evolutionary significance of dry and wet season forms in some tropical butterflies. Biol J Linnean Soc 22(1):1–12

Brakefield PM, Gates J, Keys D, Kesbeke F, Wijngaarden PJ, Monteiro A, French V, Carroll SB (1996) Development, plasticity and evolution of butterfly eyespot patterns. Nature 384 (6606):236–242

Kodandaramaiah U (2009) Eyespot evolution: phylogenetic insights from Junonia and related butterfly genera (Nymphalidae: Junoniini). Evol Dev 11(5):489–497

Kodandaramaiah U, Wahlberg N (2007) Out-of-Africa origin and dispersal-mediated diversification of the butterfly genus Junonia (Nymphalidae: Nymphalinae). J Evol Biol 20(6):2181–2191

Maddison WP, Maddison DR (2015) Mesquite: a modular system for evolutionary analysis. Version 3.04. http://mesquiteproject.org

McLeod L (1968) Controlled environment experiments with Precis octavia Cram (Nymphalidae). J Res Lepidoptera 8(2):53–54

Monteiro A, Tong X, Bear A, Liew SF, Bhardwaj S, Wasik BR, Dinwiddie A, Bastianelli C, Cheong WF, Wenk MR, Cao H (2015) Differential expression of ecdysone receptor leads to variation in phenotypic plasticity across serial homologs. PLoS Genet 11(9):e1005529

Nijhout HF (1991) The development and evolution of butterfly wing patterns, Smithsonian series in comparative evolutionary biology. Smithsonian Institution Press, Washington

Oostra V, de Jong MA, Invergo BM, Kesbeke F, Wende F, Brakefield PM, Zwaan BJ (2011) Translating environmental gradients into discontinuous reaction norms via hormone signalling in a polyphenic butterfly. Proc R Soc Lond B Biol Sci 278(1706):789–797

Prudic KL, Stoehr AM, Wasik BR, Monteiro A (2015) Eyespots deflect predator attack increasing fitness and promoting the evolution of phenotypic plasticity. Proc R Soc B 282 (1798):20141531. The Royal Society

Rountree DB, Nijhout HF (1995) Genetic control of a seasonal morph in Precis coenia (Lepidoptera: Nymphalidae). J Insect Physiol 41(12):1141–1145

Schneider CA, Rasband WS, Eliceiri KW (2012) NIH Image to ImageJ: 25 years of image analysis. Nat Method 9(7):671–675

Wahlberg N (2006) That awkward age for butterflies: insights from the age of the butterfly subfamily Nymphalinae (Lepidoptera: Nymphalidae). Syst Biol 55(5):703–714

Wahlberg N, Brower AV, Nylin S (2005) Phylogenetic relationships and historical biogeography of tribes and genera in the subfamily Nymphalinae (Lepidoptera: Nymphalidae). Biol J Linnean Soc 86(2):227–251

Win NZ, Choi EY, Park J, Park JK (2016) Taxonomic review of the tribe Junoniini (Lepidoptera: Nymphalidae: Nymphalinae) from Myanmar. J Asia-Pacific Biodiv 9(3):383–388

Chapter 14
Estimating the Mating Success of Male Butterflies in the Field

Nayuta Sasaki, Tatsuro Konagaya, Mamoru Watanabe, and Ronald L. Rutowski

Abstract Sexual dimorphism in wing coloration is pervasive in butterflies and has been attributed to the process of sexual selection. However, this view has rarely been tested, partly owing to difficulties in estimating the mating success of males in the field. In the present study, we describe a method for assessing the mating success of male pipevine swallowtail (*Battus philenor*) butterflies, based on the appearance of their reproductive tracts. Laboratory experiments indicated that, in response to mating, components of the males' reproductive tracts become shorter, decrease in mass, and change in appearance, irrespective of age; and these changes persist for at least 2 days. Using these indicators of recent mating, we examined the reproductive tracts of 68 field-caught males and found that the color of the dorsal hindwing, a feature that females use in mate choice, was significantly greener in males that had recently mated than in males that had not.

Keywords *Battus philenor* • Ejaculate substance • Male mating success • Ornaments • Sexual selection

N. Sasaki (✉)
Field Science Center for Northern Biosphere, Hokkaido University, 053-0035 Takaoka, Tomakomai, Hokkaido, Japan
e-mail: nayutaSSK@gmail.com

T. Konagaya
Graduate School of Science, Kyoto University, 606-8502 Kyoto, Japan
e-mail: konagaya@ethol.zool.kyoto-u.ac.jp

M. Watanabe
Graduate School of Life and Environmental Sciences, University of Tsukuba, 305-8572 Ibaraki, Japan
e-mail: papilio-platycnemis@nifty.com

R.L. Rutowski
School of Life Sciences, Arizona State University, Tempe, AZ 85287-4501, USA
e-mail: R.RUTOWSKI@asu.edu

T. Sekimura, H.F. Nijhout (eds.), *Diversity and Evolution of Butterfly Wing Patterns*, DOI 10.1007/978-981-10-4956-9_14

14.1 Introduction

There is a long history of interest in the diversity of butterfly wing pattern and coloration. Starting with work of Darwin (1874) and Wallace (1889), researchers have observed and discussed various issues related to wing pattern, such as interspecific similarity and variation (Nijhout 1990), ecological relevance (Rutowski 1997), color production mechanisms (Koch et al. 1998), evolutionary and developmental plasticity (Beldade et al. 2002), and genetics (Carroll et al. 1994), as well as intersexual differences. Because male butterflies typically exhibit brighter wing coloration and sometimes exhibit pattern elements that are not found in females, many researchers, including Darwin (1874), have speculated that the coloration of male wings results from female mating preferences associated with exaggerated visual signals (Kemp and Rutowski 2011; but see Allen et al. 2011).

A considerable amount of research has also been motivated by the intersexual variation of butterfly wing coloration; however, relative to other groups of colorful animals, such as birds, fish, and lizards (Blount et al. 2003; Grether et al. 2005; Hill and Montgomerie 1994; Keyser and Hill 1999), relatively little is known about the selective factors that promote the sexual dimorphism of wing color in butterflies (Kemp 2007). This deficit has partly stemmed from the difficulty of setting up the necessary assays of female preference. In addition, since sexual selection ultimately results from biased reproductive success, it is necessary to elucidate the relationship between male traits and reproductive success. However, the highly dispersed, cryptic, and ephemeral nature of butterfly copulation hinders the estimation of male mating success in the field (e.g., Rutowski 1997; Takeuchi 2016).

Here we report a new technique to assess the recent mating success of males in Lepidoptera that relies on changes that occur in the appearance of internal reproductive organs during mating. In some lepidopteran species, males transfer an ejaculate to females that can account for as much as 15% of the male body mass (e.g., Rutowski et al. 1983; Svärd and Wiklund 1989), and in many species, males can produce more than one spermatophore; however, it takes time for males to produce an ejaculate that is comparable in size to the one transferred during the previous mating (Bissoondath and Wiklund 1996; Watanabe and Hirota 1999). Therefore, the internal reproductive organs of mated males might differ in size, contents, or appearance from those of unmated males, at least for a few days after mating.

The typical arrangement of internal reproductive organs in male butterflies includes two fused testes that give rise to a pair of vas deferens, which are secretory ducts, that lead to the duplex, which is a pair of sperm storage organs. Two duplex ducts unite caudally to form the simplex, which is a single duct that leads to the intromittent organ, or aedeagus. Sperm move from the testes into the duplex via the vas deferens (Riemann et al. 1974; LaChance et al. 1977). Due to the arrangement of the reproductive organs in the male body (c.f. Fig. 14.1), the spermatophore materials and accessory substances in the simplex are transferred to the female body during mating before the sperm are transferred (Watanabe and Sato 1993). Thus,

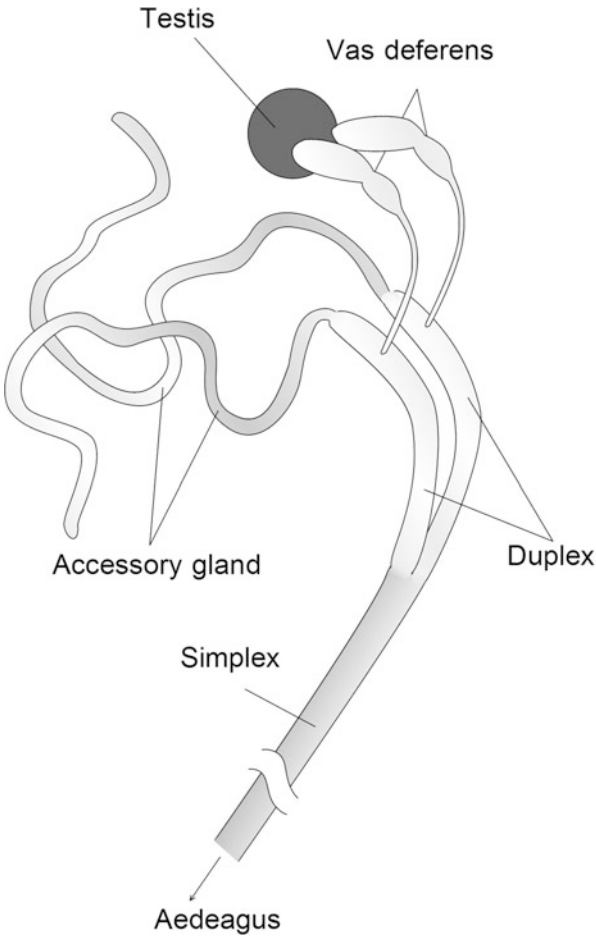

Fig. 14.1 A schematic representation of the internal reproductive organs of a *B. philenor* male (After Sasaki et al. 2015)

males might not be able to reserve spermatophore materials or accessory substance in the simplex and so the quantity or nature of these materials might be a good indicator of recent mating activity.

The aims of the present study were (1) to document any changes that occur in the appearance of reproductive structures in male pipevine swallowtail (*Battus philenor*) butterflies as a result of mating, as well as the persistence of such changes after mating, in order to develop criteria for identifying males that had recently mated and (2) to examine the reproductive tracts of field-caught *B. philenor* males, assess the variation in their recent mating history, and determine whether their recent mating success was related to their phenotypes. Rutowski and Rajyaguru (2013) have reported that, in a captivity *B. philenor*, females use the dorsal hindwing coloration of males in mate choice.

This issue is mainly reporting previously published results and ideas in Sasaki et al. (2015).

14.2 Materials and Methods

14.2.1 Source of Animals Used

All specimens were from a population of *B. philenor* that thrives near the confluence of Mesquite Wash and Sycamore Creek in the Mazatzal Mountains, Arizona (33° 43′ 50″ N, 111° 30′ 50″ W). Animals used in the mating studies were reared from eggs and early instar larvae collected in the field from early June to mid-July in 2011. All larvae were reared in a walk-in environmental chamber, programmed for 14 h of light at 30 °C and 10 h of dark at 24 °C with relative humidity held constant at 55%, and were fed ad libitum on cuttings of the local larval food plant, *Aristolochia watsonii*. On the day of eclosion, males were weighed, their forewing length measured, and given an individual number. Sexes were kept separately in small flight cages (~1 m^3) at room temperature (~24 °C) and individually fed 20% sucrose solution for about 20 min each day.

14.2.2 Examination of Reproductive Tracts of Virgin and Mated Males

To examine the effect of mating on the appearance of the male's reproductive tract, we hand-paired males with 0–3-day-old virgin females using the method of Watanabe and Hirota (1999). Then, each male was dissected and his reproductive tract examined to assess changes in the appearance of simplex with age and with mating experience. We divided males into three experimental groups: (1) males that never mated and dissected on the day of eclosion or 3 or 6 days after eclosion; (2) males that mated 1, 3, or 5 days after eclosion and dissected immediately after the mating; and (3) males mated 1 day after eclosion and dissected right after the mating or 1, 2, 3, or 5 days after mating.

Before dissection, each male was immobilized by gently pinching their thorax. Each male's abdomen was then removed from the body and placed in a petri dish filled with fresh insect Ringer's solution. The reproductive organs including the simplex and duplex were carefully removed from his abdomen. To describe the simplex of each male, we measured its length, appearance, and mass. We first imaged each simplex after removing any fat bodies attached to it and then recorded its appearance with a digital camera attached to a microscope. After capturing images, each simplex was separated from the attached duplex and aedeagus. Wet mass of each simplex was then determined to the nearest 0.01 mg.

14.2.3 Estimation of Recent Mating Success of Field-Caught Male

Sixty-eight wild males were collected from 16 July to 1 August 2011 in the morning near Sunflower, Arizona. Each captured male was scored as to his wing wear as an indicator of his age. Age-class was scored on the scale (I (least worn) to V (most worn)) described by Watanabe et al. (1986). The forewing length of each male was measured from the wing base to the wing tip. All males were dissected on the day of capture. To assess recent mating success of males, the mass, length, and transparency differences of each male's simplex were measured.

14.2.4 Spectral Analyses of Iridescent Wing Areas

In preparation for spectral measurements, the left hindwing of each butterfly was removed from the thorax and mounted dorsal side up on black card stock with spray adhesive. Reflectance spectra were collected from these wings using techniques described in Rutowski et al. (2010). Reflectance relative to a magnesium oxide white standard was measured between 300 and 700 nm from the wings. Because the reflectance spectra of these iridescent wing surfaces are unimodal, we extracted three color parameters, intensity, hue, and chroma, to describe and analyze the properties of the wing reflectance (Montgomerie 2008).

14.3 Results

14.3.1 Virgin Male Reproductive Tract

For virgin males, the simplex mass adjusted for forewing length ((simplex mass)$^{1/3}$/forewing length), simplex length adjusted for forewing length (simplex length/forewing length), and the transparency difference of simplex was approximately 0.5, 1.3, and 1.3, respectively, and these did not change with male age [mass (ANOVA, $F_{2,21}$=1.554, $p = 0.237$); length (ANOVA, $F_{2,21}$=2.276, $p = 0.130$); transparency difference (ANOVA, $F_{2,21}$=0.475, $p = 0.629$)]. Consequently, simplex of virgin males did not change in appearance with time since eclosion.

14.3.2 Reproductive Tract of Males Immediately After Mating

For males, immediately after the termination of copulation, the simplex mass adjusted for forewing length, the simplex length adjusted for forewing length, and the transparency difference were approximately 0.32, 0.5, and 0.3, respectively, and these did not vary with the age of the male at mating [mass (ANOVA, $F_{2,16}$=0.027, $p = 0.974$); length (ANOVA, $F_{2,16} = 1.331$, $p = 0.296$); transparency difference (ANOVA, $F_{2,16}$=0.170, $p = 0.845$)]. Although the simplex of males just after the termination of copulation was different in appearance from that of virgin males, these were not affected by age at mating.

14.3.3 Changes in the Male's Reproductive Tract with Time Since Mating

Although the simplex of males just after the termination of copulation was short, it lengthened and refilled again as time passed since mating. During this period, the color of the simplex turned from yellow to colorless, and the amount granular substances increased in the basal end of the tube. Statistically, the mass, length, and transparency difference of simplex all changed with time between mating and dissection (Fig. 14.2; mass: ANOVA: $F_{5,61} = 59.202$, $p < 0.001$; length: ANOVA: $F_{5,55} = 42.770$, $p < 0.001$; transparency difference: ANOVA: $F_{5,55} = 17.139$, $p < 0.001$). After copulation, simplex mass (A) and length (B) dropped to half their precopulatory values, but returned to precopulatory values in about 2 days. The transparency difference decreased with mating but also returned to premating values within about 2 days (C).

Using the results of these analyses, we developed criteria for assessing whether a male's reproductive tract showed evidence of recent mating. The distribution of simplex mass adjusted for forewing length of males within 1 day after mating was 0.251–0.453, whereas that of virgin males was 0.465–0.565, with no overlap in these ranges. The observed ranges of simplex length adjusted for forewing length and the transparency difference of males within 1 day after mating and virgin males also did not overlap (length, 0.401–0.940 vs 1.084–1.628; transparency difference, 0.013–0.964 vs 1.105–2.148). So, we set the lower end of the ranges of values for simplex characteristics of virgin males as the value below which would indicate that the male had recently mated. That is, a field-caught male that had a simplex of less than 0.46 in mass, less than 1.0 in length, or less than 1.0 in transparency difference was taken as indicating that the male had recently mated.

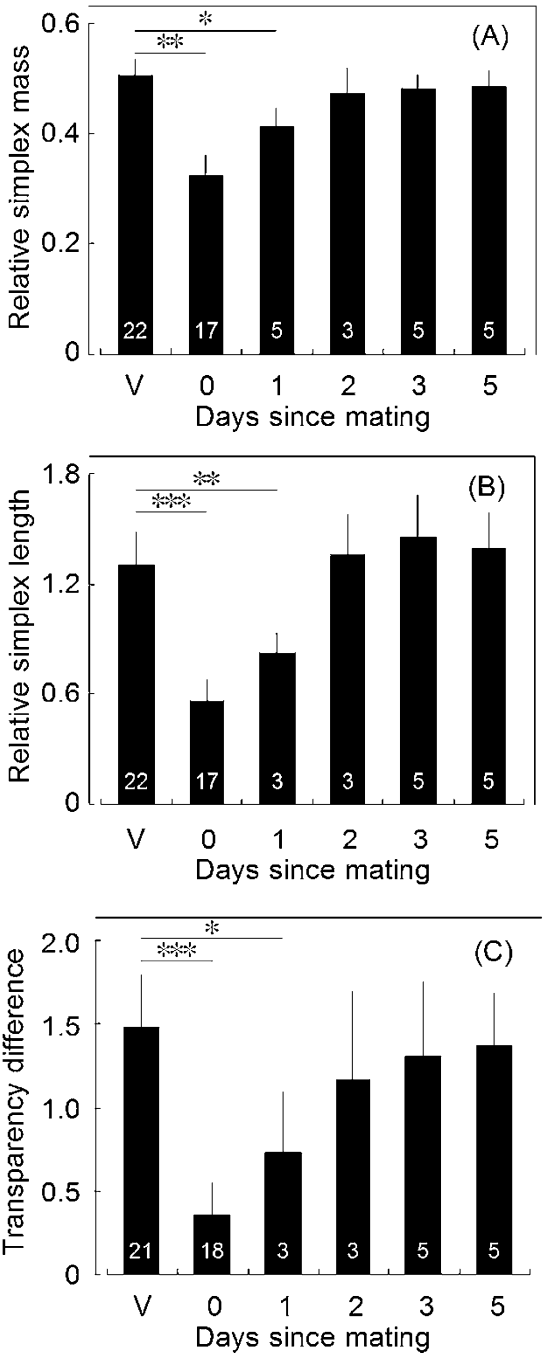

Fig. 14.2 Simplex mass (**a**), length (**b**), and transparency difference (**c**) of simplex for virgin males (V, 0, 3, 6 days old) and for mated males (1, 3, 5 days old) dissected at various number of days after mating (mean±S.D.) (After Sasaki et al. 2015). *,** and *** represent $p < 0.05$, $p < 0.01$, and $p < 0.001$ in Tukey's HSD test, respectively

14.3.4 Mating Success of Field-Caught Males

All field-caught males were evaluated and placed in groups based on which of the three criteria for recent mating they met and which they did not (Table 14.1). For the eight possible groups and to maximize contrasts any group that met two or more of the criteria (Groups E to H) we labeled as showing strong evidence of recent mating. However, because there were no individuals in Group G, we regarded males in Group E, F, and H as recently mated males. Of the 68 males in the list, 12 showed this strong evidence of having mated recently. We also confidently labeled as not recently mated, males that met none of the criteria (Group A).

Using GLM with binomial errors and a logit link function, we compared the phenotypic characteristics of those that had recently mated (Groups E, F, and H) with those that had not (Group A). The characters included in the analysis were the intensity and hue of the iridescent area of male dorsal hindwing and age-class. Chroma was not included as an independent variable in the analysis because there were significant correlations between chroma and all other characteristics (Table 14.2). As shown in Table 14.3, while intensity was not related to their recent mating success, hue and age-class significantly affect their recent mating success. Recently mated males were older and had a higher hue value (were greener) than males that had not recently mated (Figs. 14.3 and 14.4).

Table 14.1 A summary of the state of reproductive tract components of 68 males caught in the field

	Group							
Criterion	A	B	C	D	E	F	G	H
Simplex mass	–	–	–	+	–	+	+	+
Simplex length	–	–	+	–	+	–	+	+
Transparency difference	–	+	–	–	+	+	–	+
N	23	30	2	1	2	5	0	5

After Sasaki et al. (2015)
A plus sign means that the state of that component met the criteria we set for indicating the male recently mated. A minus sign means it did not meet the criteria. In later analysis, any group that met two or more of the criteria (Groups E to H) and males that met none of the criteria (Group A) were used as recently mated males and as not recently mated males, respectively

Table 14.2 Spearman correlation coefficients for the relationship between male age and the various color parameters for the dorsal hindwing coloration

Measure	1	2	3	4
1. Intensity	–			
2. Chroma	0.584*	–		
3. Hue	−0.087	−0.383*	–	
4. Age-class	−0.102	−0.581*	0.211	–

After Sasaki et al. (2015)
Significant correlation between intensity and chroma, chroma and hue, and chroma and age-class were found
*$p < 0.01$

Table 14.3 Results of an ANOVA (GLM) of factors that contribute to variation in recent mating success of wild males

Effect	df	Deviance
	34	45.004
Intensity	1	0.669
Hue	1	4.744**
Age	1	1.760*

After Sasaki et al. (2015)
Effect of hue and age-class on male recent mating success were significant. * and ** represent $p < 0.05$ and $p < 0.01$, respectively

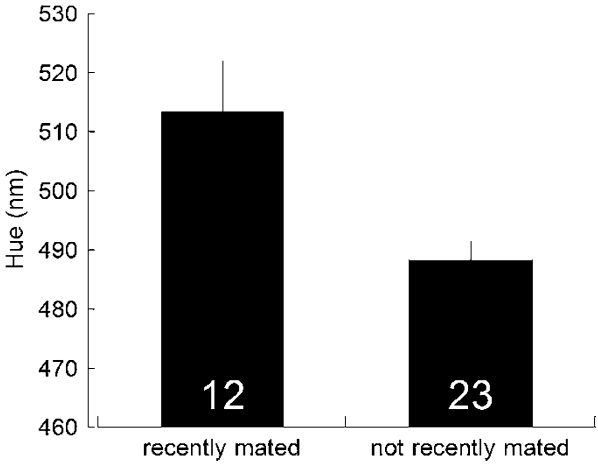

Fig. 14.3 The hue (wavelength of maximum reflectance) of the dorsal hindwing for field-caught males that met the criteria for evidence of having recently mated and those males that did not meet the criteria (±S.E.) (After Sasaki et al. 2015)

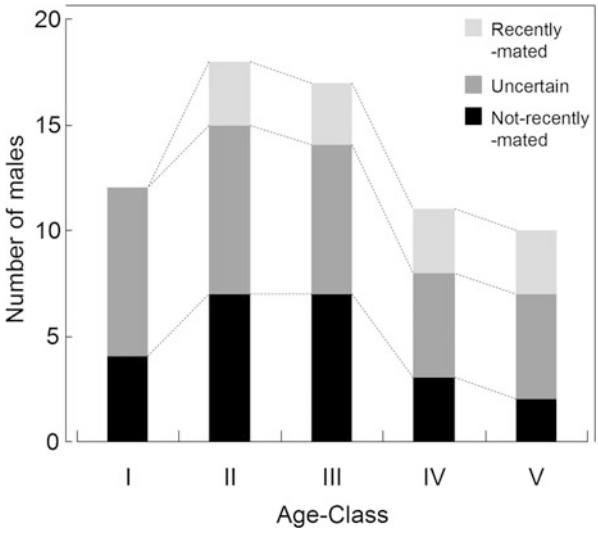

Fig. 14.4 Change with age-class in the number of clearly recently mated males (*light-gray bar*), clearly not recently mated males (*black bar*), and males of uncertain recent mating history (*dark-gray bar*) for field-caught males (After Sasaki et al. 2015)

14.4 Discussion

14.4.1 Assessing the Mating History of Male Butterflies in the Field

The most convincing demonstrations of the evolutionary significance of mating preferences are those in which the results of manipulative experiments are matched by observations in the wild or in wild-caught populations (Kemp 2007). In butterflies, many laboratory experiments have demonstrated the occurrence of female preference for particular male traits, including wing coloration (Krebs and West 1988; Robertson and Monteiro 2005; Andersson et al. 2007). However, the conclusions of these studies have rarely been validated against data obtained in more natural field-based settings (Kemp and Rutowski 2011). In other insects, the comparison of traits from copulating males and unattached males in the field has been extensively used to make inferences about population mating biology (Flecker et al. 1988; Harari et al. 1999; Alcock and Kemp 2006). However, this strategy has not been used in butterflies, except in cases of extremely high density, owing to the difficulty of observing butterfly mating in the field (Kemp and Rutowski 2011). Therefore, to determine the effect of female preference on the evolution of traits in male butterflies, it was necessary to establish an alternative method for evaluating male mating success.

Tsubaki and Matsumoto (1998) estimated the mating frequency of male *Luehdorfia japonica* by assessing the degree of scale loss from males' claspers. In this species, males consume scales and use them to form a mating plug on the female abdomen during copulation. Kazuma (1987) reported that the degree of scale loss in laboratory-reared males increased with repeated hand pairing. The degree of scale loss was scored on a scale of 0 (slight scale loss) to 3 (almost all scales were lost), and each stage corresponded to 0, 1, 2, and 3 or more matings. Since mating frequency must have a strong relationship to lifetime reproductive success, this method may provide an accurate estimation of reproductive success in wild males. However, because the mating-related loss of scales is not the rule among lepidopterans, this method is not applicable to all species.

In the present study, we reported a new technique for assessing male mating success that relies on changes that occur in the appearance of internal reproductive organs during mating. Since the internal reproductive organs of butterflies are not much different between species and it is common for males to ejaculate spermatophores and accessory substances during mating (e.g., Drummond 1984), this method can likely be applied to any butterfly species. In fact, it is known that the status of the male simplex just after mating is also different from that before mating in *Papilio xuthus* (Sasaki, personal observation), *P. machaon* (Sasaki, personal observation), *Byasa alcinous* (Sasaki, personal observation), and *Eurema hecabe* (Konagaya, personal communication). In addition, this new strategy can be used at

both middle- or low-density mating sites, since it can detect the occurrence of male mating within a few days, and even though the technique only distinguishes between males that have recently mated and those that have not, it still holds promise for examining variation in male mating success and, thereby, investigating traits that correlate with mating success and the intensity of sexual selection.

We note that, when using this method, there might be some traits that are not suitable for investigating the relationship with mating history. For example, it is impossible, in principle, to investigate the relationship between recent mating success and spermatophore production capacity, which is closely related to the reproductive success of both male and female butterflies.

14.4.2 Phenotypic Correlates of Mating Success in Male **B. philenor** *in the Field*

Our results indicate that males that exhibit signs of having recently mated differ from those that do not, in that they are older and have a greener coloration. This could mean that age and coloration are important determinants of male mating success and under selection, either in the context of (1) female choice, in which females prefer older and greener males, or (2) male competition, in which older and greener males are, for some reason, more effective competitors. In general, the results of the present study support the prediction that male coloration and mating success are related. However, Rutowski and Rajyaguru (2013) reported that the dorsal hindwings of successfully mated *B. philenor* males possessed more chromatic iridescence than those that failed to mate, rather than a different hue, as reported here.

Such differences between field and laboratory study have also been reported by previous studies. For example, in-copula males of *Eurema hecabe* were reportedly older than their free-flying counterparts and possessed significantly less bright markings, while brighter males were preferred by females in the laboratory (Kemp 2008). In this case, the difference was caused by the existence of newly emerged females that could not reject mating, and since the density of individuals at the study site was high and activity is centered at localized breeding sites, males could profitably locate such females.

The reasons for difference the color parameters correlated with the mating success of male *B. philenor* have not yet been clarified. It is possible that the data reported here about the specifics of male age and color associated with recent mating success were affected by the several significant correlations among color parameters and between coloration and age. We made efforts to control for these correlations by excluding variables, such as chroma, from our analysis, but in the end, it is difficult to make conclusions with confidence about the reasons for the

connections between male color, age, and male mating success suggested by our data set. In addition, we have not controlled or taken into consideration several other variables that might affect male mating history, such as body size, population density, time during the breeding season, and weather. To convincingly identify factors that determine male mating success in *B. philenor*, the experimental manipulation of candidate variables is needed.

Acknowledgments We thank Masaru Hasegawa and the members of Rutowski Laboratory, especially Sean Hannam, for assistance in the field and laboratory work as well as for valuable discussions. This study was supported by the Japan Society for the Promotion of Science for the Institutional Program for Young Researcher Overseas Visits to NS and TK and in part by JSPS KAKENHI Grant Number 24570019 (MW) and by NSF Grant IOS 1145654 (to R. L. Rutowski). We would like to thank Editage (www.editage.jp) for English language editing.

References

Alcock J, Kemp DJ (2006) The behavioral significance of male body size in the tarantula hawk wasp *Hemipepsis ustulata* (Hymenoptera: Pompilidae). Ethology 112:691–698

Allen CE, Zwaan BJ, Brakefield PM (2011) Evolution of sexual dimorphism in the Lepidoptera. Ann Rev Entomol 56:445–464

Andersson J, Karlson AKB, Vongvanich N, Wiklund C (2007) Male sex pheromone release and female mate choice in a butterfly. J Exp Biol 210:964–970

Beldade P, Koops K, Brakefield PM (2002) Developmental constraints versus flexibility in morphological evolution. Nature 416:844–847

Bissoondath CJ, Wiklund C (1996) Male butterfly investment in successive ejaculates in relation to mating system. Behav Ecol Sociobiol 39:285–292

Blount JD, Metcalfe NB, Birkhead TR, Surai PF (2003) Carotenoid modulation of immune function and sexual attractiveness in zebra finches. Science 300:125–127

Carroll SB, Gates J, Keys DN, Paddock SW, Panganiban GE, Selegue JE, Williams JA (1994) Pattern formation and eyespot determination in butterfly wings. Science 265:109–114

Darwin C (1874) The descent of man and selection in relation to sex. John Murray and Sons, London

Drummond BA (1984) Multiple mating and sperm competition in the Lepidoptera. In: Smith RL (ed) Sperm competition and the evolution of animal mating systems, pp 291–370

Flecker AS, Allan JD, McClintock NL (1988) Male body size and mating success in swarms of the mayfly *Epeorus longimanus*. Ecography 11:280–285

Grether GF, Cummings ME, Hudon J (2005) Countergradient variation in the sexual coloration of guppies (*Poecilia reticulata*): drosopterin synthesis balances carotenoid availability. Evolution 59:175–188

Harari AR, Handler AM, Landolt PJ (1999) Size-assortative mating, male choice and female choice in the curculionid beetle *Diaprepes abbreviatus*. Anim Behav 58:1191–1200

Hill GE, Montgomerie R (1994) Plumage color signals nutritional condition in the house finch. Proc R Soc Lond B 258:47–52

Kazuma M (1987) Mating patterns of a sphragis-bearing butterfly, *Luehdorfia japonica* Leech (Lepidoptera: Papilionidae), with descriptions of mating behavior. Res Popul Ecol 29:97-110

Kemp DJ (2007) Female butterflies prefer males bearing bright iridescent ornamentation. Proc R Soc London B 274:1043–1047
Kemp DJ (2008) Female mating biases for bright ultraviolet iridescence in the butterfly *Eurema hecabe* (Pieridae). Behav Ecol 19:1–8
Kemp DJ, Rutowski RL (2011) The role of coloration in mate choice and sexual interactions in butterflies. Adv Study Behav 43:55–92
Keyser AJ, Hill GE (1999) Condition-dependent variation in the blue-ultraviolet coloration of a structurally based plumage ornament. Proc R Soc Lond B 266:771–777
Koch PB, Keys DN, Rocheleau T, Aronstein K, Blackburn M, Carroll SB (1998) Regulation of dopa decarboxylase expression during colour pattern formation in wild-type and melanic tiger swallowtail butterflies. Development 125:2303–2313
Krebs RA, West AD (1988) Female mate preference and the evolution of female-limited Batesian mimicry. Evolution 42:1101–1104
LaChance LEO, Richard RD, Ruud RL (1977) Movement of eupyrene sperm bundles from the testis and storage in the ductus ejaculatoris duplex of the male pink bollworm: effects of age, strain, irradiation, and light. Ann Entomol Soc Am 70:647–651
Montgomerie R (2008) CLR, version 1.05. Queen's University, Kingston, Canada. Available as of 14 December 2011 at http://post.queensu.ca/~mont/color/analyze.html
Nijhout HF (1990) A comprehensive model for colour pattern formation in butterflies. Proc R Soc London B 239:81–113
Riemann JG, Thorson BJ, Ruud RL (1974) Daily cycle of release of sperm from the testes of the Mediterranean flour moth. J Insect Physiol 20:195–207
Robertson KA, Monteiro A (2005) Female *Bicyclus anynana* butterflies choose males on the basis of their dorsal UV-reflective eyespot pupils. Proc R Soc London B 272:1541–1546
Rutowski RL (1997) Sexual dimorphism, mating systems and ecology in butterflies. In: Choe JC, Crespi BJ (eds) The evolution of mating systems in insects and arachnids. Cambridge University Press, Cambridge, pp 257–272
Rutowski RL, Nahm A, Macedonia JM (2010) Iridescent hindwing patches in the pipevine swallowtail: differences in dorsal and ventral surfaces relate to signal function and context. Funct Ecol 24:767–775
Rutowski RL, Newton M, Schaefer J (1983) Interspecific variation in the size of the nutrient investment made by male butterflies during copulation. Evolution 34:708–713
Rutowski RL, Rajyaguru PK (2013) Male-specific iridescent coloration in the pipevine swallowtail (*Battus philenor*) is used in mate choice by females but not sexual discrimination by males. J Insect Behav 26:200–211
Sasaki N, Konagaya T, Watanabe M, Rutowski RL (2015) Indicators of recent mating success in the pipevine swallowtail butterfly (*Battus philenor*) and their relationship to male phenotype. J Insect Physiol 83:30–36
Svärd L, Wiklund C (1989) Mass and production rate of ejaculates in relation to monandry/polyandry in butterflies. Behav Ecol Sociobiol 24:395–402
Takeuchi T (2016) Agonistic display or courtship behavior? A review of contests over mating opportunity in butterflies. J Ethol:1–10
Tsubaki Y, Matsumoto K (1998) Fluctuating asymmetry and male mating success in a sphragis-bearing butterfly *Luehdorfia japonica* (Lepidoptera: Papilionidae). J Insect Behav 11:571–582
Wallace AR (1889) Darwinism: an exposition of the theory of natural selection, with some of its applications. Macmillan & Co, London
Watanabe M, Hirota M (1999) Effects of sucrose intake on spermatophore mass produced by male swallowtail butterfly *Papilio xuthus* L. Zool Sci 16:55–61

Watanabe M, Sato K (1993) A spermatophore structured in the bursa copulatrix of the small white *Pieris rapae* (Lepidoptera, Pieridae) during copulation, and its sugar content. J Res Lepid 32:26–36

Watanabe M, Nozato K, Kiritani K (1986) Studies on ecology and behavior of Japanese black swallowtail butterflies (Lepidoptera: Papilionidae): V. Fecundity in summer generations. Appl Entomol Zool 21:448–453

Part V
Color Patterns of Larva and Other Insects

Chapter 15
Molecular Mechanisms of Larval Color Pattern Switch in the Swallowtail Butterfly

Hongyuan Jin and Haruhiko Fujiwara

Abstract In lepidopterans (butterflies and moths), larval body color pattern, which is an important mimicry trait involved in prey–predator interactions, presents a great diversity of pigmentation and patterning. Unlike wing patterns, larval body color patterns can switch during development with larval molting. For example, in the Asian swallowtail butterfly *Papilio xuthus*, a younger larva (first–fourth instar) has a white/black color pattern that mimics bird droppings, whereas the final instar (fifth) larva drastically changes to a greenish pattern that provides camouflage on plants. Insect mimicry has interested scientists and the public since Darwin's era. Broadly, mimicry is an antipredation strategy whereby one creature's color, shape, or behavior resembles another creature or object. In this review, I address basic knowledge about larval cuticular pigmentation and advanced understanding of its regulatory mechanism in *P. xuthus*; I also discuss larval body color patterns among members of the genus *Papilio*, followed by conclusions and prospects for further research.

Keywords Larval pigmentation • Lepidoptera • Mimicry • Cuticular melanization • Ecdysteroid • Juvenile hormone • *Papilio xuthus* • *Papilio polytes* • *Papilio machaon*

15.1 Introduction

About 150 years ago, following H.W. Bates' report on mimicry in insects (Bates 1862), Charles Darwin wrote to Bates and said: "In my opinion, it is one of the most remarkable & admirable papers I ever read in my life. The mimetic cases are truly marvelous. . ." (Darwin 1863). Today, the mimicry phenomenon remains as an interesting evolutionary theme as ever, attracting the interest of both scientists and the public. To better understand the molecular mechanisms behind insect mimicry, we need to understand how wing and body color patterns evolve.

H. Jin (✉) • H. Fujiwara
Department of Integrated Biosciences, Graduate School of Frontier Sciences, The University of Tokyo, Kashiwa, Chiba 277-8562, Japan
e-mail: 1169399970@edu.k.u-tokyo.ac.jp

T. Sekimura, H.F. Nijhout (eds.), *Diversity and Evolution of Butterfly Wing Patterns*, DOI 10.1007/978-981-10-4956-9_15

Lepidopterans (butterflies and moths) show highly diverse wing colors and patterns and are considered to be an ideal model system for examining color pattern formation and evolution. In lepidopterans, evidence for wing color and pattern evolution has been frequently reported (Nijhout 1991; Reed et al. 2011; Heliconius Genome 2012; Kunte et al. 2014), whereas our knowledge of larval body coloration and pattern formation is relatively limited.

Generally, lepidopteran larvae are soft bodied and cannot escape by flight from predators. Natural selection has led to the development of many chemical and morphological devices in larvae that aid survival in the wild (Scoble and Scoble 1992). Among those, body color pattern is particularly interesting because it is important in visual recognition. Two different strategies are commonly used for predator defense. Toxic larvae tend to warn predators with their colorful markings which act as warning signals. The majority of larvae, which are palatable and nonpoisonous, mimic an item in the surroundings (such as a bud, a twig, or even a moss) or conceal their bodies in the environmental background (Pasteur 1982).

In the case of *P. xuthus*, a larva switches its body color pattern with larval molting (Fig. 15.1). A younger larva (first–fourth instar) mimics bird droppings with a black/white body color (denoted mimetic pattern, Fig. 15.1a). The fifth (final) instar larva dramatically switches to a greenish body pattern with a pair of eyespots on the metathorax, which allows it to blend in with the color and pattern of its host plant (denoted cryptic pattern, Fig. 15.1b). A similar switching of body color pattern is observed in other *Papilio* species (Prudic et al. 2007) and is considered to be a successful survival strategy for this genus (Tullberg et al. 2005). Recent studies have reported that two critical insect hormones, ecdysone (Fig. 15.2a, b) and juvenile hormone (JH), directly regulate pigmentation and color pattern switch in the larva of *P. xuthus* (Futahashi and Fujiwara 2007, 2008a).

In this chapter, I review recent progress in understanding the molecular mechanisms underlying cuticular melanization and the hormonal regulation of pigmentation in the larva of *P. xuthus*. I also discuss possible evolutionary changes among three *Papilio* species, followed by conclusions and prospects for further research.

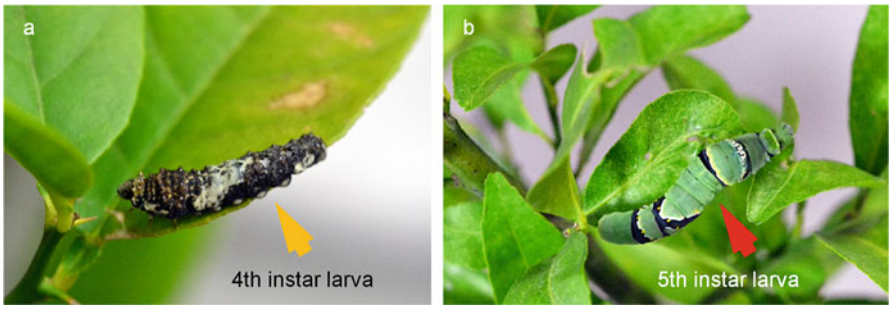

Fig. 15.1 (**a**) Fourth instar larva with bird-dropping body pattern; (**b**) Fifth instar larva with *green* body pattern of *P. xuthus*

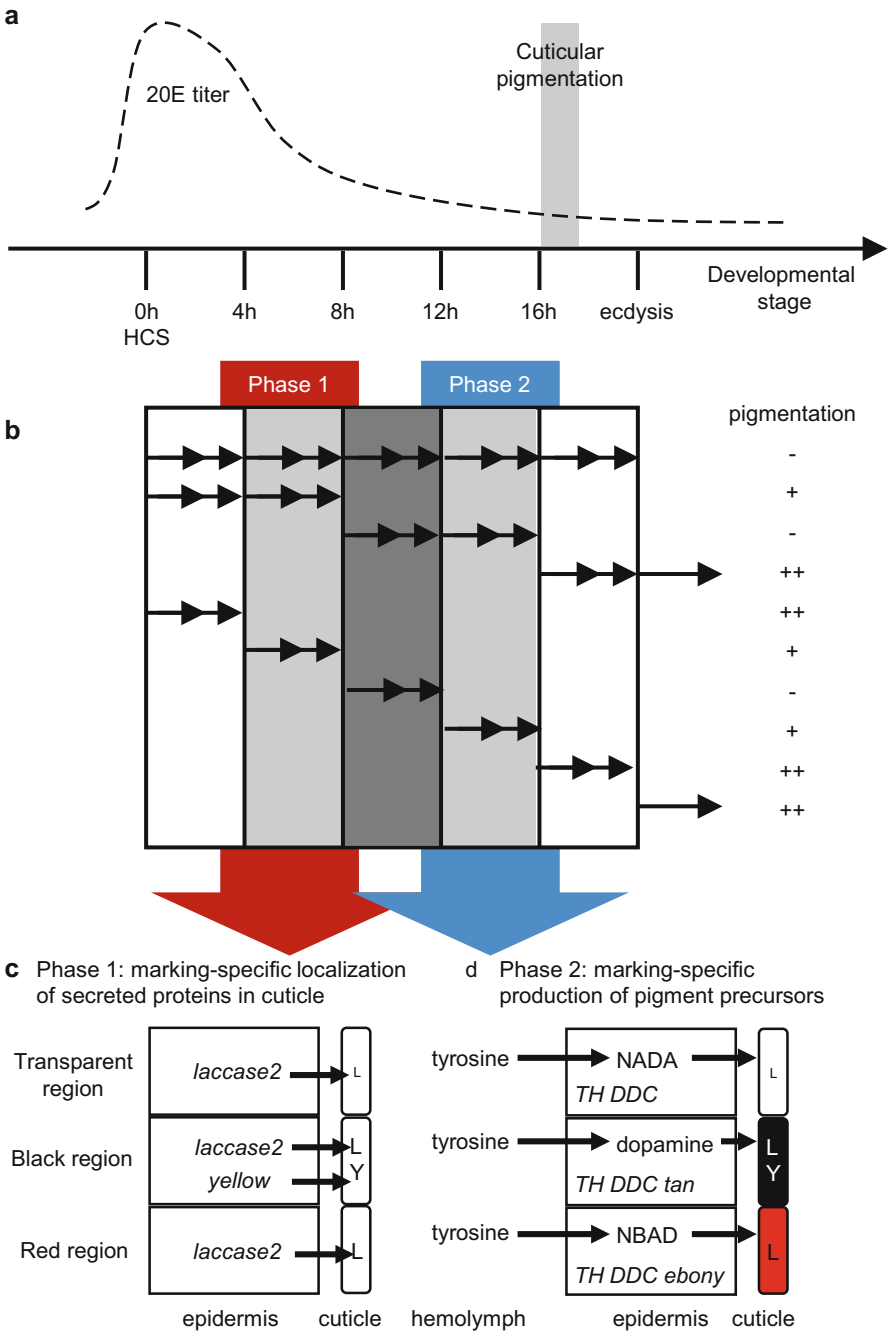

Fig. 15.2 A working model for the two-phase cuticular pigmentation in larvae of *P. xuthus*. (**a**) 20E titer in hemolymph during the fourth molt; (**b**) The timing effect of 20E on *black* pigment synthesis. The intervals of 20E applications (*arrows*, every 2 h); (**c**) phase 1; (**d**) phase 2. N-b-alanyldopamine (NBAD). N-acetyldopamine (NADA). L and Y in cuticle indicate laccase 2 and Yellow proteins (Modified from Futahashi et al. 2010)

15.2 Pigmentation of Larval Cuticle in *P. xuthus*

An insect cuticle is a hardened exoskeleton composed of chitin and proteins. In lepidopteran larvae, black cuticular pigments mainly comprise melanin, which is produced by the oxidization of dopamine or L-3,4-dihydroxyphenylalanine (DOPA) (Kramer and Hopkins 1987; Hiruma and Riddiford 2009; Wright 1987). In both *P. xuthus* and *Manduca sexta* (tobacco hornworm), the pigmentation procedure of larval cuticle can be summarized in two steps: localization of secreted proteins (Fig. 15.2c, phase 1) and production of pigment precursors (Fig. 15.2d, phase 2) (Hiruma and Riddiford 2009; Futahashi et al. 2010; Walter et al. 1991). These steps occur in the cuticle and the epidermal cell, respectively (Fig. 15.2).

In phase 1, laccase 2 (Lac2), which is a phenol oxidase (PO), and other pigment-related proteins (such as Yellow) are synthesized and deposited into the newly forming cuticle (Fig. 15.2c) (Futahashi and Fujiwara 2007; Kramer and Hopkins 1987; Hiruma and Riddiford 1988, 2009). Lac2 catalyzes the oxidation of dopamine to dopamine–melanin in many species (Hiruma and Riddiford 2009; Noh et al. 2016; Futahashi et al. 2011). In *Tribolium castaneum*, laccase 2 (coded by *TmLac2*) is the major PO involved in the tanning of larval, pupal, and adult cuticles (Arakane et al. 2005).

In *P. xuthus*, Futahashi et al. (2010) found that *Pxlaccase2* (*Pxlac2*) expression is strongly associated with the presumptive black pigment (11 h after head capsule slippage (HCS) at the fourth molt) (Futahashi et al. 2010). Typically, expression of Lac2 begins in the middle period of molting, and the deposited Lac2 is on standby until the pigment precursors reach the cuticular surface. These events precede the expression of melanin synthesis genes at mRNA levels and the production of pigment precursors (Walter et al. 1991; Hiruma and Riddiford 1988; True et al. 1999; Futahashi and Fujiwara 2005). Another pigmentation-related protein, Yellow (coded by *Pxyellow*), shows an expression pattern similar to that of Lac2 in phase 1. However, the precise function of *Pxyellow* gene remains unclear (Futahashi et al. 2010; Noh et al. 2016). It is inferred that PxYellow may be secreted into the cuticle and probably acts as a cofactor (Futahashi and Fujiwara 2005).

In phase 2, the precursors of melanin compounds are synthesized from phenolic amino acids (mainly tyrosine) (Fig. 15.2c). The dopamine–melanin synthesis pathway is conserved in many insects (Hiruma and Riddiford 2009; Noh et al. 2016; Futahashi and Fujiwara 2005; Massey and Wittkopp 2016). First, tyrosine is converted to DOPA by tyrosine hydroxylase (TH), and then dopamine is synthesized from DOPA by DOPA decarboxylase (DDC) (Futahashi and Fujiwara 2005). Dopamine is a prominent black pigment precursor in many insects (Hiruma et al. 1985). After its synthesis in an epidermal cell, dopamine is incorporated into the cuticle and converted to dopamine–melanin by PO and other proteins. However, it also can be converted to a reddish brown pigment by ebony or to a transparent pigment called N-acetyldopamine (NADA) by dopamine N-acetyltransferase (DAT) activity (Futahashi et al. 2010; Futahashi and Fujiwara 2005; Massey and Wittkopp 2016; Wittkopp et al. 2002).

In *P. xuthus*, spatially specific localization of melanin synthesis genes contributes to the color pattern (Futahashi and Fujiwara 2005). Futahashi and Fujiwara (2005) showed that the spatial expression of melanin synthesis genes (*TH*, *DDC*, and *tan*) perfectly corresponds with the presumptive black pigment (Futahashi et al. 2010; Futahashi and Fujiwara 2005) and that the expression of *ebony* is limited to the red area within the eyespot (Futahashi and Fujiwara 2005). They also demonstrated that the addition of excess tyrosine did not promote pigmentation, whereas the application of DOPA with 3-iodotyrosine (3IT, a competitive inhibitor of TH protein) led to a clear color pattern with an overall pigmentation in vitro (Futahashi and Fujiwara 2005). Their results indicate that cuticle color patterns form from spatially specific localization of melanin synthesis genes rather than the differential uptake of melanin precursors into individual epidermal cells.

Cuticular pigmentation occurs in the latter half of the molting period just before ecdysis (16–18 h after HCS during the fourth molting period). When Futahashi and Fujiwara (2005) examined the timing of expression of *PxTH*, *PxDDC*, *Pxebony*, and *Pxtan*, they noticed that the expression of these melanin synthesis genes precisely coincides with melanization onset. Therefore, cuticular pigmentation is predictably strictly controlled by ecdysteroid, the molting hormone (Futahashi and Fujiwara 2005, 2007; Futahashi et al. 2010).

15.3 Hormonal Regulation of Larval Pigmentation

Ecdysone and juvenile hormone are directly and indirectly involved in larval pigmentation in insects (Futahashi and Fujiwara 2008a; Hiruma and Riddiford 1990, 2009; Hwang et al. 2003).

15.3.1 Ecdysone-Induced Cuticular Pigmentation

Ecdysone is a steroid hormone and the central regulator in insect development and reproduction (Kopec 1926). The periodic release of ecdysone triggers larval molting and pupal metamorphosis (Yamanaka et al. 2013).

The first evidence of ecdysone-regulated pigmentation was reported by Karlson and Sekeris in 1976. They showed that ecdysone causes elevated activity of DDC in *Calliphora* (Hiruma and Riddiford 2009; Karlson and Sekeris 1976). In *M. sexta*, regulation of DDC expression requires exposure of 20-hydroxyecdysone (also known as 20E, an active form of ecdysone), followed by its withdrawal during larval molting (Hiruma and Riddiford 1986, 1990; Hiruma et al. 1995; Hiruma and Riddiford 2007). Hiruma et al. (1995) found continuous exposure of 20E insufficient for DDC expression, unless there is a 20E-free period (Hiruma et al. 1995).

In *P. xuthus*, Futahashi and Fujiwara (2007) successfully tested the effect of 20E exposure on larval pigmentation using a topical application method in vivo.

Consistent with the results in *M. sexta*, they demonstrated that cuticular melanization and epidermal pigmentation are inhibited through 20E treatment during the molt and confirmed that the removal of ecdysone is necessary for the onset of normal coloration. Moreover, they showed that 20E inhibited pigmentation if it was applied at the middle of the molt when native ecdysone titers decline (Fig. 15.2b) (Futahashi and Fujiwara 2007). As expected, the expression of melanin synthesis genes, including *TH*, *DDC*, and *ebony*, was repressed by high 20E concentration (Futahashi and Fujiwara 2007). Unexpectedly, the expression of *Pxyellow* was promoted by a high concentration of 20E. This led Futahashi and Fujiwara to hypothesize that PxYellow must function as a cofactor for other melanin synthesis enzymes since it alone is not sufficient for melanization (Futahashi and Fujiwara 2007).

Like the pigment synthesis genes, some upstream regulatory factors are also controlled by ecdysone. In the ecdysone signaling pathway, 20E acts as a hormonal signal and regulates the expression of downstream transcription factors (Yamanaka et al. 2013; Yao et al. 1992). Hiruma and Riddiford (2007) found that two nuclear transcription factors, E75B and MHR4, are 20E-induced inhibitors of *Msddc* in vitro (Hiruma and Riddiford 2007). Evidence also showed that there is at least one other suppressive protein other than E75B and MHR4 that binds to a specific sequence (GGCTTATGCGCTGCA) in the DDC promoter when the ecdysone titer decreases (Hiruma et al. 1995). In *Drosophila melanogaster*, *DmDDC* is directly modulated by an ecdysone response element (EcRE), located at position −97 to −83 bp relative to the transcription initiation site (Chen et al. 2002). In *D. melanogaster*, Yellow is known to be a prepattern factor as well as a pigmentation factor in adult body patterning (Massey and Wittkopp 2016). Recently, comprehensive yeast one-hybrid and RNAi screens were carried out by Kalay et al. (2016). They screened and identified four ecdysone-induced nuclear reporters (*Hr78*, *Hr38*, *Hr46*, and *Eip78C*) that showed a statistically significant interaction with at least one Yellow enhancer. In an RNAi experiment, all four caused altered pigmentation when knocked down (Kalay et al. 2016). In *Bombyx mori*, Yamaguchi et al. (2013) used a type of *L* (multi lunar) mutant with twin-spot markings on the sequential segments and proved that the gene responsible for this phenotype (*BmWnt1*) can be induced by high concentrations of 20E in vitro (Yamaguchi et al. 2013).

In *P. xuthus*, Futahashi et al. (2012) used a microarray EST dataset to recognize *E75A* and *E75B*, which are transcription factors involved in ecdysone signaling, as candidates involved in specific marking-specific patterning (Futahashi et al. 2012). The expression of *E75A* and *E75B* is specifically localized at the eyespot marking region, and temporal expression patterns are similar to those of *Pxyellow*, as described before. It is known that *E75* is active early in ecdysone signaling (Palli et al. 1995; Jindra et al. 1994; Jindra and Riddiford 1996). Taken together, this suggests that 20E-induced *E75A* and/or *E75B* expression may regulate both the prepattern of marking and the stage specificity of several black marking-associated genes (Futahashi et al. 2012). Interestingly, 3-dehydroecdysone 3β-reductase (coded by the *3DE 3β-reductase* gene) has a clear marking-specific expression in

the presumptive black region, similar to TH or DDC. Since its function is converting inactivated 3-dehydroecdysone to ecdysone, localized marking-specific ecdysone synthesis may be critical for complex cuticular pigmentation and patterning (Futahashi et al. 2012).

The evidence above shows that there is a complicated relationship between ecdysone signaling and larval cuticular pigmentation and patterning. However, because only some of the regulatory genes have been identified, the detailed regulatory mechanisms remain to be uncovered.

15.3.2 Juvenile Hormone Directly Regulates Larval Color Pattern Switch

Juvenile hormone (JH) is a group of acyclic sesquiterpenoids secreted from the corpora allata (CA), which is an endocrine gland near the brain (Jindra et al. 2013). Like ecdysteroids, JH plays a critical role in molting, metamorphosis, reproduction, and other physiological processes in insects (Jindra et al. 2013). JH is also known as "*status quo* hormone," because the presence of JH prevents insect metamorphosis (Riddiford 1996). In a simplified model, a lepidopteran progresses through a larva-to-larva molt when JH is present and a larva-to-pupa metamorphosis when JH is absent at the final molting stage. It has been hypothesized that JH modulates the action of ecdysteroid-molting hormones, but the detailed mechanisms of the modulation are still unclear (Jindra et al. 2013; Urena et al. 2014; Kayukawa et al. 2016).

There is some evidence that JH has an effect on larval pigmentation. Lack of sufficient JH (caused by the artificial removal of the CA from the larva) causes black larvae in the tobacco hornworm, *M. sexta*. In addition, when the larvae of the black strain are treated with JH, they revert to their normal green color (Riddiford 1975).

As described above, *P. xuthus* larvae markedly switch from a black/white body pattern to a greenish one after the fourth–fifth larval ecdysis (Fig. 15.1). Futahashi (2006) found that when 20E was injected at the early fourth instar stage, precociously molted fifth larva appeared with a black/white mimetic pattern instead of the normal green pattern (Futahashi 2006). It is known and proven that JH controls the action of ecdysteroid at least through direct inhibition of *Broad–Complex* (*BR-C*) activity (Kayukawa et al. 2016; Nijhout and Wheeler 1982; Ogihara et al. 2015). To define the role of JH in facilitating larval color pattern regulation, Futahashi and Fujiwara (2008a) performed experiments using three types of JH analogs (JHA), which they artificially applied on the integument of fourth instar larvae (Fig. 15.3). Their results showed that some individuals failed to switch color patterns, either completely or partially, after the fourth molt. The larvae treated with fenoxycarb (JHA) kept a fourth instar-like black/white pattern or developed an intermediate color pattern with elements of both fourth and fifth instars (Fig. 15.3).

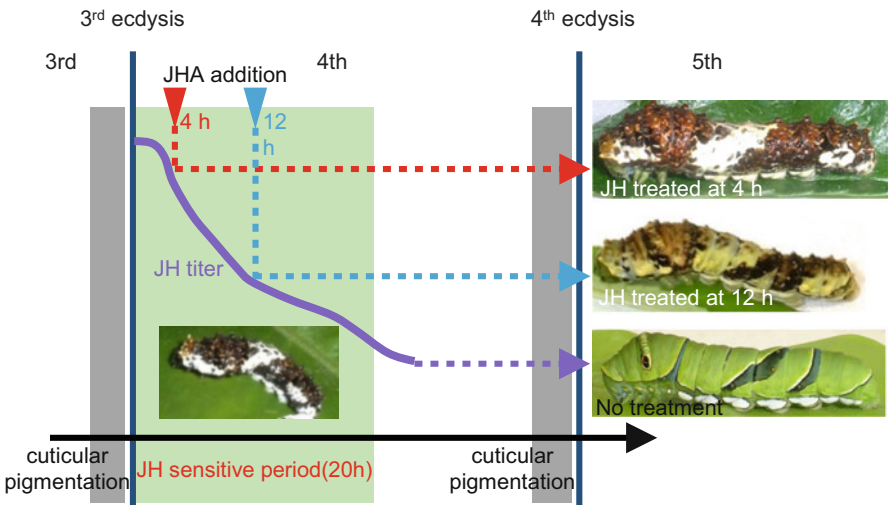

Fig. 15.3 Treatment of juvenile hormone analogs during the JH-sensitive period (Modified from Futahashi and Fujiwara 2008a)

Furthermore, they noticed that the epidermis is only sensitive to JHA during the first 20 h of the fourth instar stage. Exposure after this relatively short time frame did not prevent the color pattern switch. Hence, they named that specific time window "JH-sensitive period." In nontreated species, JH titer in the hemolymph was measured and found to be decreasing continuously during the early days of the fourth instar stage. Taken together, this evidence indicates that the decline of JH titer within a restricted developmental stage regulates the body color pattern switch in *P. xuthus* larvae (Futahashi and Fujiwara 2008a).

Because of our fragmentary knowledge of JH pathways, the molecular mechanisms underlying how JH alters color patterning and controls pigment synthesis are still under investigation (Jindra et al. 2013). Jin et al. have found some candidate genes involved in the larval color pattern switch by RNAi screening using the latest genomic information of *P. xuthus* (unpublished data). In my opinion, future studies may shed light on the downstream regulation of the JH cascade in larval pigmentation.

15.4 Species-Specific Color Patterns in the *Papilio* Genus

15.4.1 A Combination of Yellow and Blue Makes the Larval Body Green

A greenish body pattern follows the bird-dropping pattern in many *Papilio* species, making us wonder what the identity of the "green" pigment is. Green body

coloration seems to be a beneficial adaptation for the final instar larvae of *Papilio*, which helps them conceal themselves in the host plant. The chemical nature of caterpillar's green pigment was once misunderstood as chlorophyll derived from the plant because of the strong color resemblance (Meldola 1873). However, studies show that larval green pigmentation is instead formed by a particular combination of yellow and blue pigments (Przibram and Lederer 1933). Przibram and Lederer (1933) proposed that the yellow pigments are carotenoids and that most of the blue pigments are biliverdins (Przibram and Lederer 1933). Later investigations led to a model that postulates that pigments are intimately associated with specific proteins and that the complex of pigment-conjugated proteins presents the visible coloration (Kawooya et al. 1985).

The blue pigment-binding protein (or bilin-binding protein, BBP) has been isolated and identified in various lepidopterans (Riley et al. 1984; Huber et al. 1987; Saito and Shimoda 1997; Kayser et al. 2009). In *M. sexta*, insecticyanin (INS) was identified to be a bilin-binding protein. Riddiford et al. (1990) found that INS is synthesized in the epidermis and is mainly stored in epidermal pigment granules or secreted into the hemolymph and cuticle (Riddiford et al. 1990). Other pigment-binding proteins are less well known. Although carotenoid-binding protein (CBP) has been well studied in vertebrates (Bhosale and Bernstein 2007), few homologs have been recognized among the Lepidoptera. In Lepidoptera, the *yellow-blood* mutant (Y) of *B. mori* (which produces yellow cocoon) was identified (Tsuchida and Sakudoh 2015); however, the expression of *BmCBP* was not detected in the epidermis. Using next-generation sequencing (NGS) technology, whole genomes of several lepidopteran species were recently released (Suetsugu et al. 2013; Li et al. 2015; Nishikawa et al. 2015; Kanost et al. 2016). Putative BmCBP homologs in other lepidopteran species can be found by BLAST search. Nonetheless, no biological experiment has been performed, and the molecular functions of these putative CBPs are largely unknown.

In *P. xuthus*, two related genes, *bilin-binding protein 1* (*BBP1*) and *yellow-related protein* (*YRG*), were identified to be associated with greenish epidermal coloration by Futahashi and Fujiwara (2008a, b) and Shirataki et al. (2010), respectively. In addition, two *putative carotenoid-binding proteins* (*PCBP1*, *PCBP2*) and other members of BBP family were later identified, which proved to be specifically expressed in the green epidermal regions during the final larval ecdysis (Futahashi et al. 2012).

15.4.2 Species-Specific Color Pattern Among Papilio *Species*

Another vital question in adaptive evolution is how the larval body pattern evolves among closely related species. There are about 200 species included in the genus *Papilio*, and these cover more than one-third of all Papilionidae (Prudic et al. 2007). In the genus *Papilio*, all the larvae share a similar bird-dropping coloration (mimetic pattern) until the fourth or fifth (final) instar (Prudic et al. 2007). The

color pattern in the final instar stage is divided into three patterns: bird-dropping mimetic pattern, green cryptic pattern, and aposematic pattern with orange or black spots and black or white stripes (Prudic et al. 2007; Yamaguchi et al. 2013).

Shirataki et al. (2010) investigated the larval color pattern formation using three *Papilio* species: *P. xuthus*, *P. machaon*, and *P. polytes* (Shirataki et al. 2010). In 2015, whole-genome sequences of those three species were released and made freely accessible (Li et al. 2015; Nishikawa et al. 2015). The last instar larvae of *P. xuthus* and *P. polytes* exhibit similar green cryptic body patterns, with a pair of eyespots on the metathorax and a V-shaped marking on the abdomen, whereas the fourth and fifth instar larvae of *P. machaon* have aposematic color patterns, with a greenish epidermis covered by black bands and an orange twin-spot marking. However, *P. xuthus* and *P. machaon* are more closely related to each other than either is to *P. polytes* (Fig. 15.4) (Zakharov et al. 2004).

Shirataki et al. (2010) cloned several pigmentation-related genes, including *TH*, *DDC*, *yellow*, *BBP1*, and *YRG*, from all three species and compared their expression patterns using in situ hybridization (Fig. 15.4). The results showed a perfect correlation between gene expression and pigmentation among species. Expression of TH, DDC, and yellow matched the black regions in the eyespot, the V-shaped markings of *P. xuthus* and *P. polytes*, and the black bands of *P. machaon*. Regardless of the universal expression of BBP1 and YRG in the green regions among all the three species, BBP1 was specifically expressed in the blue spots in *P. polytes*, and YRG was tightly associated with the orange spots in *P. machaon*. Notably, a unique expression pattern of *ebony* was only detected in the red area within the eyespot region in *P. xuthus*. This work led to the model described in Fig. 15.3.

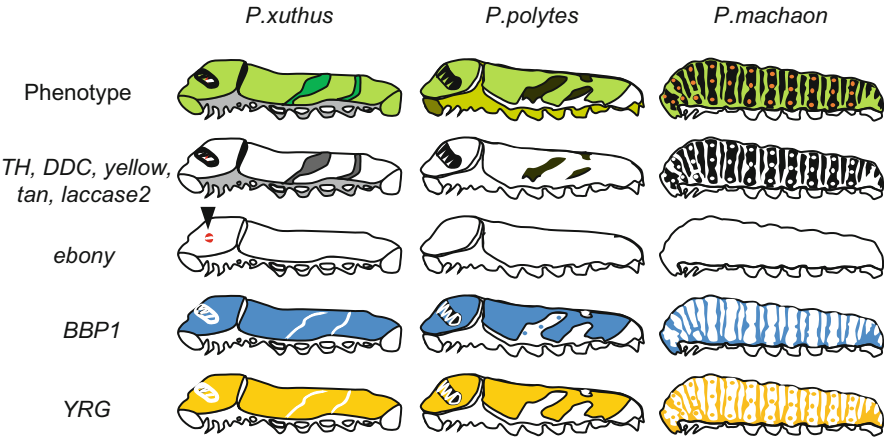

Fig. 15.4 Schema of species-specific body color pattern among three *Papilio* species (Modified from Shirataki et al. 2010)

15.4.3 *Trans-regulation of YRG in the Genus* Papilio

Morphological and phenotypic differences arising from evolutionary change, particularly using large-scale genetic information, have been recently identified in lepidopterans (Kunte et al. 2014; Nishikawa et al. 2015; Wallbank et al. 2016). Some studies have examined the genetic basis underlying intraspecific differences among members of the genus *Drosophila (*Massey and Wittkopp 2016; Wittkopp et al. 2009*)*. F1 hybrids allow researchers to understand regulation changes between close species (Wittkopp et al. 2003, 2008; Wittkopp and Kalay 2012).

Although hybrids of *Papilio* species are difficult to breed under laboratory conditions (Watanabe 1968), Shirataki et al. (2010) successfully bred an F1 hybrid by hand-pairing a *P. xuthus* male with a *P. polytes* female (Clarke and Sheppard 1956), and the fifth instar larvae showed intermediate characteristics between parents (Shirataki et al. 2010). One pigment-related gene, *YRG*, was selected to study expression patterns in the F1 hybrid because both the nucleotide and amino acid sequences had diverged enough to include species-specific regions. Species-specific YRG probes (PxYRG and PpYRG) were designed, and the spatial expression pattern was detected in the last instar larvae of the F1 hybrid. Both the PxYRG and PpYRG probes showed similar expression patterns, indicating that changes in expression of the *YRG* gene are mainly caused by trans-regulatory changes (Shirataki et al. 2010).

15.5 Conclusion and Future Prospects

In the swallowtail butterfly, the larval body color pattern is a vital ecological trait that affects prey–predator interactions. It is precisely regulated by ecdysteroid and juvenile hormone. In *P. xuthus*, pigmentation mechanisms and pathways have been recently elucidated. However, the details of hormonal regulation need to be understood, and the molecular mechanism underlying larval body color patterning has not been studied. New information from next-generation whole-genome sequencing projects will provide a valuable resource that can be used to gain insight into the genetic basis underlying those questions. Moreover, pioneering functional analysis methods, like electroporation-mediated transgenic methods (Ando and Fujiwara 2013) and the CRISPR/Cas9 system (Li et al. 2015), may also lead to new approaches for examining gene functions in non-model species, such as *P. xuthus*.

References

Ando T, Fujiwara H (2013) Electroporation-mediated somatic transgenesis for rapid functional analysis in insects. Development 140(2):454–458. doi:10.1242/dev.085241

Arakane Y, Muthukrishnan S, Beeman RW, Kanost MR, Kramer KJ (2005) Laccase 2 is the phenoloxidase gene required for beetle cuticle tanning. Proc Natl Acad Sci U S A 102 (32):11337–11342. doi:10.1073/pnas.0504982102

Bates HW (1862) XXXII. Contributions to an insect fauna of the Amazon valley. Lepidoptera: Heliconidæ. Trans Linn Soc Lond 23(3):495–566. doi:10.1111/j.1096-3642.1860.tb00146.x

Bhosale P, Bernstein PS (2007) Vertebrate and invertebrate carotenoid-binding proteins. Arch Biochem Biophys 458(2):121–127. doi:10.1016/j.abb.2006.10.005

Chen L, Reece C, O'Keefe SL, Hawryluk GW, Engstrom MM, Hodgetts RB (2002) Induction of the early-late Ddc gene during Drosophila metamorphosis by the ecdysone receptor. Mech Dev 114(1–2):95–107

Clarke CA, Sheppard PM (1956) Hand-pairing of butterflies. Lepid News New Haven 10:47–53

Darwin CR (1863) To H.W. Bates "Letter no.3816,". Cleveland Health Sciences Library, Cleveland

Futahashi R (2006) Molecular mechanisms of mimicry in larval body marking of the swallowtail butterfly, Papilio xuthus. The University of Tokyo, Tokyo

Futahashi R, Fujiwara H (2005) Melanin-synthesis enzymes coregulate stage-specific larval cuticular markings in the swallowtail butterfly, Papilio xuthus. Dev Genes Evol 215 (10):519–529. doi:10.1007/s00427-005-0014-y

Futahashi R, Fujiwara H (2007) Regulation of 20-hydroxyecdysone on the larval pigmentation and the expression of melanin synthesis enzymes and yellow gene of the swallowtail butterfly, Papilio xuthus. Insect Biochem Mol Biol 37(8):855–864. doi:10.1016/j.ibmb.2007.02.014

Futahashi R, Fujiwara H (2008a) Juvenile hormone regulates butterfly larval pattern switches. Science 319(5866):1061. doi:10.1126/science.1149786

Futahashi R, Fujiwara H (2008b) Identification of stage-specific larval camouflage associated genes in the swallowtail butterfly, Papilio xuthus. Dev Genes Evol 218(9):491–504. doi:10.1007/s00427-008-0243-y

Futahashi R, Banno Y, Fujiwara H (2010) Caterpillar color patterns are determined by a two-phase melanin gene prepatterning process: new evidence from tan and laccase2. Evol Dev 12 (2):157–167. doi:10.1111/j.1525-142X.2010.00401.x

Futahashi R, Tanaka K, Matsuura Y, Tanahashi M, Kikuchi Y, Fukatsu T (2011) Laccase2 is required for cuticular pigmentation in stinkbugs. Insect Biochem Mol Biol 41(3):191–196. doi:10.1016/j.ibmb.2010.12.003

Futahashi R, Shirataki H, Narita T, Mita K, Fujiwara H (2012) Comprehensive microarray-based analysis for stage-specific larval camouflage pattern-associated genes in the swallowtail butterfly, Papilio xuthus. BMC Biol 10:46. doi:10.1186/1741-7007-10-46

Heliconius Genome C (2012) Butterfly genome reveals promiscuous exchange of mimicry adaptations among species. Nature 487(7405):94–98. doi:10.1038/nature11041

Hiruma K, Riddiford LM (1986) Inhibition of dopa decarboxylase synthesis by 20-hydroxyecdysone during the last larval moult of Manduca sexta. Insect Biochem 16 (1):225–231. doi:10.1016/0020-1790(86)90100-9

Hiruma K, Riddiford LM (1988) Granular phenoloxidase involved in cuticular melanization in the tobacco hornworm: regulation of its synthesis in the epidermis by juvenile hormone. Dev Biol 130(1):87–97

Hiruma K, Riddiford LM (1990) Regulation of dopa decarboxylase gene expression in the larval epidermis of the tobacco hornworm by 20-hydroxyecdysone and juvenile hormone. Dev Biol 138(1):214–224

Hiruma K, Riddiford LM (2007) The coordination of the sequential appearance of MHR4 and dopa decarboxylase during the decline of the ecdysteroid titer at the end of the molt. Mol Cell Endocrinol 276(1–2):71–79. doi:10.1016/j.mce.2007.07.002

Hiruma K, Riddiford LM (2009) The molecular mechanisms of cuticular melanization: the ecdysone cascade leading to dopa decarboxylase expression in Manduca sexta. Insect Biochem Mol Biol 39(4):245–253. doi:10.1016/j.ibmb.2009.01.008

Hiruma K, Riddiford LM, Hopkins TL, Morgan TD (1985) Roles of dopa decarboxylase and phenoloxidase in the melanization of the tobacco hornworm and their control by 20-hydroxyecdysone. J Comp Physiol B 155(6):659–669

Hiruma K, Carter MS, Riddiford LM (1995) Characterization of the dopa decarboxylase gene of Manduca sexta and its suppression by 20-hydroxyecdysone. Dev Biol 169(1):195–209. doi:10.1006/dbio.1995.1137

Huber R, Schneider M, Mayr I, Muller R, Deutzmann R, Suter F, Zuber H, Falk H, Kayser H (1987) Molecular structure of the bilin binding protein (BBP) from Pieris brassicae after refinement at 2.0 A resolution. J Mol Biol 198(3):499–513

Hwang JS, Kang SW, Goo TW, Yun EY, Lee JS, Kwon OY, Chun T, Suzuki Y, Fujiwara H (2003) cDNA cloning and mRNA expression of L-3,4-dihydroxyphenylalanine decarboxylase gene homologue from the silkworm, Bombyx mori. Biotechnol Lett 25(12):997–1002

Jindra M, Riddiford LM (1996) Expression of ecdysteroid-regulated transcripts in the silk gland of the wax moth, Galleria mellonella. Dev Genes Evol 206(5):305–314. doi:10.1007/s004270050057

Jindra M, Sehnal F, Riddiford LM (1994) Isolation, characterization and developmental expression of the ecdysteroid-induced E75 gene of the wax moth Galleria mellonella. Eur J Biochem 221(2):665–675

Jindra M, Palli SR, Riddiford LM (2013) The juvenile hormone signaling pathway in insect development. Annu Rev Entomol 58:181–204. doi:10.1146/annurev-ento-120811-153700

Kalay G, Lusk R, Dome M, Hens K, Deplancke B, Wittkopp PJ (2016) Potential direct regulators of the Drosophila yellow gene identified by yeast one-hybrid and RNAi screens. G3 (Bethesda) 6(10):3419–3430. doi:10.1534/g3.116.032607

Kanost MR, Arrese EL, Cao X, Chen YR, Chellapilla S, Goldsmith MR, Grosse-Wilde E, Heckel DG, Herndon N, Jiang H, Papanicolaou A, Qu J, Soulages JL, Vogel H, Walters J, Waterhouse RM, Ahn SJ, Almeida FC, An C, Aqrawi P, Bretschneider A, Bryant WB, Bucks S, Chao H, Chevignon G, Christen JM, Clarke DF, Dittmer NT, Ferguson LC, Garavelou S, Gordon KH, Gunaratna RT, Han Y, Hauser F, He Y, Heidel-Fischer H, Hirsh A, Hu Y, Jiang H, Kalra D, Klinner C, Konig C, Kovar C, Kroll AR, Kuwar SS, Lee SL, Lehman R, Li K, Li Z, Liang H, Lovelace S, Lu Z, Mansfield JH, McCulloch KJ, Mathew T, Morton B, Muzny DM, Neunemann D, Ongeri F, Pauchet Y, Pu LL, Pyrousis I, Rao XJ, Redding A, Roesel C, Sanchez-Gracia A, Schaack S, Shukla A, Tetreau G, Wang Y, Xiong GH, Traut W, Walsh TK, Worley KC, Wu D, Wu W, Wu YQ, Zhang X, Zou Z, Zucker H, Briscoe AD, Burmester T, Clem RJ, Feyereisen R, Grimmelikhuijzen CJ, Hamodrakas SJ, Hansson BS, Huguet E, Jermiin LS, Lan Q, Lehman HK, Lorenzen M, Merzendorfer H, Michalopoulos I, Morton DB, Muthukrishnan S, Oakeshott JG, Palmer W, Park Y, Passarelli AL, Rozas J, Schwartz LM, Smith W, Southgate A, Vilcinskas A, Vogt R, Wang P, Werren J, Yu XQ, Zhou JJ, Brown SJ, Scherer SE, Richards S, Blissard GW (2016) Multifaceted biological insights from a draft genome sequence of the tobacco hornworm moth, Manduca sexta. Insect Biochem Mol Biol. doi:10.1016/j.ibmb.2016.07.005

Karlson P, Sekeris CE (1976) Control of tyrosine metabolism and cuticle sclerotization by ecdysone. The insect integument. l-571. Elsevier Scientific Publishing Company, Amsterdam/Oxford/New York

Kawooya JK, Keim PS, Law JH, Riley CT, Ryan RO, Shapiro JP (1985) Why are green caterpillars green. ACS Symp Ser 276:511–521

Kayser H, Mann K, Machaidze G, Nimtz M, Ringler P, Muller SA, Aebi U (2009) Isolation, characterisation and molecular imaging of a high-molecular-weight insect biliprotein, a member of the Hexameric Arylphorin protein family. J Mol Biol 389(1):74–89. doi:10.1016/j.jmb.2009.03.075

Kayukawa T, Nagamine K, Ito Y, Nishita Y, Ishikawa Y, Shinoda T (2016) Kruppel homolog 1 inhibits insect metamorphosis via direct transcriptional repression of broad-complex, a pupal specifier gene. J Biol Chem 291(4):1751–1762. doi:10.1074/jbc.M115.686121

Kopec S (1926) Experiments on metamorphosis of insects. Bull Int Acad Polon Sci Cracow B 1917:57–60

Kramer KJ, Hopkins TL (1987) Tyrosine metabolism for insect cuticle tanning. Arch Insect Biochem Physiol 6(4):279–301. doi:10.1002/arch.940060406

Kunte K, Zhang W, Tenger-Trolander A, Palmer DH, Martin A, Reed RD, Mullen SP, Kronforst MR (2014) Doublesex is a mimicry supergene. Nature 507(7491):229–232. doi:10.1038/nature13112

Li X, Fan D, Zhang W, Liu G, Zhang L, Zhao L, Fang X, Chen L, Dong Y, Chen Y, Ding Y, Zhao R, Feng M, Zhu Y, Feng Y, Jiang X, Zhu D, Xiang H, Feng X, Li S, Wang J, Zhang G, Kronforst MR, Wang W (2015) Outbred genome sequencing and CRISPR/Cas9 gene editing in butterflies. Nat Commun 6:8212. doi:10.1038/ncomms9212

Massey JH, Wittkopp PJ (2016) The genetic basis of pigmentation differences within and between Drosophila species. Curr Top Dev Biol 119:27–61. doi:10.1016/bs.ctdb.2016.03.004

Meldola R (1873) On a certain class of cases of variable protective colouring in insects. Proc Zool Soc:153–162

Nijhout HF (1991) The development and evolution of butterfly wing patterns. Smithsonian series in comparative evolutionary biology: the development and evolution of butterfly wing patterns. Smithsonian Institution Press, Washington, DC/London

Nijhout HF, Wheeler DE (1982) Juvenile-hormone and the physiological-basis of insect polymorphisms. Q Rev Biol 57(2):109–133

Nishikawa H, Iijima T, Kajitani R, Yamaguchi J, Ando T, Suzuki Y, Sugano S, Fujiyama A, Kosugi S, Hirakawa H, Tabata S, Ozaki K, Morimoto H, Ihara K, Obara M, Hori H, Itoh T, Fujiwara H (2015) A genetic mechanism for female-limited Batesian mimicry in Papilio butterfly. Nat Genet. doi:10.1038/ng.3241

Noh MY, Muthukrishnan S, Kramer KJ, Arakane Y (2016) Cuticle formation and pigmentation in beetles. Curr Opin Insect Sci 17:1–9. doi:10.1016/j.cois.2016.05.004

Ogihara MH, Hikiba J, Iga M, Kataoka H (2015) Negative regulation of juvenile hormone analog for ecdysteroidogenic enzymes. J Insect Physiol. doi:10.1016/j.jinsphys.2015.03.012

Palli SR, Sohi SS, Cook BJ, Lambert D, Ladd TR, Retnakaran A (1995) Analysis of ecdysteroid action in Malacosoma disstria cells: cloning selected regions of E75- and MHR3-like genes. Insect Biochem Mol Biol 25(6):697–707

Pasteur G (1982) A classificatory review of mimicry systems. Annu Rev Ecol Syst 13:169–199

Prudic KL, Oliver JC, Sperling FA (2007) The signal environment is more important than diet or chemical specialization in the evolution of warning coloration. Proc Natl Acad Sci U S A 104 (49):19381–19386. doi:10.1073/pnas.0705478104

Przibram H, Lederer E (1933) Das Tiergrun der Heuschrecken als Mischung aus Farbstoffen. Anz Akad Wiss Wien 70:163–165

Reed RD, Papa R, Martin A, Hines HM, Counterman BA, Pardo-Diaz C, Jiggins CD, Chamberlain NL, Kronforst MR, Chen R, Halder G, Nijhout HF, McMillan WO (2011) Optix drives the repeated convergent evolution of butterfly wing pattern mimicry. Science 333 (6046):1137–1141. doi:10.1126/science.1208227

Riddiford LSLM (1975) The biology of the black larval mutant of the tobacco hornworm, Manduca sexta. J Insect Physiol 21(12):1931–1933, 1935–1938

Riddiford LM (1996) Juvenile hormone: the status of its "status quo" action. Arch Insect Biochem Physiol 32(3–4):271–286. doi:10.1002/(SICI)1520-6327(1996)32:3/4<271::AID-ARCH2>3.0.CO;2-W

Riddiford LM, Palli SR, Hiruma K, Li W, Green J, Hice RH, Wolfgang WJ, Webb BA (1990) Developmental expression, synthesis, and secretion of insecticyanin by the epidermis of the tobacco hornworm, Manduca sexta. Arch Insect Biochem Physiol 14(3):171–190. doi:10.1002/arch.940140305

Riley CT, Barbeau BK, Keim PS, Kezdy FJ, Heinrikson RL, Law JH (1984) The covalent protein structure of insecticyanin, a blue biliprotein from the hemolymph of the tobacco hornworm, Manduca sexta L. J Biol Chem 259(21):13159–13165

Saito H, Shimoda M (1997) Insecticyanin of Agrius convolvuli: purification and characterization of the biliverdin-binding protein from the larval hemolymph. Zool Sci 14(5):777–783. doi:10.2108/zsj.14.777

Scoble MJ, Scoble MJ (1992) The Lepidoptera. British Museum/Oxford University Press, London/Oxford

Shirataki H, Futahashi R, Fujiwara H (2010) Species-specific coordinated gene expression and trans-regulation of larval color pattern in three swallowtail butterflies. Evol Dev 12 (3):305–314. doi:10.1111/j.1525-142X.2010.00416.x

Suetsugu Y, Futahashi R, Kanamori H, Kadono-Okuda K, Sasanuma S, Narukawa J, Ajimura M, Jouraku A, Namiki N, Shimomura M, Sezutsu H, Osanai-Futahashi M, Suzuki MG, Daimon T, Shinoda T, Taniai K, Asaoka K, Niwa R, Kawaoka S, Katsuma S, Tamura T, Noda H, Kasahara M, Sugano S, Suzuki Y, Fujiwara H, Kataoka H, Arunkumar KP, Tomar A, Nagaraju J, Goldsmith MR, Feng Q, Xia Q, Yamamoto K, Shimada T, Mita K (2013) Large scale full-length cDNA sequencing reveals a unique genomic landscape in a lepidopteran model insect, Bombyx mori. G3 (Bethesda) 3(9):1481–1492. doi:10.1534/g3.113.006239

True JR, Edwards KA, Yamamoto D, Carroll SB (1999) Drosophila wing melanin patterns form by vein-dependent elaboration of enzymatic prepatterns. Curr Biol 9(23):1382–1391

Tsuchida K, Sakudoh T (2015) Recent progress in molecular genetic studies on the carotenoid transport system using cocoon-color mutants of the silkworm. Arch Biochem Biophys 572:151–157. doi:10.1016/j.abb.2014.12.029

Tullberg BS, Merilaita S, Wiklund C (2005) Aposematism and crypsis combined as a result of distance dependence: functional versatility of the colour pattern in the swallowtail butterfly larva. Proc Biol Sci 272(1570):1315–1321. doi:10.1098/rspb.2005.3079

Urena E, Manjon C, Franch-Marro X, Martin D (2014) Transcription factor E93 specifies adult metamorphosis in hemimetabolous and holometabolous insects. Proc Natl Acad Sci U S A 111 (19):7024–7029. doi:10.1073/pnas.1401478111

Wallbank RW, Baxter SW, Pardo-Diaz C, Hanly JJ, Martin SH, Mallet J, Dasmahapatra KK, Salazar C, Joron M, Nadeau N, McMillan WO, Jiggins CD (2016) Evolutionary novelty in a butterfly wing pattern through enhancer shuffling. PLoS Biol 14(1):e1002353. doi:10.1371/journal.pbio.1002353

Walter MF, Black BC, Afshar G, Kermabon AY, Wright TR, Biessmann H (1991) Temporal and spatial expression of the yellow gene in correlation with cuticle formation and dopa decarboxylase activity in Drosophila development. Dev Biol 147(1):32–45

Watanabe K (1968) A study of interspecific hybrids between Papilio machaon hippocrates and P. xuthus. Trans Lep Soc Jpn 19(1&2):3

Wittkopp PJ, Kalay G (2012) Cis-regulatory elements: molecular mechanisms and evolutionary processes underlying divergence. Nat Rev Genet 13(1):59–69. doi:10.1038/nrg3095

Wittkopp PJ, Vaccaro K, Carroll SB (2002) Evolution of yellow gene regulation and pigmentation in Drosophila. Curr Biol 12(18):1547–1556

Wittkopp PJ, Carroll SB, Kopp A (2003) Evolution in black and white: genetic control of pigment patterns in Drosophila. Trends Genet 19(9):495–504. doi:10.1016/S0168-9525(03)00194-X

Wittkopp PJ, Haerum BK, Clark AG (2008) Regulatory changes underlying expression differences within and between Drosophila species. Nat Genet 40(3):346–350. doi:10.1038/ng.77

Wittkopp PJ, Stewart EE, Arnold LL, Neidert AH, Haerum BK, Thompson EM, Akhras S, Smith-Winberry G, Shefner L (2009) Intraspecific polymorphism to interspecific divergence: genetics of pigmentation in Drosophila. Science 326(5952):540–544. doi:10.1126/science.1176980

Wright TR (1987) The genetics of biogenic amine metabolism, sclerotization, and melanization in Drosophila melanogaster. Adv Genet 24:127–222

Yamaguchi J, Banno Y, Mita K, Yamamoto K, Ando T, Fujiwara H (2013) Periodic Wnt1 expression in response to ecdysteroid generates twin-spot markings on caterpillars. Nat Commun 4:1857. doi:10.1038/ncomms2778

Yamanaka N, Rewitz KF, O'Connor MB (2013) Ecdysone control of developmental transitions: lessons from Drosophila research. Annu Rev Entomol 58:497–516. doi:10.1146/annurev-ento-120811-153608

Yao TP, Segraves WA, Oro AE, McKeown M, Evans RM (1992) Drosophila ultraspiracle modulates ecdysone receptor function via heterodimer formation. Cell 71(1):63–72

Zakharov EV, Caterino MS, Sperling FA (2004) Molecular phylogeny, historical biogeography, and divergence time estimates for swallowtail butterflies of the genus Papilio (Lepidoptera: Papilionidae). Syst Biol 53(2):193–215. doi:10.1080/10635150490423403

Chapter 16
Drosophila guttifera as a Model System for Unraveling Color Pattern Formation

Shigeyuki Koshikawa, Yuichi Fukutomi, and Keiji Matsumoto

Abstract A polka-dotted fruit fly, *Drosophila guttifera*, has a unique pigmentation pattern made of black melanin and serves as a good model system to study color pattern formation. Because of its short generation time and the availability of transgenics, it is suitable for dissecting the genetic mechanisms of color pattern formation. While the ecology and life history of *D. guttifera* in the wild are not well understood, it is known to be resistant to a mushroom toxin, and this physiological trait is under molecular scrutiny. Pigmentation around crossveins and longitudinal vein tips is common in closely related species of the *quinaria* group, in addition to which *D. guttifera* has evolved species-specific pigmentation spots around the campaniform sensilla. Regulatory evolution of the Wnt signaling ligand Wingless, which locally induces pigmentation in the developing wing epithelium, has driven the evolution of distinct aspects of wing and body pigmentation. A melanin biosynthesis pathway gene, *yellow*, is also involved in the elaboration of these traits, downstream of *wingless*. Unraveling the detailed mechanism of pigmentation pattern formation of this species sheds light on the general principles of morphological evolution and foreshadows potential parallels with other systems, such as the pigmented wings of butterflies.

Keywords *Drosophila guttifera* • Pigmentation • Color pattern • Evolution • Development • Transgenic • *Cis*-regulatory element • Phylogeny • Ecology • Life history • Taxonomy

S. Koshikawa (✉)
The Hakubi Center for Advanced Research, Kyoto University, Sakyo-ku, Kyoto 606-8501, Japan

Graduate School of Science, Kyoto University, Sakyo-ku, Kyoto 606-8501, Japan
e-mail: koshikawa@mdb.biophys.kyoto-u.ac.jp

Y. Fukutomi
Graduate School of Science, Kyoto University, Sakyo-ku, Kyoto 606-8501, Japan

K. Matsumoto
Graduate School of Science, Kyoto University, Sakyo-ku, Kyoto 606-8501, Japan

Graduate School of Science, Osaka City University, Sumiyoshi-ku, Osaka 558-8585, Japan

T. Sekimura, H.F. Nijhout (eds.), *Diversity and Evolution of Butterfly Wing Patterns*, DOI 10.1007/978-981-10-4956-9_16

16.1 Introduction

Research on butterfly color patterns has greatly advanced in recent years. Knowledge of the characteristics of the genome, mechanisms of pattern formation, and the function and evolutionary mode of the pattern is rapidly growing. This was enabled by utilization of multiple model species, including species of *Bicyclus*, *Heliconius*, *Junonia*, *Vanessa*, *Papilio*, and others, and by the best use of characteristics of materials (Nijhout 1991; Carroll et al. 1994; Brakefield et al. 1996; Joron et al. 2011; Reed et al. 2011; The Heliconius Genome Consortium 2012; Martin et al. 2012; Kunte et al. 2014; Monteiro 2015; Nishikawa et al. 2015; Beldade and Peralta 2017).

In vertebrates, zebrafish (*Danio rerio*) has been a model of color pattern formation, and recently, domestic and wild cats and a four-striped mouse (*Rhabdomys pumilio*) were also used for research, making this an exciting time for color pattern studies (Singh and Nüsslein-Volhard 2015; Kaelin et al. 2012; Mallarino et al. 2016).

We have been using a dipteran insect, *Drosophila guttifera*, to study a mechanism of color pattern formation (Fig. 16.1). *D. guttifera* has a pattern on its wings, which is a commonality with butterflies; however, there are also some important differences. In contrast with the pigmented scales of butterflies and moths (as an exception, see Stavenga et al. 2010), *Drosophila* pigmentation is embedded in the cuticle layers of the wing membrane. This pigmentation is believed to be made of black melanin. A congeneric species, *Drosophila melanogaster*, is a model organism widely used in genetics and various biological researches, and we can utilize its knowledge, techniques, and resources to study *D. guttifera*. This phylogenetic proximity is an asset, as it is possible to transfer a part of the genetic system, such as an enhancer involved in pattern formation, into *D. melanogaster* and analyze its function in a heterologous context. *D. guttifera* has the potential to

Fig. 16.1 Adult male of *Drosophila guttifera*. The pigmentation pattern is very similar between the sexes